Lysine-specific histone demethylase 1 (LSD1): A novel molecular target for tumor therapy

Thesis

Submitted for a Doctoral Degree
in Natural Sciences (Dr. rer.nat.)
Mathematics and Natural Sciences Faculty
Rheinische Friedrich Wilhelms University, Bonn

Submitted by

Soyoung Lim

from

South Korea

Bonn, 2009

Angefertigt mit Genehmigung der Mathematisch-Naturwissenschaftlichen Fakultät der Rheinischen Friedrich-Wilhelms-Universität Bonn

Supervisor:	Prof. Dr. Reinhard Büttner
First reviewer:	Prof. Dr. Christa E. Müller
Second reviewer:	Prof. Dr. Evi Kostenis
Third reviewer:	Prof. Dr. Hubert Schorle

Date of Submission: 14. Jul. 2009
Date of Examination: 12. Nov. 2009

Declaration

I solemnly declare that the work submitted here is the result of my own investigation, except where otherwise stated. This work has not been submitted to any other university or institute towards the partial fulfillment of any degree.

Soyoung Lim

Table of contents

Summary

Aberrant epigenetic changes in DNA methylation and histone acetylation are hallmarks of most cancers, while histone methylation had been considered to be irreversible and less versatile. Recently, several histone demethylases were identified catalyzing the removal of methyl groups from histone H3 lysine residues and thereby influencing gene expression. Lysine-specific histone demethylase 1 (LSD1) modulates demethylation of mono- and dimethylated lysines at residues 4 or 9 in histone H3, thereby allowing transcription factors or co-repressor complexes to selectively initiate or repress transcription. Although the physiological role of histone methylation is actively investigated, little is known about the implication of LSD1 in tumorigenesis. Here, we addressed the functional significance of LSD1 in different tumor types.

Neuroblastoma is the most common extracranial tumor of childhood originating from undifferentiated precursor cells of the peripheral sympathetic nervous system. Despite advances in multimodal therapy, neuroblastomas remain a clinical challenge. In this work, we found that LSD1 is strongly expressed in very aggressive neuroblastomas. LSD1 expression was inversely correlated with differentiation in primary neuroblastic tumors and correlated with adverse clinical outcome. *In vitro* differentiation of neuroblastoma cells resulted in downregulation of LSD1, suggesting that LSD1 is involved in maintaining the undifferentiated, malignant phenotype of neuroblastoma cells. siRNA-mediated knock-down of LSD1 decreased cellular growth and induced expression of differentiation-associated genes like *TNS1, TPM1, DNM2* and *DNAL4*. Upon knock-down of LSD1, putative tumor suppressor genes like *TFPI2* and *XRCC5* were increased accompanied by the increase in target gene specific H3K4 methylation. Since the catalytic domain of LSD1 has a high sequence homology to monoaminoxidases (MAOs), MAO inhibitors (MAOIs) were reported as LSD1 inhibitors. LSD1 inhibition using MAOIs resulted in an increase of global H3K4 methylation and growth inhibition of neuroblastoma cells *in vitro*. A xenograft mouse model was used to assess the potential therapeutic value of targeting LSD1 in neuroblastic tumor *in vivo*. For the first time, we could show that the treatment with MAOI tranylcypromine reduced significantly xenograft tumor growth, suggesting that LSD1 may serve as a drug target in neuroblastoma. However, MAOIs were shown to be inadequate for tumor treatment due

to their excessive side effects such as seizures caused by their modulation of neurotransmitter deamination. Instead, specific LSD1 inhibitors must be developed which do not inhibit type A and B MAOs.

In industrialized countries, breast cancer is the most common tumor in women. Expression level of estrogen receptors (ERs) is an important predictive diagnostic marker indicating a favourable clinical course and response to hormone therapy. In this work, I developed an ELISA to examine LSD1 protein levels in tissue specimens of breast cancer. We determined very high LSD1 expression in ER-negative tumors which are known to have a poorer prognosis than ER-positive tumors. Pharmacological LSD1 inhibition resulted in growth inhibition of breast cancer cells. Genetic knock-down of LSD1 induced downregulation of proliferation-associated genes such as *CCNA2* and *ERBB2* and increased target gene-specific H3K9 methylation. These data indicate that LSD1 may serve as a predictive marker for aggressive biology and targeting LSD1 in ER-negative breast cancers might provide more specific treatment.
In summary, I could show that LSD1 is strongly expressed in malignant neuroblastoma and breast cancer and functions as an oncogene.

Although histone methylation has been shown to be implicated in tumorigenesis, to date, no specific chemical modulator of LSD1 has been described. To identify selective LSD1 inhibitors from a compound library comprising 768 compounds selected by cheminformatics approach, a LSD1-HRP coupled assay was developed and applied for a high-throughput kinetic study. In this screening, a putative LSD1 inhibitor was identified and further experiments are going on to evaluate its LSD1 inhibitory actions. The identification of a new LSD1 inhibitor may serve as a starting point toward the development of a new class of LSD1 inhibitors which would help to evaluate the therapeutic potential of targeting LSD1 for tumor therapy.

Abbreviations

APS	Ammonium persulfate
AR	Androgen receptor
Bp	Basepair
BSA	Bovine serum albumin
CCNA2	Cyclin A2
ChIP	Chromatin immunoprecipitation
CpG	Cytosine phosphate guanine
CpGI	CpG islands
DMSO	Dimethylsulfoxide
DNMT	DNA methyltransferase
dNTP	Deoxynucleosides
E.coli	Escherichia coli
EDTA	Disodium ethylendiamine tetraacetic acid
EGTA	Ethylenglycol-bis-(β-aminoethylether) *N,N,N',N'* tetra acetic acid
ELISA	Enzyme-linked immunosorbent assay
Em	Molar extinction coefficient
ER	Estrogen receptor
ERBB2	v-erb-b2 erythroblastic leukemia viral oncogene homolog 2, neuro/glioblastoma derived oncogene homolog
FAD	Flavin adenine dinucleotide
FCS	Fetal calf serum
GN	Ganglioneuroma
GNB	Ganglioneuroblastoma
H3K4	Histone H3 lysine 4
H3K4me2	Histone H3 di-methylated at lysine 9
H3K9	Histone H3 lysine 4
H3K9me2	Histone H3 di-methylated at lysine 9
HAT	Histone acetyltransferase
HDAC	Histone deacetylase
HEPES	*N*-2-Hydroxyethylpiperazin-*N'*-2-ethansulfonic acid
Her2	Human epidermal growth factor receptor2
HMT	Histone methyltransferase
HP1	Heterochromatin protein 1
HRP	Horseradish peroxidase
IC50	The inhibitory concentration yielding 50 % inhibition
IPTG	Isopropyl-beta-D-thiogalactopyranoside
JmjC	Jumonji C
JMJD	Jumonji domain containing demethylase
Kb	kilobase
KDM	Lysine demethylase
Km	The Michaelis constant in Michaelis-Menten kinetics
LB	Luria-bertani-medium
LSD1	Lysine-specific histone demethylase 1
MAO	Monoaminoxidase
MAOI	Monoaminoxidase inhibitor
MTT	(3-(4,5-Dimethylthiazol-2-y)-2,5-diphyltetrazoliumbromid
NB	Neuroblastoma

NP40	Nonyl phenoxylpolyethoxylethanol 40
PAO	Polyamineoxidase
PBS	Phosphate buffered Saline
PBST	Phosphate buffered Saline-tween
PCR	Polymerase chain reaction
PR	Progesterone receptor
PVDF	Polyvinyliden fluoride
qRT-PCR	Quantitative real time polymerase chain reaction
rpm	Revolutions per minute
RT-PCR	Reverse transcription polymerase chain reaction
SDS	Sodium dodecyl sulfate
siRNA	Short interference ribonucleic acid
TAE	Tris-acetate EDTA
TCM	Tranylcypromine
TEMED	*N,N,N´,N´* -Tetramethylethylendiamine
TMA	Tissue microarray
Tris	2-amino-2-hydroxymethyl-1,3-propanediol
TSG	Tumor suppressor gene
Tween	Tween 20, polyoxyethylenesorbitan nonolaurate
U	Unit (s)
V_0	Initial velocity
WB	Western blotting
X-gal	5-Bromo-4-chloro-3-indolyl-ß-D-galactoside

1. Introduction

1.1. What is epigenetics?

Epigenetics is defined as heritable changes in gene activity and expression that occur without alteration in DNA sequence (Goldberg *et al.*, 2007; Bird 2007). The best example of an epigenetic change is the differentiation process in which cells carrying identical DNA differentiate into different cell type. Genomic imprinting which results in monoallelic expression or X chromosome inactivation in female mammalian cells are also referred to the epigenetic phenomena. Epigenetic changes are preserved when cells divide (Jaenisch, 2008). Thus, epigenetics is considered a bridge between genotype and phenotype (Bernstein *et al.*, 2007; Jaenisch *et al.*, 2003; Reik, 2007).
Different epigenetic phenomena are linked largely by the fact that DNA is not “naked” but exists as an intimate complex with histones (and histone variants) and other chromatin-related proteins such as chromatin remodeling proteins. Mainly, epigenetic information is stored as chemical modifications to cytosine bases and to the histone protein. These chemical changes regulate chromatin structure and DNA accessibility. Small non-coding RNAs also play an important role in targeting chromatin-modifying effectors to the specific chromatin loci. In the last decade, epigenetic processes were known to be fundamental to normal development and they are increasingly recognized as being involved in human diseases (Ozanne *et al.*, 2007; Feinberg *et al.*, 2004; Esteller, 2008). Here, two main epigenetic modifications, DNA methylation and histone modifications are discussed in detail with emphasis on their roles in transcription.

1.2. Chromatin structure

Genomic DNA in eukaryotic cells is packaged with histones to form protein/DNA complexes called chromatin. The basic unit of chromatin is the nucleosome, which is composed of ~147 base pairs of DNA wrapped around an octamer of the four core histones (H2A, H2B, H3, and H4) (Figure 1.1). The core histones are tightly packed in globular regions with amino-terminal tails that extend from the globular region, making them accessible to histone modifying enzymes (Luger *et al.*, 1997) (Figure 1.1). Another protein, termed linker histone H1, interacts with DNA links between nucleosomes. It

functions in the compaction of chromatin into higher-order structures that comprise chromosomes.

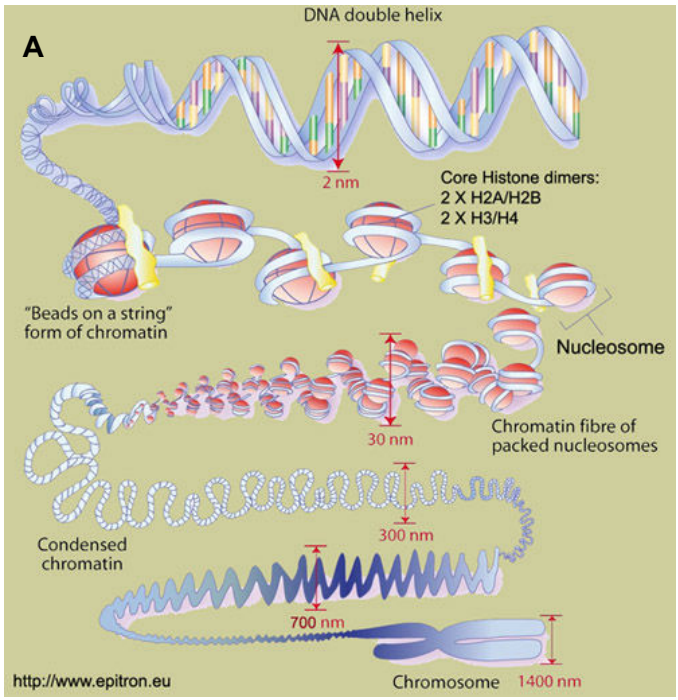

Figure 1.1. Higher order structuring of chromatin and structure of nucleosome. (A) DNA is compacked with core histones (red) forming chromatin. Linker Histone H1 (yellow) functions in compaction of chromatin into higher order chromosomes. (Picture from www.epitron.eu)
(B) Nucleosome, the basic unit of chromatin, is composed of 146 base pairs of DNA (black) wrapped around an octamer of the four core histones. The amino-terminal tails extrude from the nucleosome core.

In a non-dividing cell, chromatin can be divided into two functional states: euchromatin or heterochromatin. Euchromatin accounting for a less than 4 % of the genome is the region where DNA is accessible, representing an open conformation due to the relaxed state of nucleosome arrangement. Euchromatin contains genes in active and inactive transcriptional states (Koch *et al.*, 2007). Some of the genes are ubiquitously expressed (housekeeping genes); others are developmentally regulated or stress-induced in response to environmental cues.

Conversely, heterochromatin comprising 95 % of the genome constitutes an area where DNA is packaged into highly condensed forms that are inaccessible to transcription factors or chromatin-associated proteins (Jenuwein *et al.*, 2001; Talbert *et al.*, 2006; Huang *et al.*, 2004). Heterochromatin primarily consists of noncoding and repetitive sequences and the repressed genes associated with morphogenesis or differentiation (imprinting or X chromosome inactivation) (Reik, 2007; Feinberg *et al.*, 2004).

Heterochromatin has critical functions in controlling chromosomal stability and the prevention of mutations and translocations (Muegge, 2005; Huang *et al.*, 2004).

1.3. DNA methylation

DNA methylation is the first recognized and most well-characterized epigenetic modification. In mammalian cells, DNA methylation occurs at the 5´ position of the cytosine ring within CpG dinucleotides via addition of a methyl group to create a 5-methylcytosine (m^5C) (Figure 1.2). Three mammalian DNA methyltransferases (DNMTs) have been described (Chen *et al.*, 2004; Bestor, 2000). DNMT3a and DNMT3b function primarily as "*de novo"* methyltransferases, targeting unmethylated CpGs to initiate methylation. The process of *de novo* methylation can occur in early embryonic stem cells or cancer cells (Okano *et al.*, 1999). In contrast, DNMT1 acts as a "maintenance" methyltransferase, which has specificity for hemi-methylated CpG dinucleotides. After DNA replication, DNMT1 recognizes hemi-methylated CpGs and copies DNA methylation patterns to a newly synthesized DNA strand based on the DNA methylation pattern in the complementary template strand. By this process DNA methylation patterns can be inherited through DNA replication (Groth *et al.*, 2007; Li *et al.*, 1992).

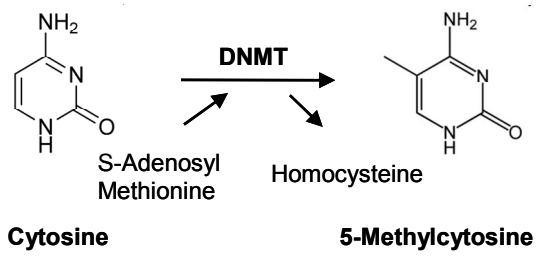

Figure 1.2. The formation of 5-methylcytosine. Using S-adenosyl methionine as a methyl group donor, DNMT catalyzes the methylation reaction of cytosine.

CpGs tend to cluster in regions termed CpG islands (CpGIs). CpGIs are characterized by more than 50% (G+C) and CpG content, spanning at least 200 bases. On a genome scale, methylated DNA is enriched at noncoding regions (e.g., centromeric heterochromatin) and interspersed at repetitive elements (transposons), thus linked to transcriptional silencing and formation of heterochromatin (Feinberg *et al.*, 2004). In euchromatin, CpGIs are found at 60% of the 5´ends of many genes. CpG methylation at the gene promoter-associated regions is believed critical for the control of gene silencing (Muegge, 2005; Huang *et al.,* 2004). The 5` regions of genes involved in imprinting, X chromosome inactivation, and tissue-specific differentiation are hypermethylated, while the 5` regions of most housekeeping genes and many regulated genes are frequently unmethylated, remaining accessible to transcription factors and chromatin-associated proteins (Jones *et al.*, 2007; Laird, 2003).

1.4. Histone modifications

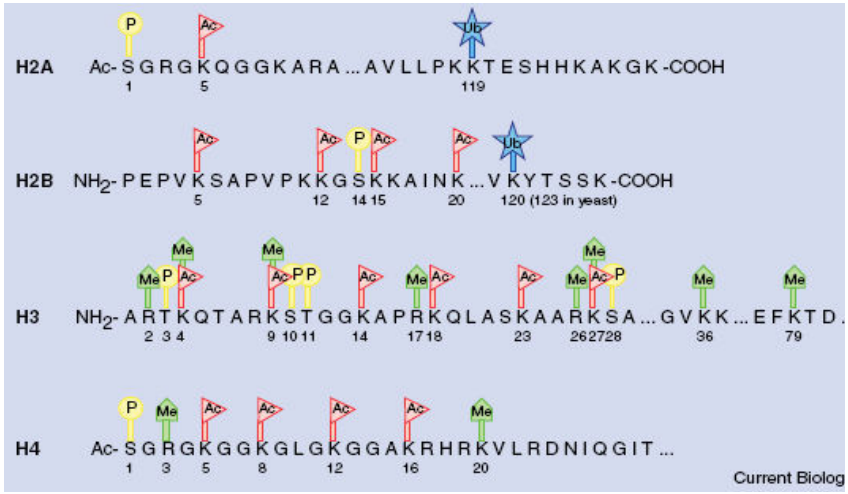

Figure 1.3. Post-translational modifications of the core histones. Histone methylation at lysines is represented as green pentagons and phosphorylation at serines or threonines as yellow circles, upiquitination as blue stars and acetylation at lysines as red triangles (Peterson *et al.*, 2004).

The N-terminals of the core histones are subjected to several types of post-translational modifications, including acetylation, methylation, phosphorylation, ubiquitination and sumoylation (Kouzarides, 2007; Ruthenburg *et al.*, 2007) (Figure 1.3). Site-specific combinations of histone modifications termed “histone code” correlated well with particular biological functions, such as transcriptional activation/repression, DNA replication, DNA repair, histone deposition, mitosis/meiosis, formation of euchromatin/heterochromatin and X inactivation (Peterson *et al.*, 2004). In contrast to DNA methylation, which is relatively stable, histone modifications are more dynamic responding to hormonal signals, environmental factors or drug treatment (Jones *et al*., 2005).

Table 1.1. Chromatin modification

Modification	Position	Enzymes		Transcriptional role
DNA methylation				
		Methyltransferase		
Methylated cytosine	CpG islands	DNMT 1-3		Repression
Histone modifications				
Lys methylation		Lysine methyltransferase	Lysine demethylase	
	H3 K4	MLL, ALL-1, Set9/7, ALR-1/2, ALR, Set1, ASH1	LSD1, Jarid1A-D	Activation
	H3 K9	Suv39h, G9a, Eu-HMTase I, ESET/SETBD1	LSD1/AR, JHDM2A, JMJD2A-D	Repression, Activation
	H3 K27	EZH2	UTX, JMJD3	Repression
	H3 K36	HYPB, Smyd2, NSD1, Set2	JHDM1, JMJD2A-C, FBXL10	Elongation Recruiting the Rpd3S to repress internal initiation
	H3 K79	Dot1		Activation
	H4 K20	PR-Set7, SET8		Silencing
Arg methylation		Arginine methyltransferase	Arginine demethylase	
	H3 R2/17/26	CARM1	Not found	Activation
	H4 R3	PRMT1		
Phosphorylation		Ser/Thr kinase	Phosphatase	
	H3 S10			Activation
Acetylation		Acetyltransferase	Deacetylase	
	H3 K9	PCAF/GCN5,	HDACs show no specificity for a particular aectyl group, except SirT2. (Kouzarides *et al*., 2007)	Activation
	H3 K14	PCAF/GCN5, CBP/p300, TIP60, ScSAS3		
	H3 K18	PCAF/GCN5, CBP/p300		
	H3 K23	ScSAS3		
	H3 K56	ScRTT109		
	H4 K5	CBP/p300, HAT1, TIP60, HB01		
	H4 K8	CBP/p300, TIP60, HB01		
	H4 K12	TIP60, HB01, HAT1		
	H4 K16	TIP60, ScSAS2	SirT2	
	H2A K5	CBP/p300		
	H2B K12	CBP/p300		
	H2B K15	CBP/p300		
Ubiquitination		Ubiquitin ligase		
	H2B K120	UbcH6, RNF20/40		Activation
	H2A K119	hPRC1L/Bmi/Ring1A		Repression

(Kourarides, 2007; Peterson *et al*., 2004; Li *et al*., 2007)

1.4.1. Acetylation of histones

In 1996, the first nuclear histone acetyltransferase (HAT) Gca5 was identified which had previously been characterized as a transcriptional co-activator protein. Subsequently, a variety of other transcriptional co-activators, such as CBP/p300 were found to have intrinsic HAT activity, and many co-repressors, such as Rpd3, were found to have histone deacetylase (HDAC) activity (Peterson *et al*., 2004).
Acetylation of lysine residues at the N-terminus of histone tails is connected with transcriptional activation by directly affecting chromatin structure (Feinberg *et al*., 2004). Acetylation removes positive charges of the lysine residues and reduces the affinity between histones and negatively charged DNA, thereby opening the condensed chromatin structure to allow transcriptional machinery easier access to promoter regions. Thus, histone acetylation relies primarily on the number of lysines modified, which is termed a cumulative effect (Li *et al*., 2007). The known acetylation sites and HAT/HDAC enzymes are summarized in table 1.1.

1.4.2. Lysine methylation

While acetylation is positively correlated with actively transcribed genes (Roh *et al*., 2005) methylation can either activate or repress transcription, depending upon the site and degree (mono-, di-, and trimethylation) of modifications (Ruthenburg *et al*., 2007). In contrast to acetylation, histone methylations are regulated with enormous specificity. One histone methyltransferase (HMT) modifies one single lysine on a single histone (Kuzarides, 2007). Histone methylation had been thought of as an irreversible epigenetic mark until the first lysine specific histone demethylase LSD1 (also known as AOF2 and KDM1) was discovered in 2004 (Shi *et al*., 2004). Subsequent to the discovery of LSD1, another family of more than 30 histone demethylases structurally different from LSD1 was described, all of which sharing a motif designated the Jumonji C (JmjC) domain and revealing a substrate specificity. Identification of these enzymes opened a new era in understanding how chromatin dynamic is regulated and further understanding of the regulation of these enzymes will provide significant insight into fundamental mechanisms of many biological processes and human diseases. Currently known site-specific HMTs and histone lysine demethylases (KDMs) are listed in table 1.1.

Six lysine (K) residues on histone H3 and H4 (H3K4, H3K9, H3K27, H3K36, H3K79 and H4K20) are subjected to mono-, di- and tri-methylation. Importantly each methylation state represent a specific epigenetic mark with a precise biological meaning and well-defined chromatin localization (Figure 1.3) (Margueron *et al.,* 2005). H3K4, H3K36 and H3K79 are implicated in activation of transcription, whereas H3K9, H3K27 and H4K20 are connected to transcriptional repression.

1.4.3. Arginine methylation, phosphorylation and ubiquitination

In contrast to lysine acetylation and methylation, the function of the following three histone modifications has not been fully elucidated yet. Arginine methylation can be either activatory or repressive for transcription. Arginine methylation is mediated by arginine methyltransferases (PRMTs), but there are no enzymes yet identified that can reverse arginine methylation (Kouzarides, 2007).

Ubiquitination is a very large modification and has been found on H2A (K119) and H2B (K120). Ubiquitylation of H2AK119 is mediated by the Bmi/Ring1A protein and is associated with transcriptional repression. In contrast, H2BK120 ubiquitylation is mediated by RNF20/RNF40 and activates transcription.

Little is known about phosphorylation and gene expression. A role for H3S10 phosphorylation has been demonstrated for the activation of “immediate early” genes. For example, concomitant with this phosphorylation, a phosphor-binding protein 14-3-3 was shown to appear on chromatin (Kourarides, 2007).

1.5. Interpretation of epigenetic modifications

The global genome-analyses revealed that distribution of histones and histone modifications correlates with transcription state (Figure 1.4). In activated gene regions, there is an enrichment of active histone markers such as methylation at H3K4, H3K36, or H3K79 and global acetylation at core histone (Koch *et al*., 2007; Heintzman *et al*., 2007; Edmunds *et al*., 2008; Steger *et al*., 2008; Krivtsov *et al.,* 2008). "Tri or di-methylation" at H3K4 and H3/H4ac are heavily enriched around the transcriptional start

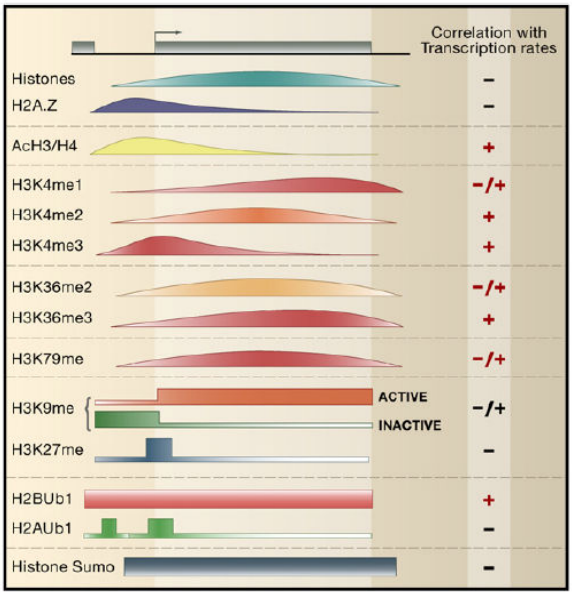

Figure 1.4. Genome-wide distribution pattern of histone modification from a transcription perspective. The distribution of histones and their modifications are illustrated on an arbitrary gene relative to its promoter. The location of a modification is tightly regulated with distinct patterns within the upstream region, the core promoter, the 5´ end of the open reading frame (ORF) and the 3´end of the ORF. This distribution of modifications is crucial for its effect on transcription. Acetylation of histone 3 and histone 4 or di- or trimethylation of H3K4, are associated with active transcription, whereas, modifications, such as H3K9me and H3K27me, are localized to inactive genes or regions termed heterochromatin (Li *et al*., 2007).

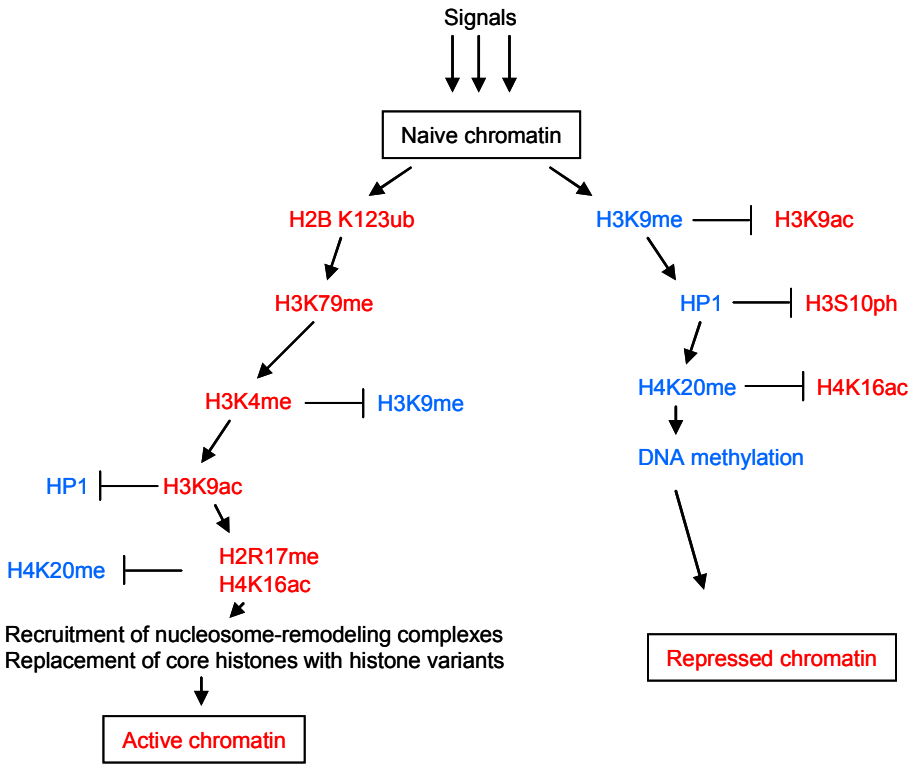

Figure 1.5. Coordinated modification of chromatin. The transition of a naive chromatin template to active euchromatin or establishment of repressive heterochromatin involves a series of coordinated chromatin modifications. Active marks are represented as red, and repressive marks as blue (modified from Allis *et al*., 2007).

sites, while methylation at H3K36 and H3K79 are distributed downstream of activated gene regions. H3K36me3 at the 3´end of active genes was found to have a function in the suppression of inappropriate initiation from cryptic start sites within the coding region (Kuzarides, 2007). Moreover, histone H2A is replaced with histone variant H2A.Z around the transcriptional start sites. In contrast, for genes that are not expressed or are expressed at low levels, high levels of repressive histone markers such as H3K27me2 and H3K9me2/3 are enriched around the transcriptional start sites.

Histone modifications occur in a combinatorial manner. The transition of a naive chromatin template to active euchromatin or establishment of repressive heterochromatin involves a series of coordinated chromatin modifications. As shown in figure 1.5, combinations of active marks are progressively induced while simultanously

counteracting repressive modifications (Allis *et al*., 2007). Especially, histone lysine methylation has been linked to DNA methylation and is thus implicated in gene silencing.

Once the "histone code" is established at a given locus, then how can this epigenetic information be interpreted to bring biological consequences? Some "effector" proteins have been reported that can recognize these specific histone modifications and bind to the modified histone tails (Figure 1.6) (Allis *et al*., 2007). For example, proteins that have chromodomains bind to methylated lysines, whereas bromodomains within proteins specifically bind to acetylated lysines. Heterochromatin protein 1 (HP1) which has a chromodomain interacts specifically with dimethylated H3K9, leading to the silencing of euchromatic genes as well as the formation of silent heterochromatin (Figure 1.5 and 1.6). The chromodomain within the Polycomb protein binds specifically to a dimethylated K27 of histone H3, resulting in the silencing of the homeobox protein (HOX) gene expression (Figure 1.6). The binding of bromodomains to different acetylated lysines, however, does not show as much specificity. In the case of DNA methylation, methyl-CpG-binding domain proteins (MBD) are considered the "reader/binder" of DNA methylation, functioning in silencing of chromatin (Figure 1.6).

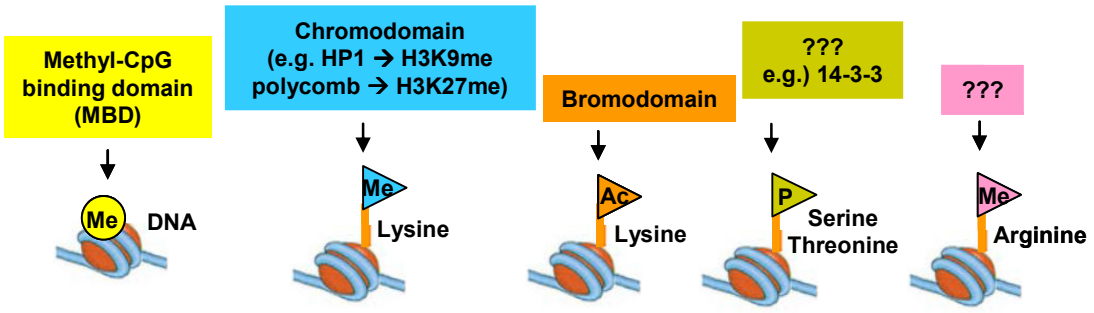

Figure 1.6. From epigenetic modification to biological consequences. "Effector" proteins can recognize specific histone modification. Chromodomains within proteins bind to methylated lysine and bromodomains within proteins bind to acetylated lysine. There are no protein domains yet identified that can bind specifically to arginine-methylated histones or serine/threonine-phosphorylated histones.

1.6. Lysine-specific histone demethylase 1 (LSD1)

It was recently demonstrated that methylation marks are not static but dynamically regulated by both histone methyltransferases and histone demethylases. LSD1 is the first discovered histone demethylase which catalyzes the demethylation reaction of mono- and dimethylated histone H3 lysine 4 (Shi *et al*., 2004). LSD1 is highly conserved in organisms ranging from *Schizosaccharomyces pombe* to human and consists of three major domains: an N-terminal SWIRM (Swi3p/Rsc8p/Moira) domain, a C-terminal AOL (amine oxidase-like) domain, and a central protruding Tower domain (Figure 1.7). The C-terminal catalytic domain reveals high sequence homology to amine oxidases

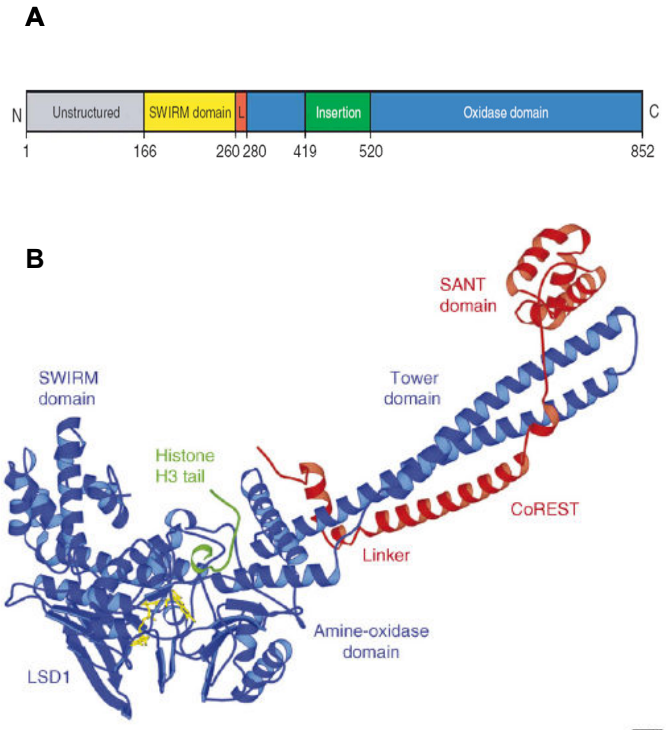

Figure 1.7. Structure of human LSD1. (A) Domain structure. Gray, unstructured N-terminal region; yellow, SWIRM domain; red, SWIRM-oxidase connector; blue, oxidase domain; green, helical insertion (Stavropoulos *et al*., 2006). (B) Structure of LSD1 in complex with CoREST and a peptide substrate. LSD1 (blue) tightly associates with the CoREST C-terminal SANT domain (red). The histone H3 N-terminal peptide (residues 1-16; green) binds in the LSD1 amine oxidase domain in proximity to the flavin cofactor (yellow) (Forneris *et al*., 2008).

that belong to the flavin adenine dinucleotide (FAD)-dependent enzyme family including mono- and polyaminoxidase. The N-terminal SWIRM domain seems to be important for chromatin binding (Anand *et al*., 2007). The Tower domain, inserted into the AOL domain, forms a long helix-turn-helix structure and serves as a platform for binding of LSD1 partner proteins such as corepresser element silencing factor, CoREST.

LSD1 acts on mono- and dimethylated H3K4 through a flavin-dependent mechanism (Shi *et al.,* 2004; Forneris *et al.,* 2005). The reaction results in a hybrid transfer with reduction of FAD to FADH2 which is reoxidized by molecular oxygen, producing hydrogen peroxide (Figure 1.8). The resulting imine intermediate is hydrolyzed to generate the demethylated H3 tail and formaldehyde. LSD1 cannot demethylate trimethylated lysine residues, since a lone pair of electrons in the unprotonated state of N of methylated lysine is required in FAD-mediated reaction. Forneris *et al.* showed that LSD1 requires the first 20 N-terminal amino acids of the histone tail for productive binding in the *in vitro* enzymatic assay (Forneris *et al*., 2005).

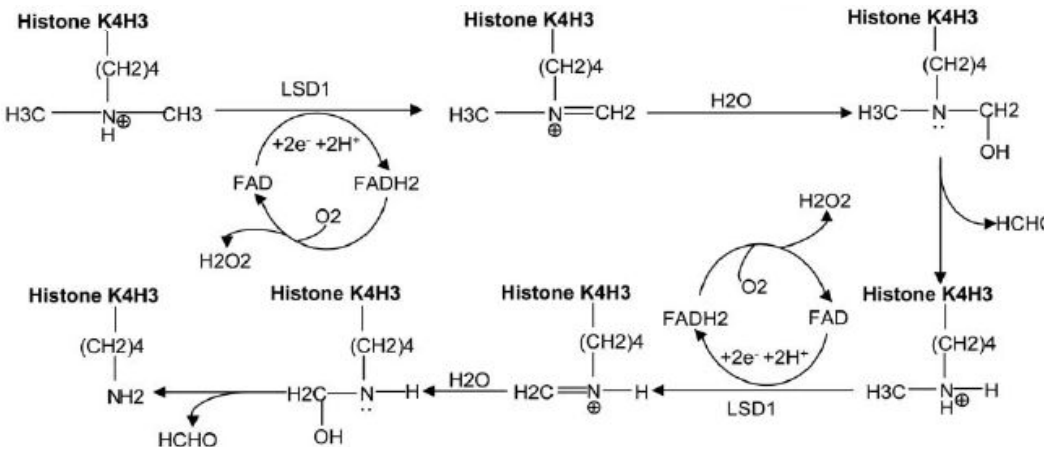

Figure 1.8. Demethylation of K4H3me2 by LSD1. First, the methylated Lys4 side chain of histone substrate is oxidized by the FAD prosthetic group with resultant reduction of oxygene to hydrogen peroxide. The resulting imine intermediates is hydrolyzed to generate the demethylated H3 tail and formaldehyde (Shi *et al.,* 2004).

The presence of other activation markers (e.g. Lys hyperacetylation or Ser 10 phosphorylation) on H3 greatly decreases catalytic activity of LSD1 (Forneris *et al*., 2005). This finding implies that other enzymes, including histone deacetylases, arginine demethylases and serin phosphatases must operate before LSD1 activity can occur. Therefore, LSD1–mediated H3K4 demethylation seems to be a final epigenetic process associated with gene repression (Forneris *et al.*, 2008).

1.6.1. Linking LSD1 to gene repression

LSD1 was originally identified as a component of transcriptional repressor complexes comprising transcriptional corepressor protein (CoREST) and HDAC1/2. In association with the transcription factor repressor element 1-silencing transcription factor (REST), the LSD1-CoREST-HDAC core mediates long-term repression of neuronal genes in non-neuronal cells and in neuronal precursors. The LSD1-CoREST-HDAC core is functionally and structurally conserved (Dallman *et al*., 2004) and was shown to be also involved in various biological processes. In hematopoiesis, the LSD1-CoREST-HDAC core associates with growth factor independent 1 transcription repressor (Gfi-1) repressing Gfi-1 target genes (Saleque *et al*., 2007). LSD1-CoREST-HDAC core is also involved in silencing mature B-cell genes through direct interaction with the transcriptional repressor B lymphocyte-induced maturation protein-1 (Blimp-1) (Su *et al.*, 2009). The constitutive transrepressor TLX also forms a complex with LSD1-CoREST-HDAC core, repressing PTEN gene and inhibiting cell proliferation (Yokoyama *et al.,* 2008).

LSD1 can also directly interact with p53 to confer p53-mediated transcriptional repression, such as the repression of the alpha-fetoprotein (AFP), whereas the well known p53 target gene p21 can be actively transcribed without recruitment of LSD1. This finding suggests that LSD1 is targeted to chromatin by p53 but likely in a gene-specific manner (Tsai *et al.,* 2008). Another important indication of LSD1 involvement in gene repression is that the DNA methylase regulator DNMT3L recognizes histone H3 tails that are unmethylated at H3K4 (Ooi *et al*., 2007). This finding suggests the importance of LSD1 in the formation and propagation of heterochromatin through LSD1-dependent H3K4 demethylation and following *de novo* DNA methylation.

1.6.2. The role of LSD1 in gene activation

Recent studies implicated LSD1 in transcriptional activation mediated by nuclear receptors (the androgen and estrogen receptors, AR and ER) functioning as an H3K9 demethylase (Garcia-Bassets *et al.,* 2007; Metzger *et al.,* 2005). This function was firstly described by Metzger *et al.* who showed that activation of AR target genes requires LSD1-dependent histone H3K9 demethylation. They demonstrated that, following hormone treatment, AR and LSD1 colocalize on promoters and stimulate H3K9 demethylation without altering the H3K4 methylation status and promote ligand dependent transcription of AR target genes resulting in enhanced tumor cell growth. Consistently, LSD1 knock-down resulted in decreased activation of AR-responsive promoters.

Recently, a genome-wide analysis of LSD1 promoter occupancy following estrogen treatment of MCF7 cells has revealed striking results regarding the activatory role of LSD1 (Garcia-Bassets *et al*., 2007). LSD1 occupies nearly 20 % of the total assayed promoters and 84 % of these promoters are associated with RNA polymerase II and additionally with activation markers such as dimethyl-H3K4 and acetyl-H3K9 suggesting that LSD1 is extensively involved in gene activation rather than repression.

The dual role of LSD1 in gene repression and activation is also demonstrated by the fine regulation of growth hormone expression during pituitary development (Wang *et al*., 2007). Activation of growth hormone expression is regulated by the transcriptional activator pituitary transcription factor 1 (Pit1) during the early phases through recruitment of a LSD1-containing mixed lineage leukemia 1 (MLL1) coactivator complex. Pit1 is later replaced by zinc finger E-box binding homeobox 1 (ZEB1), a transcriptional repressor which recruits a co-repressor complex containing C-terminal binding protein (CtBP), CoREST and LSD1, switching off growth hormone expression.

Until now it is not clear how LSD1 functions as a H3K9 demethylase in association with AR, ER or other transcription factors. So far, H3K9 demethylase activity by LSD1 has not been detected in *in vitro* enzymatic assay (Shi *et al*., 2004; Forneris *et al*., 2005). Possibly, an interacting partner or a post-translational modification of LSD1 could alter LSD1 demethylation specificity from H3K4 to H3K9 possibly through allosteric alteration. Alternatively and more likely, other H3K9-specific histone demethylases could be recruited by LSD1 or by a LSD1-associated protein. In this case, LSD1 might act as a

docking or adaptor module for different coactivator complexes that might contain a demethylase specific for H3K9. Indeed, it was observed that some chromatin-remodeling complexes contain both LSD1 and a H3K9 demethylase of the Jumonji-containing class JMJD2C (Wissmann *et al*., 2007). JMJD2C assembles into the AR complex and collaborates AR-target-gene transcription together with LSD1.

In addition to its transcriptional regulation of individual genes, LSD1 plays an important role in interchromosomal interaction and nuclear rearrangement. Hu *et al.* showed that upon treatment of estrogen, LSD1 is recruited to distinct interchromatin granules, long thought to serve as "storage" site for the splicing machinery, some transcription elongation factors and various chromatin remodeling complexes, enhancing nuclear receptor-induced transcription (Hu *et al.,* 2008).

1.6.3. The role of LSD1 in development and differentiation

Since its discovery, the functional role of LSD1 has been actively investigated. LSD1 appears to be pivotal in development and differentiation. Constitutive knockout of *LSD1* results in mouse embryonic lethality at or before embryonic day 5.5 (Wang *et al.,* 2007; Wang *et al.,* 2009). Zygotic LSD1 expression first appeared at the morular stage and became ubiquitous in postimplantation embryos. ES cells derived from LSD1 knockdown mouse showed severe growth impairment, probably due to increased cell death, impaired cell cycle progression, and defects in differentiation. Conditional knockout of LSD1 showed defects in pituitary gland development and the Notch signalling pathway (Wang *et al.,* 2007). RNAi inhibition of LSD1 in several mammalian haematopoietic lineages resulted in impairment of differentiation *in vitro* (Saleque *et al.,* 2007). In addition, LSD1 appears to play conserved roles in meiosis and germ cell development. The mammalian LSD1 shows relatively high levels of expression in mouse testes (Godmann *et al*., 2007). Mutations of the fly LSD1 homolg lead to sex-specific embryonic lethality and sterility in the surviving (primarily female) offspring, probably owing to defects in ovary development (Di Stefano *et al*., 2007). Mutant in spr-5, the Caenorhabditis elegans ortholog of LSD1, exhibited germline immortality by the misregulation of spermatogenesis-related genes (Katz *et al.,* 2009).

1.6.4. LSD1 functions beyond histone demethylation

Recent studies have identified non-histone substrates for LSD1 (Huang *et al.,* 2007; Wang *et al.,* 2009). LSD1 controls the tumor suppressor activity of p53 by demethylating a specific p53 lysine (Lys370) which is required for efficient binding to the transcriptional co-activator p53-binding protein-1. Through this interaction, LSD1 blocks p53 pro-apoptotic activity (Huang *et al*., 2007).

Very recently, a DNA methyltransferase was also indentified as a non-histone substrate for LSD1 (Wang *et al*., 2009). Methylation of DNMT1 leads to protein degradation. LSD1 can directly demethylate and stabilize DNMT1 maintaining global DNA methylation. Thus, LSD1 coordinates not only histone methylation but also DNA methylation to regulate chromatin structure and gene activity. However, its mode of recognition of a non-histone substrate remains unclear, especially in light of the dissimilar amino acid sequences surrounding non-histone substrates and H3K4.

1.7. Altered epigenetic modifications in cancer

Given that epigenetic processes are fundamental to the regulation of gene activity, it is not surprising that aberrant changes in epigenetic modifications were found in many pathological processes (Ozanne *et al*., 2007; Feinberg *et al*., 2004; Laird, 2003), especially in human tumors (Esteller, 2008; Jones *et al*., 2007; Widschwendter *et al*., 2007).

Neoplastic transformation also termed as carcinogenesis, is regarded as the multistep process whereby cells undergo a change involving uncontrolled cell proliferation, a loss of checkpoint control tolerating the accumulation of chromosomal aberrations and genomic instability, and mis-regulated differentiation (Lengauer *et al*., 1998). It is commonly thought that silencing of tumor suppressor genes (TSGs) or activation of oncogenes through dominant mutation or overexpression of a normal oncogene (proto-oncogene) initiate carcinogenesis (Hanahan *et al*., 2000). However, a growing body of data has appeared since the mid-1990s indicating that epigenetic alterations may also be critical for the evolution of all human cancer types (Jones *et al.,* 2007; Laird *et al.,* 2003).

Global DNA hypomethylation is a widespread phenotype of cancer cells. At the individual gene level, DNA hypomethylation can lead to the activation of proto-oncogenes, the derepression of genes that cause aberrant cell function, or the biallelic expression of imprinted genes (also termed loss of imprinting or LOI). On a global genomic scale, broad DNA hypomethylation becomes increasingly mutagenic to the extent of causing global genomic instability (Allis *et al*., 2007). Particularly, global DNA hypomethylation at regions of constitutive heterochromatin predisposes cell to chromosomal translocations and aneuploidy that contribute to cancer progression.
Another hallmark of cancer is CpGI hypermethylation at TSG promoter regions. Abnormal hypermethylation of CpGIs in the 5´ regions of TSGs is integral to their transcriptional silencing. Indeed, many TSGs such as RASSFIA (self-sufficiency in growth signals), E-cadherin (tissue invasion and metastasis), GST Pi and MLH1 (DNA repair capacity) and p19 or RB (limitless replicative potential) were shown to be epigenetically silenced in human cancer.

An imbalance of histone modification may also contribute to oncogenic transformation. Indeed, changes of histone modification levels were shown to be an indicator of cell normality or abnormality. As demonstrated by a study in prostate tumor progression, there is a manifest decrease in repressive histone marks and an increase in overall acetylation states (Seligson *et al*., 2005) causing elevated levels of gene transcription and genomic instability.
Mutations, overexpression or malfunction of several histone modifying enzymes such as HDACs and HMTs have been shown to be linked to cancer. For example, deregulation of a Polycomb group protein (e.g., EZH2) or trithorax group protein (e.g., MLL) HMT acts during oncogenic transformation through perturbing a cell's epigenetic identity, which consequently either transcriptionally silences or activates inappropriate genes (Schneider *et al*., 2002; Valk-Lingbeek *et al*., 2004). In fact, the deregulation of EZH2 or MLL has been shown to be associated with increased risk of prostate cancer, breast cancer, multiple myeloma, or leukemia (Lund *et al.,* 2004; Valk-Lingbeek *et al*., 2004).

1.8. Epigenetic therapy of cancer

1.8.1. DNMT and HDAC inhibitors

Targeting chromatin-modifying effector enzymes has opened up a new horizon for cancer therapeutics. There are two main classes of "epi-drugs": inhibitors of DNMTs and HDACs. The nucleoside analogs 5-azacytidine, 5-aza-2´- deoxycytidine and zebularine are powerful inhibitors of DNA cytosine methylation (Figure 1.9). These drugs are incorporated into the DNA of replicating cells and then interact with all three known DNMTs to form covalent intermediates which ultimately inhibit DNA methylation. These nucleoside analogs can reactivate silenced genes in tissue culture or in xenograft models. Zebularine is being applied for the treatment of certain hematological malignancies, particularly myeloid dysplastic syndrome. Despite the lack of specificity of nucleoside analogs which inhibit DNA methylation throughout the genome, results from clinical trials suggest that demethylation induced by azanucleosides might be of general benefit for the reversion of epigenetic lesions in cancer (Wijermans *et al.,* 2008, Mai *et al*., 2009).

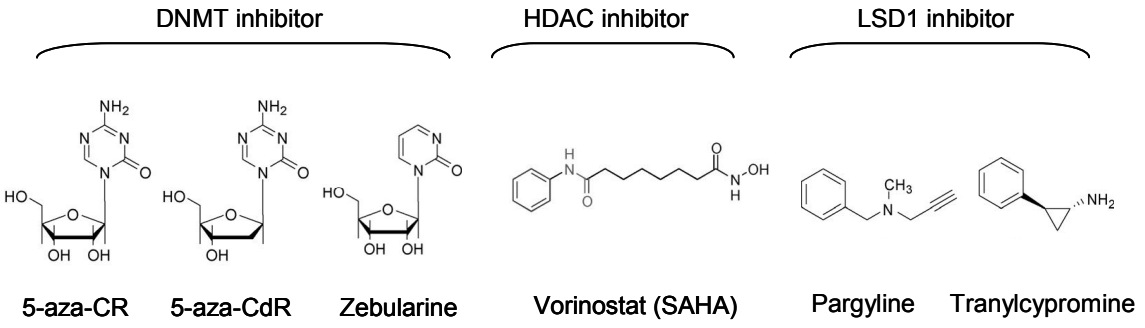

Figure 1.9. Chemical structures of epi-drugs

Clinical trials are also ongoing using inhibitors of various HDACs. Among them, SAHA (vorinostat, Zolinza®; Merck) was approved by the US FDA in 2006 for the treatment of cutaneous manifestations in patients with cutaneous T-cell lymphoma (CTCL) (Figure 1.9). The molecular mechanisms mediating the anti-cancer effects of HDAC inhibitors are very complex. In part, the antiproliferative effects of vorinostat involve the activation of aberrantly repressed TSGs, induction of differentiation and promotion of apoptosis, as

well as changes in acetylation levels and function of non-histone proteins (Witt *et a*l., 2009).

1.8.2. Targeting LSD1 in tumor therapy

Since the discovery of LSD1, there have been increasing efforts to identify or design LSD1 inhibitors that could function as antitumor therapeutic agents. Given the frequent physical association of LSD1 with HDACs and the positive cooperativity between LSD1 and HDACs in modifying chromatin, it is very likely that LSD1 and HDACs collaborate to repress the transcription of common sets of genes. Thus, chemical inhibitors of LSD1 may exhibit antitumor activities on their own and/or have synergistic effects with HDAC inhibitors (Yang *et al.,* 2007).

Moreover, LSD1 has been found upregulated in certain high-risk tumors and high levels of LSD1 correlated with tumor relapse during therapy (Metzger *et al.,* 2005; Kahl *et al*., 2006). At the cellular level, overexpression of LSD1 in prostate carcinoma was sufficient to promote AR-dependent transcription in the absence of androgens (Kahl *et al.,* 2006). Thus, the development of LSD1 inhibitors may provide an important new therapy of cancer.

LSD1 shares similar folding topology and enzymatic properties with members of the flavin-dependant amino oxidas family, including MAOs and PAOs. Owing to the similarity between LSD1 and mono-amineoxidases (MAOs)/poly-amineoxidases (PAOs), both MAO inhibitors and polyamine analogues have been shown to inhibit LSD1 enzymatic activity (Lee *et al*., 2006; Huang *et al.*, 2007). Pargyline or tranylcypromine which are well-known MAO inhibitors and used clinically as antidepressant, have been proved to be LSD1 inhibitors (Figure 1.9). Pargyline blocks demethylation by LSD1 and consequently blocks androgen-receptor-dependent transcription, suggesting that modulation of LSD1 activity offers a new strategy to regulate androgen receptor functions which are important in prostate cancer (Metzger *et al.*, 2005). Biguanide and bisguanidine polyamine analogues have been described to inhibit LSD1 and be capable of reactivating genes that are pathologically silenced in the development of colon cancer including members of the secreted frizzle-related proteins (SFRPs) and the GATA family of transcription factor (Huang *et al*., 2007). Despite the fact that MAO inhibitors and polyamine analogues may serve as a valuable starting point for the design of more

potent LSD1 inhibitors, they have limitations for the clinical use due to their action on MAOs and PAOs and anticipated side effects, and no data is yet available about their effects in cancer.

2. Aims of this work

LSD1 has been found to be upregulated in high-risk prostate cancer and overexpression of LSD1 was shown to be correlated with tumor relapse. Aberrant overexpression of LSD1 does not seem to be restricted to prostate cancer but rather represents a general phenomenon of most aggressive cancer types. The goals of my study are to analyze the functional role of LSD1 in neuroblastoma and breast cancer and to evaluate its use as a predictive marker for aggressive tumor biology. For the determination of LSD1 protein levels in tissue specimen, an ELISA for LSD1 has to be developed. Using either RNA interference method or small molecule inhibitor for LSD1 in a cell culture system, we wanted to analyze the functional role of LSD1 in proliferation and transcriptional regulation. Furthermore, we wanted to provide evidence that LSD1 could be targeted in cancer therapy. For this purpose, the effect of MAOIs on the tumor growth in a xenograft mouse model was investigated. To find specific LSD1 inhibitors, a high-throughput screening assay was developed and employed to screen a compound library for novel small molecule inhibitors of LSD1.

3. LSD1 in neuroblastoma

3.1. Neuroblastoma

Neuroblastoma is the most common extracranial tumor of childhood. This tumor originates from precursor cells of the peripheral sympathetic nervous system and usually arises in a paraspinal location in the abdomen or chest. Neuroblastoma accounts for 7-10 % of all childhood cancers and is the most common cancer diagnosed during infancy (Brodeur *et al*., 2003).

The clinical course of neuroblastoma is very heterogeneous. While neuroblastoma (NB) with favourable biology as well as the benign variants ganglioneuroblastoma (GNB) and ganglioneuroma (GN) spontaneously regress or differentiate without any therapeutic intervention, neuroblastoma with unfavourable biology often fatally progresses regardless of multimodal therapy (Brodeur *et al*., 2003; Maris *et al*., 2007). More than 60 % of neuroblastomas remain with their poor prognosis despite the application of aggressive multimodal therapies including surgery, radiation therapy, and cytotoxic chemotherapy. The survival rate for the *MYCN*-amplificated neuroblastoma with tumor stage 4 is less than 20 %. Unfortunately, new biologically based therapeutic options such as induction of differentiation using retinoic acid derivatives (Sidell *et al*., 1983), blockage of the tyrosine receptor kinase pathway or inhibition of angiogenesis have shown less significant survival advantage. Therefore, the identification of novel drug targets and development of new therapeutic options are urgently needed.

High-throughput analysis including expression profiling (Schramm *et al*., 2007; Schulte *et al*., 2008) and array CGH (Schleiermacher *et al*., 2007; Chen *et al*., 2006; Vandesompele *et al*., 2005) have identified several patterns in heterogenous neuroblastomas. Based on the patterns of genetic change, neuroblastomas can be classified into three subtypes that are predictive of clinical behaviour. The first favourable tumor group is characterized by near-triploid karyotypes with whole chromosome gains. These tumors rarely have structural rearrangements and usually express the TrkA neurotrophin receptor. The second tumor group comprises the near-diploid or tetraploid tumors with low TrkA expression and structural chromosomal aberration. The third unfavourable tumor group comprises highly aggressive and rapidly progressing tumors

with high TrkB expression, *MYCN* amplification and aberrant diploid chromosome with 1p36 and 11q deletion (Attiyeh *et al*., 2005).
MYCN amplification was shown to be predominantly associated with rapid tumor progression and a poor outcome, serving as a powerful predictor of a poor prognosis. MYC oncoproteins are transcription factors that can lead to deregulated growth proliferation by activating genes related to cell cycle progression. *MYCN* amplification was detected in 25 % of all neuroblastomas. Brodeur *et al.* revealed that the 3 year event-free survival (EFS) of infants whose tumors lacked *MYCN* amplification was 93 %, whereas those with tumors that had *MYCN* amplification had only a 10 % EFS (Brodeur *et al*., 2003). However, pharmacological intervention to modulate central oncogens like *MYCN* has not yet been achieved. Many of the genes discriminating between favourable and unfavourable neuroblastomas belong to the functional category of transcription factors which are very difficult drug targets.

A relatively new therapeutic approach is targeting epigenetic enzymes which are involved in tumor progression and modulate broad expression patterns. Indeed, histone acetylation and DNA methylation have been shown to specifically regulate central genes in aggressive neuroblastoma (de Ruijter *et al*., 2004; Stupack *et al*., 2006; Jones *et al*., 2001). Treatment with histone deacetylase (HDAC) inhibitors and DNA-demethylating agents has proven effective against neuroblastoma cells *in vitro* (de Ruijter *et al*., 2004), and are currently being evaluated for treating neuroblastoma *in vivo*.

In a previous study, our group has shown that LSD1 is involved in malignant progression of prostate cancer and controls androgen receptor-dependent transcription in the absence of androgen. In this study, we wanted to analyze the implication of LSD1 in neuroblastoma.

3.2. Results

This work was carried out in collaboration with Dr. Jutta Kirfel (Bonn), Johannes Schulte (Essen), Prof. Angelika Eggert (Essen), Ludger Klein-Hitpass (Essen) and Rogier Versteeg (The Netherlands).

3.2.1. LSD1 is strongly expressed in poorly differentiated neuroblastomas

We analyzed LSD1 expression in primary neuroblastic tumors including malignant neuroblastomas, benign ganglioneuroblastomas and ganglioneuromas. A tissue microarray was prepared for this purpose incorporating 99 primary, untreated tumors, of which 77 were neuroblastomas and 22 were ganglioneuroblastomas and ganglioneuromas. LSD1 expression was significantly higher in poorly differentiated than in differentiated neuroblastomas (Mann-Whitney-Test, $P = 2.6x10^{-5}$, Figure 3.1B). LSD1 expression was also higher in differentiated neuroblastomas than in ganglioneuromas and ganglioneuroblastomas (Mann-Whitney-Test, $P = 8.2x10^{-5}$, Figure 3.1B). LSD1 was not expressed in non-malignant cells, such as stromal tissue or infiltrating leukocytes (Figure 3.1A). Similar results were obtained in an independent cohort of 110 neuroblastic tumors previously analyzed on Affymetrix microarrays when these data were reanalyzed for LSD1 mRNA levels (Figure 3.1C). Kaplan-Meier analysis revealed that a low LSD1 mRNA expression level was predictive of event-free survival (EFS) in the latter cohort (log rank-test, p=0.021, Figure 3.1D). In contrast to mRNA expression, LSD1 protein expression which was measured semi-quantitatively on the TMA using immunohistochemistry failed to serve as a statistically significant predictive parameter of survival and relapse or progression. The amplification of the *MYCN* oncogene, a known marker for unfavourable neuroblastoma did not correlate with LSD1 expression (data not shown).

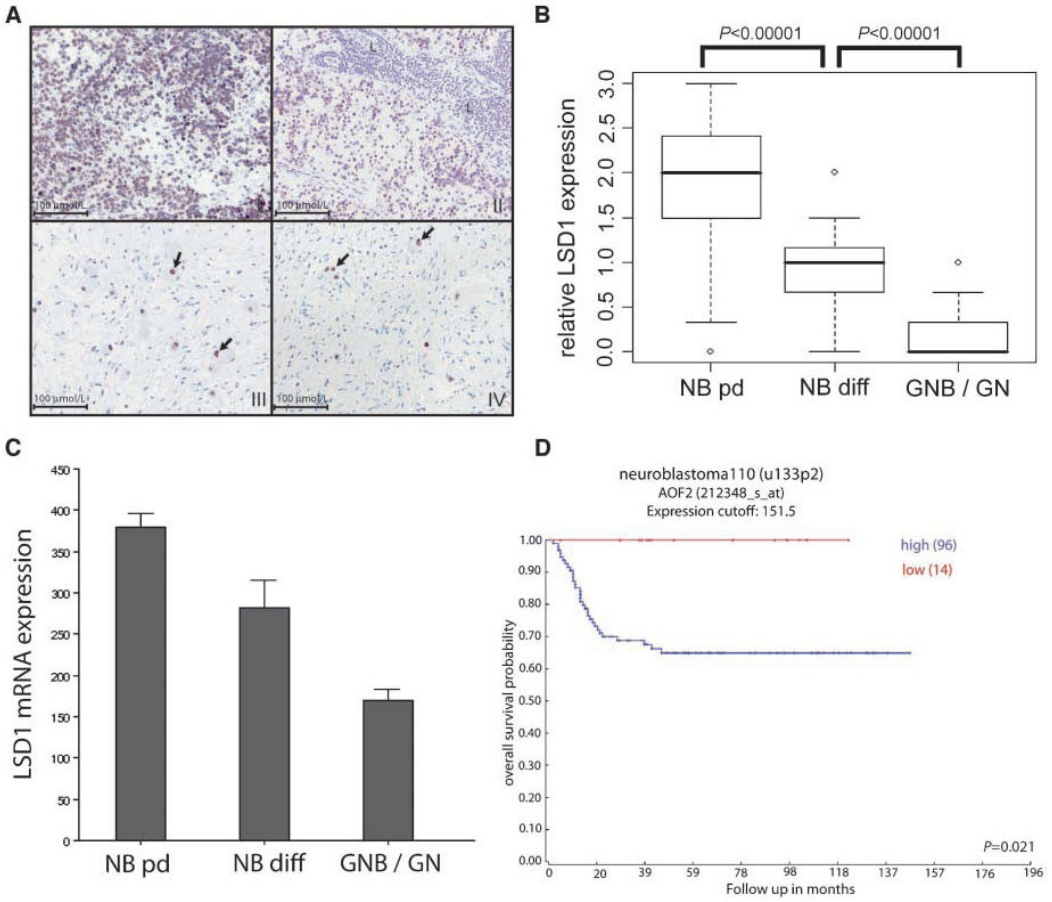

Figure 3.1. LSD1 is strongly expressed in poorly differentiated neuroblastoma. (**A)** Immunohistochemical staining of LSD1 in neuroblastic tumors. In poorly differentiated neuroblastomas (I and II), nuclear LSD1 staining is observed in almost all tumor cells. In contrast, in benign ganglioneuroblastomas (III)/ganglioneuroma (IV), LSD1 staining is mild or absent. The few signals marked by arrows in III and IV represent nucleoli of differentiated ganglia. Infiltrating leukocytes (L) in II, and Schwannian stroma do not display any immunoreactivity for LSD1 (III/IV). **(B)** A tissue microarray with 99 primary neuroblastic tumors was used to analyze LSD1 expression in neuroblastoma and its benign derivates. Expression was significantly higher in poorly differentiated neuroblastomas (NB pd) than in differentiated neuroblastomas (NB diff) or ganglioneuroblastomas/ganglioneuromas (GNB/GN). **(C)** LSD1 mRNA expression in an independant cohort of 110 neuroblastic tumors analyzed with Affymetrix microarrays. **(D)** Kaplan-Meier analysis of 110 neuroblastic tumors shows that low LSD1 mRNA expression levels are predictive of EFS.

3.2.2. LSD1 expression in neuroblastoma cell lines

LSD1 protein expression in neuroblastoma cell lines was assessed by Western blotting. All cell lines strongly expressed LSD1 (Figure 3.2A). As all existing neuroblastoma cell lines were established from undifferentiated, aggressive tumors, this result was consistent with our data from primary tumors where aggressive tumors showed high LSD1 expression. We then asked if induction of differentiation might result in down-regulation of LSD1. We therefore treated SY5Y and BE2C neuroblastoma cells with all-trans retinoic acid (RA), a drug known to induce differentiation of neuroblastoma cells (Cuende *et al.,* 2008). After 12 days, RA treatment resulted in morphological changes such as neurite development and reduced proliferation (Figure 3.2B). Upon differentiation, a significant down-regulation of LSD1 was detected (Figure 3.2C)

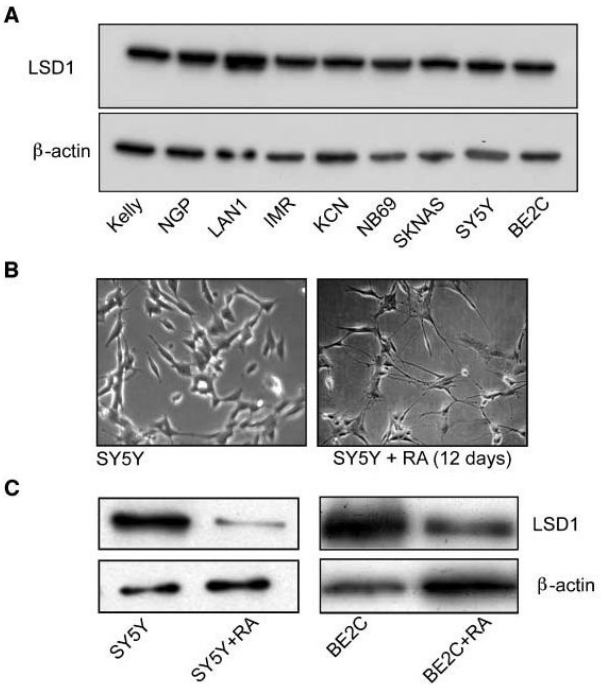

Figure 3.2. **(A)** LSD1 protein expression in different neuroblastoma cell lines. β-actin was used as the loading control. **(B)** Treatment of SH-SY5Y cells with all-trans retinoic acid (RA) resulted in a significant increase in the number and length of neurites, which served as an indicator of differentiated phenotype. **(C)** After 12 d, retinoic acid treatment induced differentiation of SH-SY5Y and BE(2)-C neuroblastoma cells. LSD1 protein levels were significantly reduced in both cell lines. β-actin served as the loading control.

3.2.3. Silencing of LSD1 impairs neuroblastoma growth and induces cellular differentiation *in vitro*

To further analyze the functional relevance of LSD1 in neuroblastic tumors, SH-SY5Y cells were transiently transfected with siRNA directed against LSD1 or with a scrambled control siRNA. A significant LSD1 knock-down was detected on protein levels after transfection with either 10 or 20 pmol of siRNA (Figure 3.3A).

Upon siRNA-induced knock-down of LSD1, a significant decrease in cell viability was detected in MTT assays (Figure 3.3B). Decreased viability was accompanied by the appearance of morphological features indicating differentiation, such as outgrowth of neurite-like structures (Figure 3.3C).

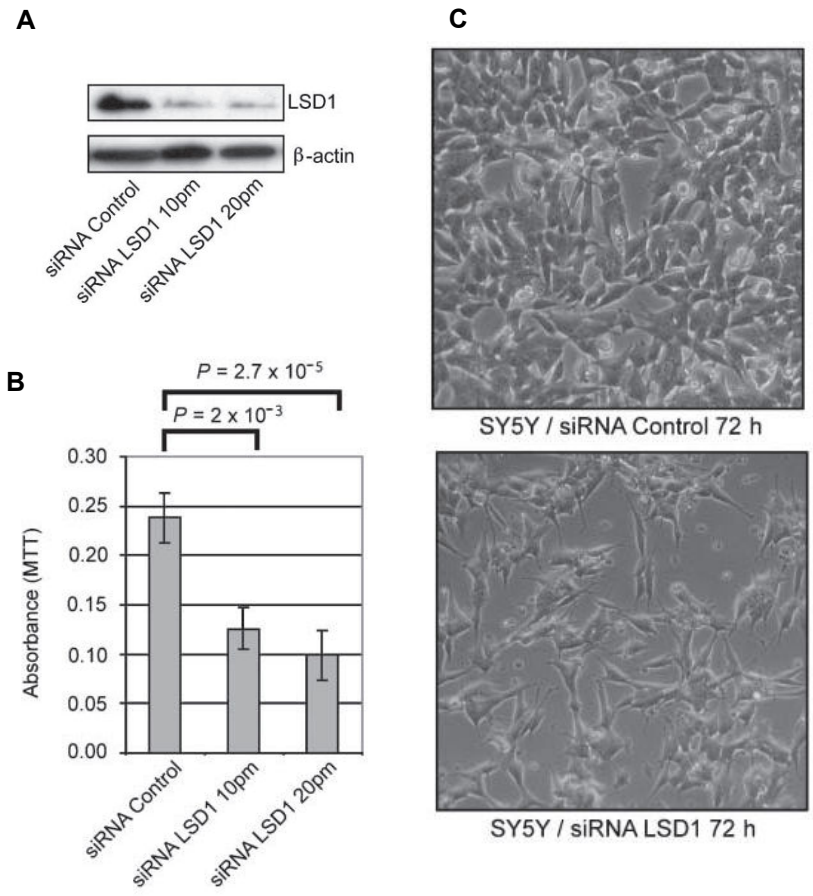

Figure 3.3. (**A**) Transfection of SH-SY5Y neuroblastoma cells with LSD1-directed siRNA resulted in reproducible knockdown of LSD1 protein levels. β-actin served as the loading control. (**B**) MTT assay of SH-SY5Y treated with siRNA against LSD1 detected a significant reduction in cell number after 72 h incubation. (**C**) Phase-contrast microscopy of SH-SY5Y cells transfected either with siRNA against LSD1 or scrambled control siRNA. Phenotypic changes were observed 72 h posttreatment.

Microarray analysis revealed changes in expression that were consistent with these observations 72 hours after LSD1 knock-down (Figure 3.4). At this time, 28 genes were significantly induced at least 1.5-fold and 29 genes were significantly repressed at least 1.5-fold. Among the 28 induced genes, 4 genes such as *TNS1, TPM1, DNM2* and *DNAL4* are known to be related to cytoskeletal remodeling and neurite dynamics (Schevzov *et al*., 2005; Dehmelt *et al*., 2006; Okamoto *et al*., 2001). *TNS1* encodes tensin1 which localizes to focal adhesions, attaching cells to the extracellular matrix. Tropomyosin1 (*TPM1*) is an integral component of actin microfilaments and is recruited to the sprouting neurite. Dynein4 (*DNAL4*) also contributes to the generation of new neurites by pushing the microtubule bundles outward. *DNM2* encodes dynamin2 which is expressed in synaptosomes and controls synaptic vesicle recycling. Upregulation of *TNS1, TPM1 DNM2* and *DNAL4* indicates the differentiation of neuroblastoma cells upon knock-down of LSD1.

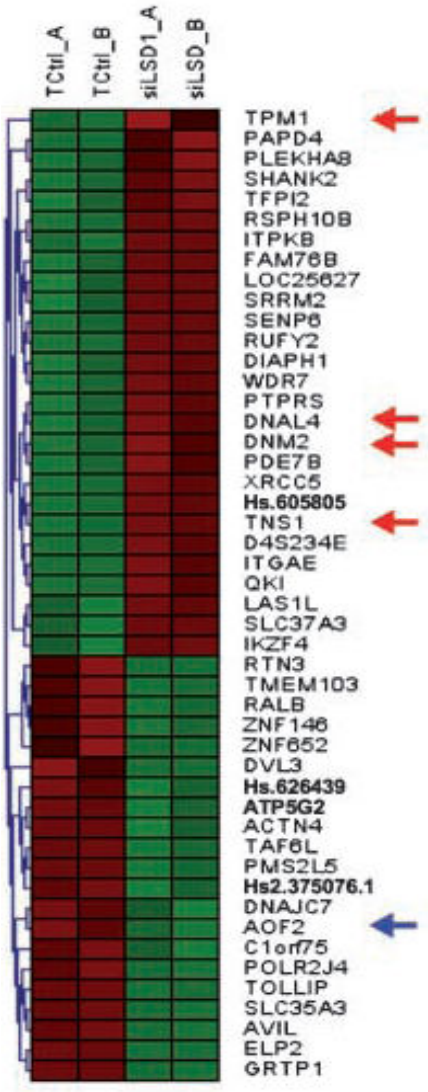

Figure 3.4. Microarray analysis of SH-SY5Y cells treated with siRNA directed against LSD1 or with scrambled control siRNA revealed an induction of genes involved in differentiation and neurite dynamics (red arrow). siRNA-mediated knockdown of LSD1/AOF2 resulted in reduction of LSD1 mRNA as expected (blue arrow).

To confirm the expression change detected via microarray analysis, TaqMan quantitative RT-PCR was performed using LSD1/AOF2, TNS1, TPM1, DNM2 and DNAL4 primers (Figure 3.5). Upon knock-down of LSD1, the LSD1 mRNA level decreased, while the identified 4 genes increased about 1.5-fold as shown in the microarray analysis.

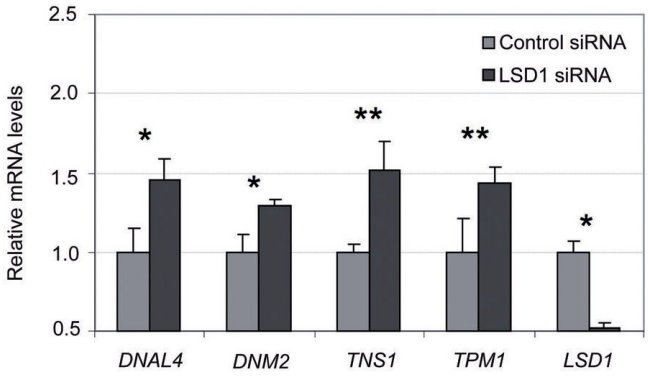

Table. Fold change in relative mRNA expression

	DNAL4	± SD	DNM2	± SD	TNS1	± SD	TPM1	± SD	LSD1	± SD
Control siRNA	1.000	0.145	1.000	0.109	1.000	0.050	1.000	0.207	1.000	0.070
LSD1 siRNA	1.451	0.133	1.294	0.037	1.515	0.186	1.431	0.106	0.522	0.024

* P < 0.1
** P < 0.5

Figure 3.5. TaqMan quantitative RT-PCR confirmed the expression changes detected via microarray analysis for LSD1, DNAL4, DNM2, TNS1 and TPM1. ** $p < 0.1$,** $p < 0.5$*

3.2.4. Knock-down of LSD1 upregulates putative tumor suppressor genes and alters gene specific H3K4 methylation

To determine whether LSD1 knock down influences the gene-specific methylation status regulating directly gene expression, *TFPI2* and *XRCC5* genes were chosen which were also induced upon knock-down of LSD1. The *TFPI2* gene encodes the protein, tissue factor pathway inhibitor 2 which is a putative tumor suppressor gene. Epigenetic silencing of TFPI2 was observed in hepatocellular carcinoma, malignant melanoma and invasive breast cancer cells (Wong *et al.,* 2007;, Nobeyama *et al.,* 2007), while ectopic expression of TFPI2 suppresses the proliferation and invasiveness of hepatocellular

carcinoma cells, suggesting its role in inhibition of the growth of neoplasm (Wojtukiewicz *et al*., 2003). *XRCC5* encodes the Ku80 protein which functions in nonhomologous DNA end joining and is involved in the double-strand break repair pathway by interacting with BRCA1 (Wei *et al.,* 2008). Epigenetic inactivation of XRCC5 in cancers such as non-small cell lung cancer was also reported (Lee *et al*., 2007).

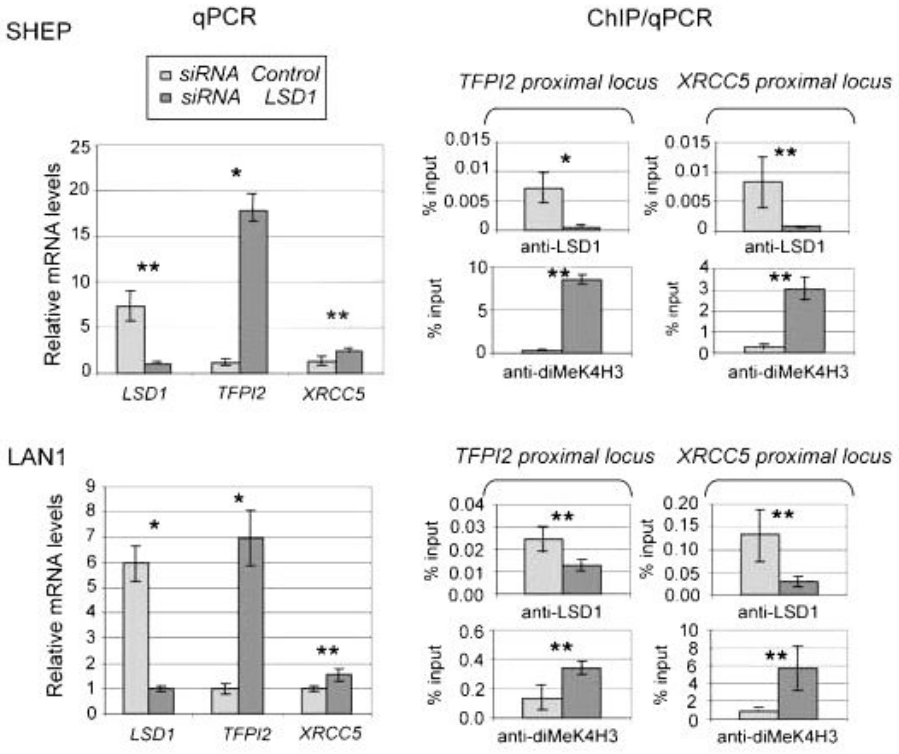

Figure 3.6. SHEP and LAN1 cells were transfected with LSD1-directed siRNA. ChIP (left) was performed with the indicated antibodies. The precipitated DNA was amplified by PCR using primers flanking the TFPI2 proximal locus or XRCC5 proximal locus. siRNA mediated knockdown of LSD1 was verified by quantitative PCR analysis (right).

For this study, SHEP and LAN1 cells were treated with siRNA directed against LSD1 or with a scrambled control siRNA and were subjected to TaqMan quantitative RT-PCR to confirm the induction of *TFPI2* and *XRCC5* as observed in the microarray. In both cell lines, *TFPI2* was 17-fold and *XRCC5* was 1.5-2 fold induced upon knock down of LSD1. To assess whether *TFPI2* and *XRCC5* are direct targets of LSD1, cells were subjected to chromatin immunoprecipitaiton (ChIP) using α-LSD1 and α-diMeK4H3 antibodies.

ChIP analysis revealed that LSD1 is present at the -300 proximal promoter regions of the *TFPI2* and *XRCC5* (Figure 3.6, right panel). Silencing of LSD1 decreased the occupancy of LSD1 on the proximal promoter regions. This was accompanied by significant increase in di-methylation on H3K4 which is consistent with up-regulation of *TFPI2* and *XRCC5*. These findings suggest that LSD1 regulates directly the transcription of *TFPI2* and *XRCC5* through demethylation of H3K4. Furthermore, knock down of LSD1 can reactivate the tumor suppressor gene *TFPI2* and the DNA repair gene *XRCC5* which are often epigenetically silenced in malignant tumors.

3.2.5. LSD1 inhibition using MAOIs impairs neuroblastoma growth *in vitro*

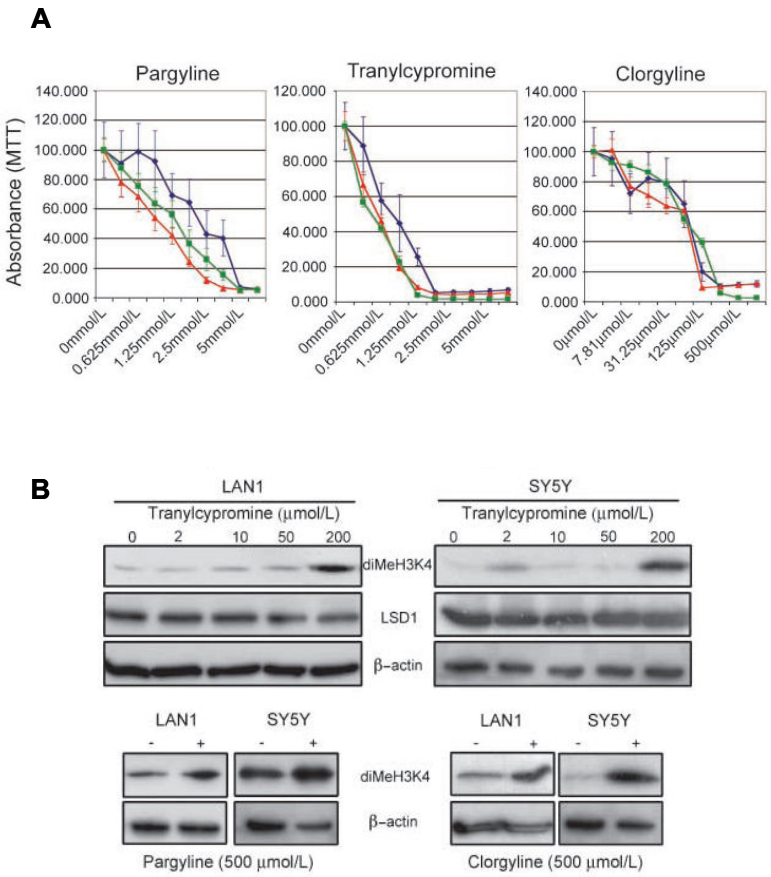

Figure 3.7. (**A)** Treatment of SHEP (red), SH-SY5Y (green), or LAN-1 (blue) neuroblastoma cells with pargyline, tranylcypromine, or clorgyline resulted in extensive reduction of cell numbers and MTT uptake. (**B)** Western blot analysis confirmed an accumulation of H3K4 dimethylation upon treatment with MAOIs. In contrast, LSD1 protein levels were not affected. β-actin served as the loading control.

We also analyzed the effect of LSD1 inhibition on cell viability and methylation levels. The catalytic domain of LSD1 has a high sequence homology to monoaminoxidase (MAO), and they share a common demethylating mechanism. Importantly, MAO inhibitors (MAOI) were shown to inhibit LSD1 activity (Lee *et al*., 2006). Treatment of neuroblastoma cell lines with the reversible MAOI, pargyline and clorgyline, or with the irreversible MAOI, tranylcypromine, impaired growth of neuroblastoma cells in a dose-dependent manner (Figure 3.7A). Reduced viability was accompanied by the increase of global di-methylation of lysine 4 in histone 3 (diMeH3K4) (Figure 3.8B).

3.2.6. Small molecule inhibitor of LSD1 inhibits xenograft tumor growth

A xenograft mouse model was used to assess the potential therapeutic value of small molecule inhibitors targeting LSD1 against neuroblastic tumors *in vivo*. 24 nude mice (nu/nu) were subcutaneously injected with $2.0x10^7$ of SH-SY5Y neuroblastoma cells in the flank. Tranylcypromine treatment by intraperitoneal injection of 2 mg tranylcypromine once daily was started at the time of xenograft injection, and sodium chloride was injected into control animals. During treatment, one mouse died of peritonitis and six mice died from tranylcypromine-induced seizures. 17 surviving mice were sacrificed 21 days after the injection of tumor cells. Xenograft tumors in the mice treated with tranylcypromine were significantly smaller than the control. (T-test, p= 0.044, Figure 8A). Histological examination revealed that the tranylcypromine treatment resulted in a higher content of fibrosis and extensive necrosis in the xenograft (Figure 3.8B).

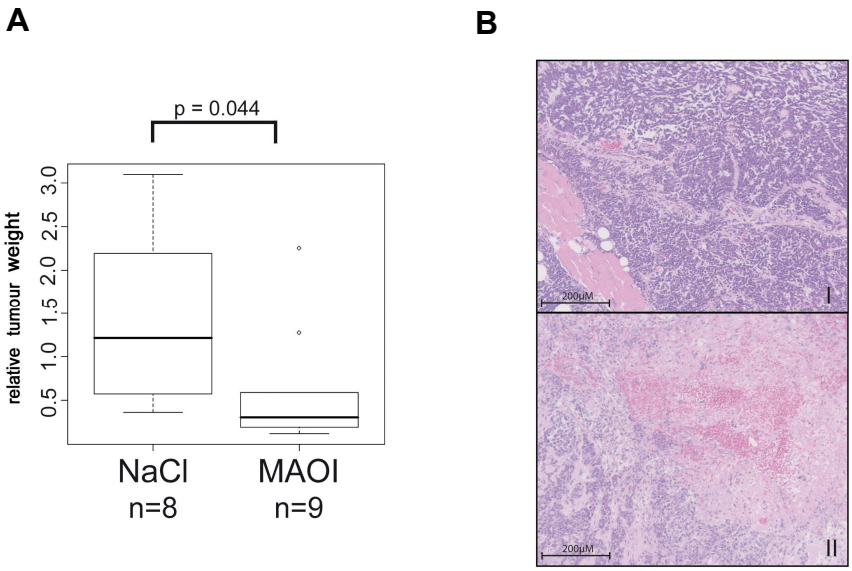

Figure 3.8. (**A)** Relative tumor weight of SH-SY5Y xenografts in nude mice treated with 2 mg tranylcypromine (MAOI) or control (NaCl). Mice were sacrificed, and the tumors were weighed 21 d after s.c. tumor cell inoculation. Tumors in mice receiving tranylcypromine were significantly smaller than mice receiving saline only. (**B)** histologic appearance of tumors treated without MAOI (saline, I) or with 2 mg tranylcypromine (II) for 21 days. Sections were stained with H&E. Note the massive necrosis and hemorrhage of tumors in the MAOI-treated xenografts (II).

4. LSD1 in breast cancer

4.1. Breast cancer

In the industrialized countries of the Western world breast cancer is the most common tumor in women, and along with lung cancer the most important cause of cancer-associated morbidity and mortality.
Breast cancer is a heterogeneous disease that has distinct histopathological features, genetic and genomic variability and diverse prognostic outcomes. In premalignant stages, atypical ductal hyperplasia (ADH) arises in the breast terminal ductal lobular unit (TDLU) and develops to ductal carcinoma in situ (DCIS). DCIS may enter malignant stages and give rise to invasive breast cancer (IBC). Once cells have invaded, the risk for developing metastasis significantly increases. During this multistage process, control of proliferation, survival, differentiation and migration become deregulated. The complexity and heterogeneity of breast cancer make it harder to identify novel therapies and to improve existing therapies for the treatment and prevention of this disease (Vargo-Gogola *et al.,* 2007).

Currently, breast cancer patients are managed based on a constellation of clinical and histopathological parameters in conjunction with assessment of hormone receptor (estrogen (ER) and progesterone receptor (PR)) status and Her2 (human epithelial receptor 2, also known as HER-2/neu or erB-2) expression and gene amplification.
ER expression is observed in 40-70 % of breast cancers which has a more favourable prognosis than ER-negative breast cancers (Corinne *et al.,* 2007). With ER positive breast cancer, homone-blocking medications, such as tamoxifen, slow the cancer's growth.
About 20 % of invasive breast cancer belong to the Her2-positive group which can spread aggressively and has a poor prognostic outcome. Trastuzumab (Herceptin) is a monoclonal antibody targeted to the Her2 protein that can be used for this type of breast cancer. However, response rate of 35 % to the Her2-targeted drugs seems to be a limiting factor for the treatment of the Her2-postive breast cancer (Osborne *et al.,* 2004).
Breast cancers that are Her2-negative and also lack receptors for estrogen and progesterone are referred to as "triple negative" and comprise approximately 20 % of all

invasive breast cancers. This form of the disease is highly aggressive with the worst prognostic outcome. Aggressive chemotherapy is the only modality of systemic therapy for the triple negative subtype. Therefore, the identification of novel drug targets and development of new therapeutic options are urgently needed for the treatment of ER-negative breast cancers with resistance to the Her2 blockers or hormone therapy.

Considering the recent evidence that LSD1 critically controls hormone-dependent gene expression, cellular growth and malignant progression of prostate cancers, we investigated for the first time the role of LSD1 in breast cancer.

4.2. Results

4.2.1. Development of LSD1 ELISA

To analyze the LSD1 expression level in breast tumor, both fresh-frozen and formalin-fixed, paraffin-embedded tissue specimens of ductal and lobular breast cancer were used for this study. Initial immunohistochemical staining of paraffin-embedded tissue specimens revealed moderate nuclear expression in luminal cells of normal breast glands and ER-positive cancers (histological grade 2). Significantly more intense staining was observed in ER-negative breast cancers (histological grade 3), in which every tumor cell showed a strong and specific nuclear staining pattern (Figure 4.1).

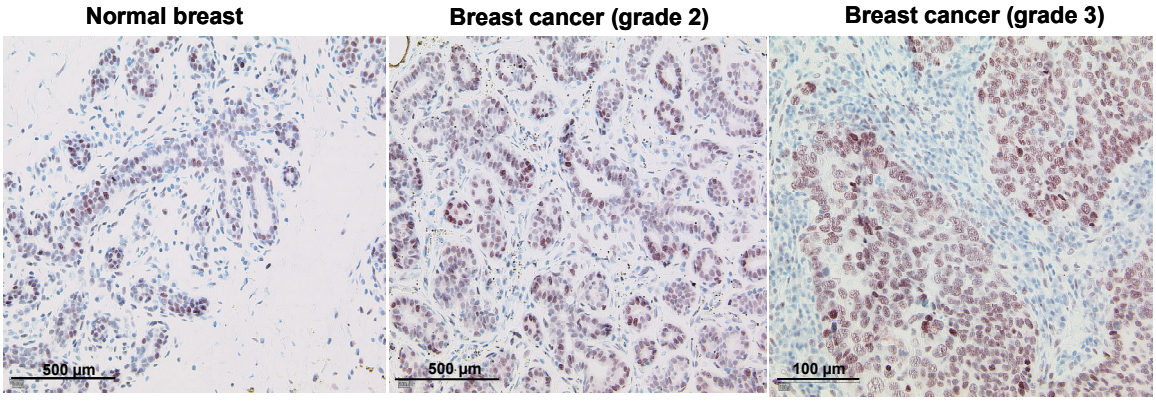

Figure 4.1. Overexpression of LSD1 in breast tumor. Immunohistochemical staining of LSD1 was shown in normal breast tissue and breast cancer (histologic grade G2 and G3).

I aimed to measure LSD1 expression levels in breast tumors using an LSD1 ELISA assay. Since no commercial ELISA for LSD1 was available, LSD1 ELISA was developed (Figure 4.2). 96-well Maxisorb microplates were incubated with tissue protein lysates (40 µg) in coating buffer (50 mM sodium carbonate buffer, pH 9.2) overnight at 4 °C. After removal of the coating solution, the wells were blocked with 200 µl blocking buffer (Roche) for 1 h at room temperature. After rinsing with washing buffer, the wells were incubated with α-LSD1 antibody in 100 µl blocking buffer for 1 h at 25 °C followed by three washing steps with 200 µl PBS-T. After addition of 100 µl HRP-labelled α-mouse, the wells were incubated for 0.5 h and washed three times. Finally, 100 µl of the TMB

substrate solution were added to each well. The conversion of substrate was stopped by addition of 100 µl of 2 N sulphuric acid solution. The optical density was determined in an ELISA reader at 450 nm. The N-terminal his_6-tagged LSD1 ΔN (166-852) protein

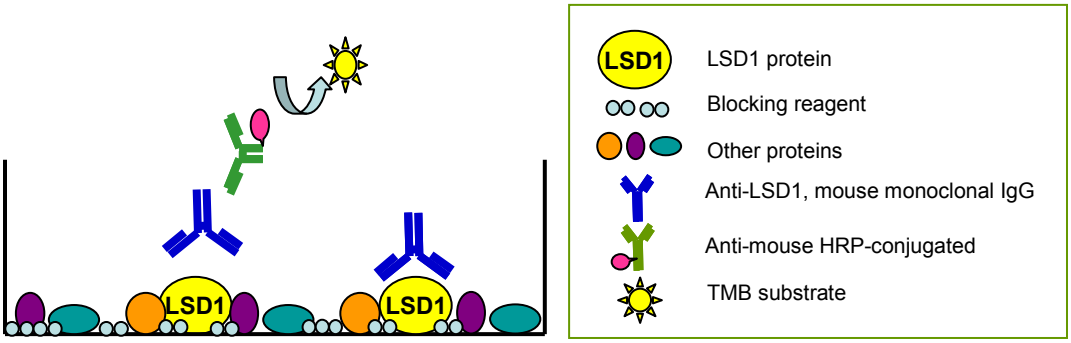

Figure 4.2. Development of LSD1 ELISA. Maxi-sorb microplates were incubated with a series of dilution of recombinant his_6-tagged LSD1 ΔN (166-852) protein (1.0, 3.1, 9.3, 27.8, 83.3 and 250.0 µg/L) and breast tumor tissue protein lysate (3, 10, 30 and 60 µg/well) in coating buffer (50 mM sodium carbonate buffer, pH 9.2) overnight at 4 °C. Antibody dilution ratio was modified for the recombinant LSD1. (α-LSD1, 1:4000; HRP-labelled α–mouse, 1:1000). Otherwise, all steps were performed as described above.

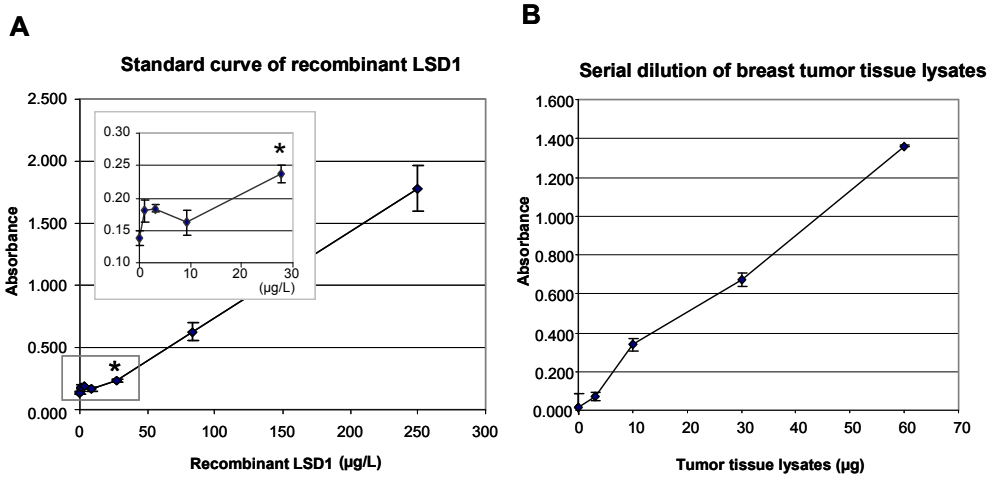

Figure 4.3. (A) Dose-response curve of LSD1 ELISA. A serial dilution of the purified his_6-tagged LSD1 ΔN (166-852) ranging from 1 to 250 µg/L was used as a calibrator in the LSD1 ELISA to generate the dose-response curve. Linear range was 27.8 -250.0 µg/L and the linear correlation coefficient (R^2) was 0.99. The detection limit was estimated as the minimum analyte concentration evoking a response significantly different from that of the zero calibrator. The detection limit of the assay was 27.8 µg/L ($P < 0.01$). **(B) Linearity of dilution curves for breast tumor lysates.** A series dilution of breast tumor tissue protein lysates was used in the linearity study. In the range of 3 – 60 µg protein lysates, the dilution curve was close to linear (R^2=0.99).

The assay was validated by recombinant LSD1 protein and performed in a quantitative manner over a broad spectrum of LSD1 protein concentrations between 1 to 250 µg/L and also after serial dilution of protein lysates from breast cancer tissue specimens (Figure 4.3). Linear range of recombinant LSD1 protein was 27.8 – 250.0 µg/L, while tumor tissue protein lysate showed linearity in the range of 3 - 60 µg. For the following ELISA assay, 40 µg protein lysates was used pro well.

4.2.2. LSD1 is strongly expressed in ER-negative breast cancer

The established ELISA was used to analyze several breast cancer specimens.

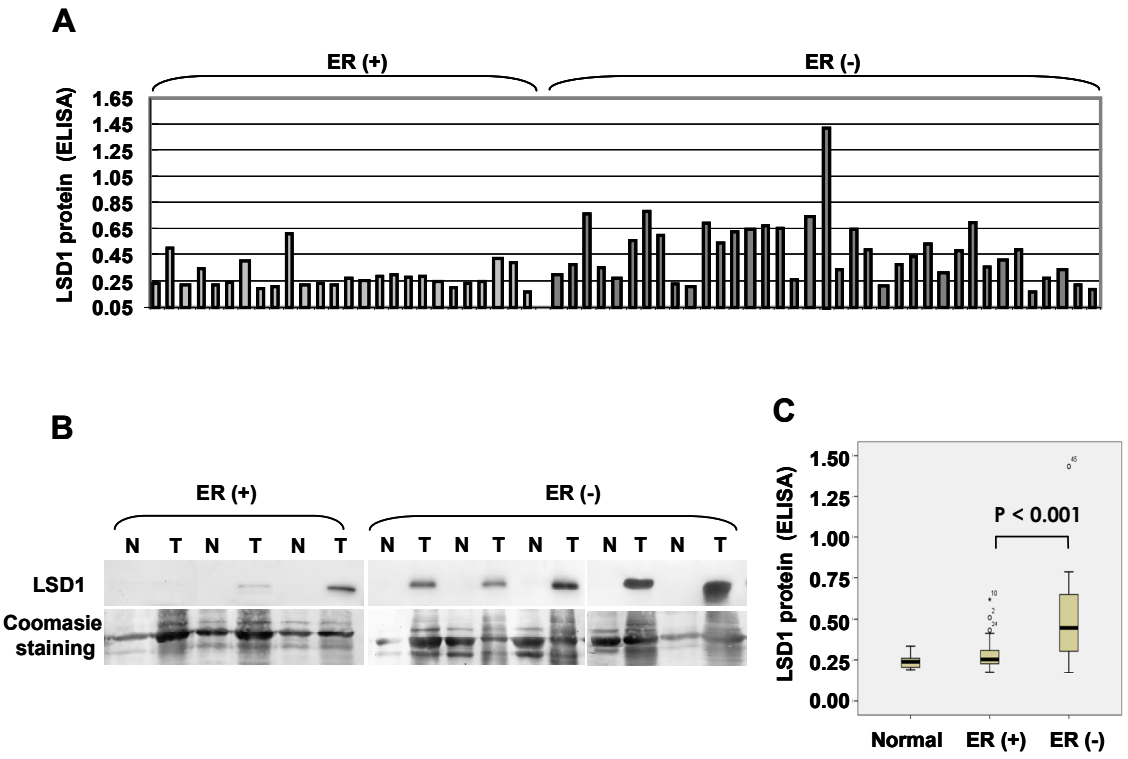

Figure 4.4. Overexpression of LSD1 in ER-negative breast tumor. (**A**) LSD1 expression level in 26 ER positive and 37 ER negative breast tumor was analyzed with ELISA for LSD1. ER (+), ER-positive; ER (-), ER-negative. (**B**) LSD1 expression in normal and tumor tissue extracts was determined by western blot. Coomasie staining was used as the loading control. N, normal breast tissue; T, breast tumor tissue. (**C**) Statistcal significance test of ELISA was done by two-sided, non-parametrical Mann-Whitney U-test to analyze differences in expression levels among normal, ER-positive and ER-negative groups. LSD1 expression was significantly higher in ER-negative breast tumor than in ER-positive tumor or normal tissue ($P < 0.001$).

In protein lysates of snap-frozen primary breast tissues including 20 normal breast tissues, 26 ER-positive and 37 ER-negative breast tumors, LSD1 protein was significantly stronger expressed in ER-negative breast cancers than in ER-positive cancers or normal tissue (Mann-Whitney-U-test, $P < 0.001$, Figure 4.4A and 4.4C). There was a trend of slightly higher expression comparing ER-positive breast cancer and normal breast tissue, but this did not reach statistical significance. Similar results were seen in a small set of breast cancer specimens analyzed by Western blot analysis. LSD1 was stronger expressed in ER-negative breast tumors compared to normal breast tissues and ER positive tumors (Figure 4.4B).

Table 4.1. Correlation between histopathological data and LSD1 expression in tumor specimens from 38 breast cancer patients

	LSD1 low[a], n (%) (*n* = 16)	LSD1 high[a], n (%) (*n* = 22)	*P* [b]
Size			
pT1	7 (44)	11 (50)	0.752
PT2-4	9 (56)	11 (50)	
Nodal status			
Neg	12 (75)	14 (64)	0.504
Pos	4 (25)	8 (36)	
ER status[c]			
Neg	3 (19)	20 (91)	**< 0.001**
Pos	13 (81)	2 (9)	
PR status[d]			
Low	7 (44)	21 (95)	**0.001**
High	9 (56)	1 (5)	
Her2/erbB2[e]			
Low	14 (88)	16 (73)	0.426
High	2 (12)	6 (27)	

[a]LSD1 low, 0 ≤ score ≤ 9; LSD1 high, 9 < score ≤ 12
[b]Fisher`s exact test (two sided).
[c]ER neg, score = 0; ER pos, score =12
[d]PR low, 0 ≤ score ≤ 6; high, 6 < score ≤ 12;
PR, progesterone receptor
[e]Her2/erbB2, low, score 0 or 1; high, score 2 or 3

Significant inverse correlation between LSD1 expression and ER status was also seen in detailed immunohistochemical analysis. To statistically calculate the association between histopathological parameters and LSD1 expression levels (Table 4.1), tumor specimens were classified into a group with low LSD1 expression (n=16) and a second group with high LSD1 expression (n=22). Results in table 4.1 clearly indicated that strong nuclear LSD1 staining (score > 9) was associated with negative ER status (score = 0) (Fisher´s exact test, $P < 0.001$, Table 4.1). Consistently high LSD1 expression also correlated with low PR expression (score ≤ 6) ($P = 0.001$). Neither tumor size and nodal status nor Her2/erbB2 status showed any correlation with LSD1 expression.
Considering that hormone receptor expression in breast cancer is associated with a significantly better prognosis (Cui *et al*., 2005), high LSD1 expression appears to provide a biomarker for aggressive tumor biology associated with hormone receptor-negative breast cancer.

4.2.3. LSD1 inhibition using MAOIs confers growth inhibition and increase of global H3K4 methylation in vitro

The catalytic domains of LSD1 and monoaminoxidases (MAOs) share structural homology and make use of the same catalytic mechanism (Lee *et al*., 2006). Therefore, we used the MAO inhibitors tranylcypromine and clorgyline to inhibit LSD1 in breast cancer cell lines *in vitro*. Four different breast cancer cell lines, all of which strongly expressed LSD1 (Figure 4.5B) were tested. Treatment with tranylcypromine and clorgyline for 72 hours impaired cell growth in a dose-dependent manner (Figure 4.5A) in all four cell lines. In contrast to our clinical data *in vivo*, LSD1 expression levels or sensitivity to MAOIs did not differ between ER-positive and ER-negative cell lines *in vitro*. To address whether reduced cell viability after treatment with MAOIs correlates with LSD1 inhibition, we analyzed the methylation status of lysine 4 in histone 3 in cells before and after treatment. Upon treatment of MAOIs, global di-methylation of lysine 4 in histone H3 increased, while LSD1 enzyme levels were not altered (Figure 4.5B).

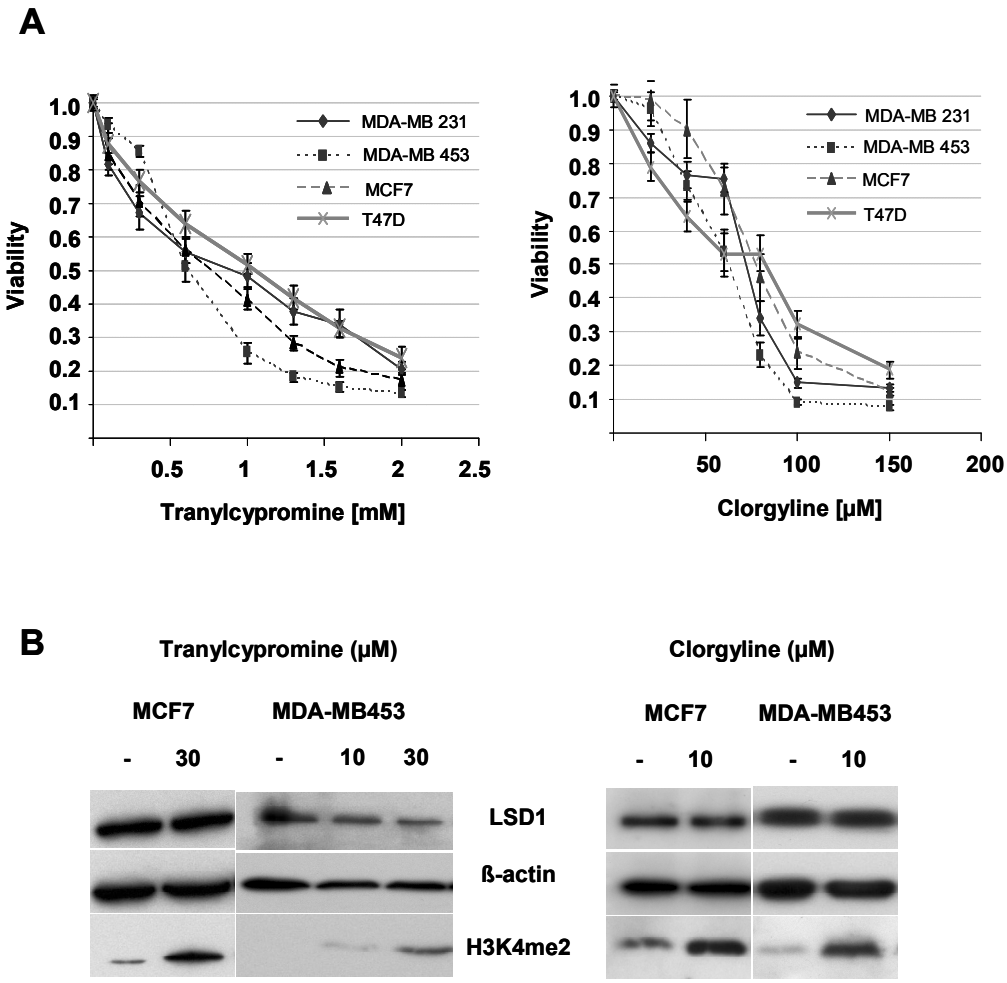

Figure 4.5. Reduction in cell growth and increase of global H3K4 methylation upon MAOIs treatment. (**A**) Four different breast cancer cells were treated with Tranylcypromine and Clorgyline for 72 h for MTT assay. MAOIs treatment resulted in extensive reduction of cell numbers. (**B**) Western blot analysis confirmed an accumulation of H3K4 di-methylation upon treatment with tranylcypromine and clorgyline for 24 h. LSD1 protein levels were not affected. β-actin served as the loading control.

4.2.4. siRNA-mediated knock down of LSD1 reduces cellular growth

To analyze the consequences of reduced LSD1 expression, MDA-MB 453 and MDA-MB 231 cells were transiently transfected with 15 nM siRNA directed against LSD1 or with 15 nM scrambled control siRNA. Significant LSD1 knock-down was detected by measuring protein levels 3 days after transfection by Western blot (Figure 4.6B). MTT assays indicated that the silencing of LSD1 caused a significant decrease in cell growth and viability (Figure 4.6A). Similar effects were also seen in MCF7 and T47D cells. Morphologically no sign of apoptosis was detected, but the LSD1 inhibition appeared to affect the number of dividing cells consistent with a previous report that knock-down of LSD1 leads to G2/M cell cycle arrest (Scoumanne *et al*., 2007).

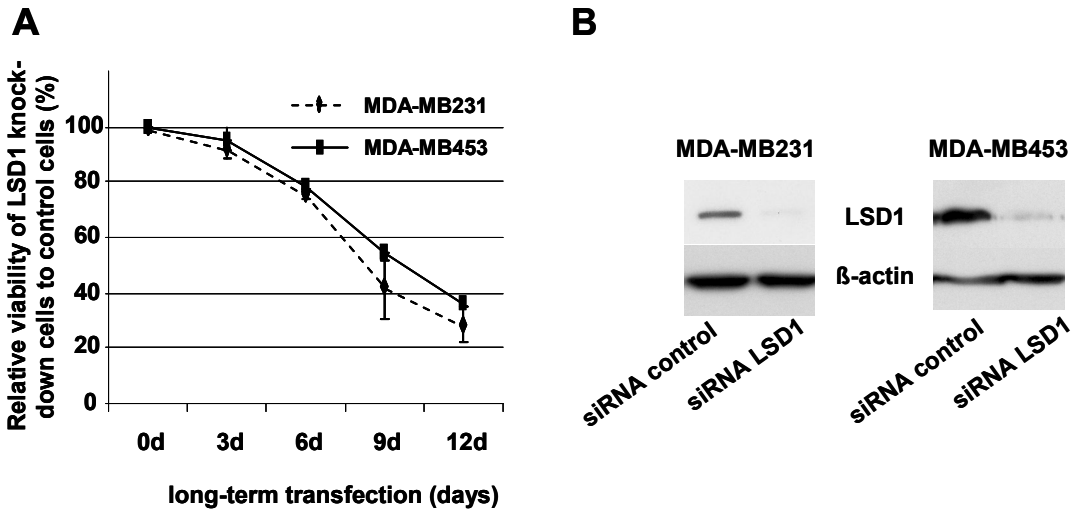

Figure 4.6. Decreased cellular growth upon siRNA mediated knock down of LSD1. (**A**) A significant reduction in cell number was observed in MTT assay upon knock-down of LSD1. MDA-MB 231 and MDA-MB 453 cells were treated with siRNA against LSD1 for 12 days. (**B**) Knock-down of LSD1 protein levels was determined 6 days after transfection by western blot. β-actin served as the loading control.

4.2.5. Knock-down of LSD1 induces downregulation of proliferation associated genes and alters target gene-specific H3K9 methylation

Considering that LSD1 regulates gene-expression through modification of histone methlyation in gene promoter regions and previous evidence that silencing of LSD1 decreased cellular proliferation, we further analyzed expression of proliferation related genes by quantitative RT-PCR (qRT-PCR). As illustrated in figure 4.7A *CCNA2* and *ERBB2* were downregulated after LSD1 knock-down both in ER-positive MCF7 or ER-negative MDA-MB 231 and MDA-MB 453 cells (66 - 83% decrease in *ERBB2* mRNA level; 40 – 65 % decrease in *CCNA2* mRNA level). Down-regulation of the Her2/erbB2 protein level was confirmed 6 days after knock-down of LSD1 in MDA-MB 231 cells (Figure 4.7B). However, in MDA-MB 453 and MCF7 cells, Her2/erbB2 protein was highly expressed and we could not detect any significant change in Her2/erbB2 protein level upon knock-down of LSD1. Possibly the transient changes in RNA levels by the transfected siRNA were not robust enough in these cell lines to cause significant and persistent changes in protein levels.

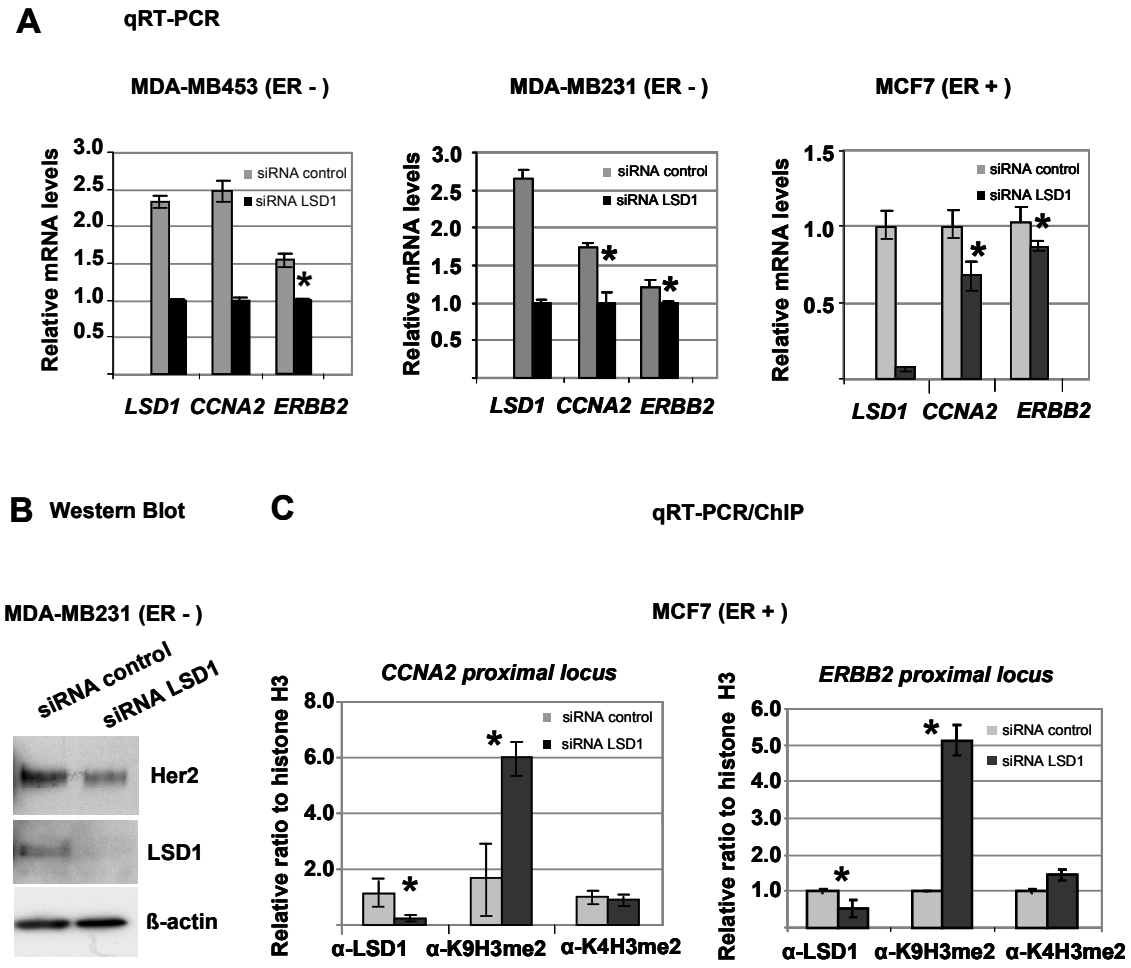

Figure 4.7. Down-regulation of *CCNA2* and *ERBB2* mRNA expression and enrichment of H3K9 di-methylation in the promoter region upon knock down of LSD1. (**A**) Quantitative PCR analysis was done in 3 different breast cancer cells treated with siRNA directed against LSD1 or with scrambled control siRNA. *CCNA2* and *ERBB2* mRNA expressions were down-regulated 3 days after knock-down of LSD1. 18S rRNA was used as the endogenous reference gene. (**B**) Reduction in Her2/erbB2 protein expression 6 days after knock down of LSD1 was determined by western blotting. (**C**) Enrichment of H3K9 di-methylation in the proximal promoter region of *CCNA2* or *ERBB2* was observed upon knock down LSD1 using ChIP assay. The sonificated chromatin of MCF7 cells was immunoprecipitated with α-LSD1, α-K9H3me2 and α-K4H3me2. The precipitated DNA was amplified by PCR using primers flanking the *CCNA2* proximal locus or *ERBB2* proximal locus. **P* < 0.05.

To asses whether the promoters of *CCNA2* and *ERBB2* are direct or rather indirect targets of histone modification by LSD1, MCF7 cells treated with siRNA directed against LSD1 or with a scrambled control siRNA were subjected to chromatin immunoprecipitation (ChIP) using α-LSD1, α-K9H3me2 and α-K4H3me2 antibodies. ChIP analysis indeed confirmed that LSD1 is present at the proximal promoter of the *CCNA2* and *ERBB2* gene. Knock down of LSD1 decreased the occupancy of LSD1 on *CCNA2* (from -137 to -30) and *ERBB2* (from -309 to -220) promoter regions (Figure 4.7C). This was accompanied by significant increase in dimethylation on H3K9 which has been previously shown to result in transcriptional repression. In contrast, after LSD1 knock-down, genomic DNA corresponding *CCNA2* and *ERBB2* proximal locus were not enriched with α-H3K4me2 antibody. This finding is consistent with results observed above for down-regulation of *ERBB2* and *CCNA2* upon knock down of LSD1, suggesting that LSD1 regulate directly the transcription of *CCNA2* and *ERBB2* through demethylation of H3K9, but not by demethylation of H3K4.

5. LSD1 enzyme assay for high-throughput screening (HTS)

5.1. Epi-drugs, a new class of cancer therapeutics

In the last years, the pharmacoepigenomic field has highly improved and epi-drugs are introduced as a new class of cancer therapeutics. The HDAC inhibitor suberoylanilidehydroxamic acid (SAHA) has recently been approved for the treatment of advanced T cell lymphoma, while other HDAC inhibitors and DNMT inhibitors are in clinical trials (Kuendgen *et al.,* 2008, Spannhoff *et al.,* 2009). Compared to that field of epigenetics, the knowledge on histone methylation and the consequences of its inhibition is still behind. Also the search for inhibitors is still in the beginning, and to date, no specific chemical modulators of endogenous LSD1 have been identified, although histone methylation has been shown to be important in epigenetic regulation of gene expression through the establishment of stable gene-expression patterns. MAOIs which are the first available small molecular inhibitors of LSD1 were shown to be inadequate for the tumor treatment due to their excessive side effects such as seizures caused by their modulation of neurotransmitter deamination. In this study, I wanted to establish a LSD1 enzyme assay for high-throughput screening to identify lead compounds for specific LSD1 inhibitors.

5.2. Results

5.2.1. Cloning and expression of recombinant human LSD1

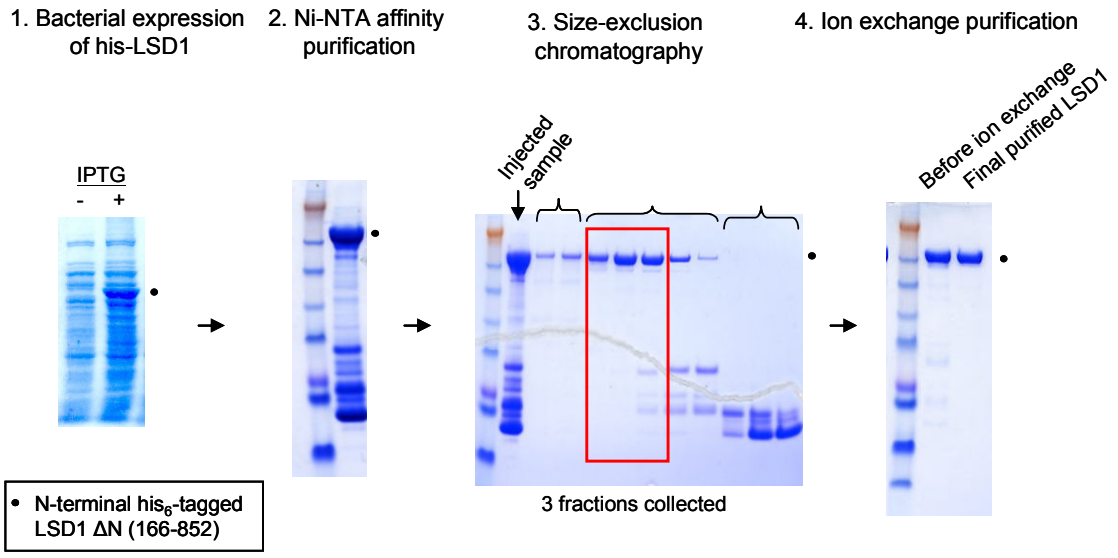

Figure 5.1. Induction and purification of N-terminal his$_6$-tagged LSD1 ΔN (166-852) (1) The fusion protein was expressed in *E. coli* BL21 (DE3) Star overnight at 20°C in the presence of 0.75 – 1 mM IPTG. (2) The lysate was applied to Ni^{2+} affinity column and his-tagged LSD1 was eluted with the elution buffer (100 mM Tris-HCl pH 8.0, 300 mM Imidazole). (3) The protein was concentrated and then purified on a Superdex 200 (16/60) size-exclusion column in 20 mM Tris-HCl pH 8.0, 100 mM NaCl. (4) Three fractions were passed through HitrapQ ion exchange column (50 mM Tris pH 8.0). Finally, purified LSD1 was stored in 20 mM Tris-HCl pH 8.0, 100 mM NaCl, 5 % Glycerol, 2 mM DTT.

The purification of LSD1 was done in collaboration with Dr. Young-Jun Im (NIH, U.S.A).

To establish an *in vitro* enzyme assay for LSD1, we purified the recombinant human LSD1 from *E. coli*. Firstly, the gene encoding the LSD1 construct (166–852 amino acids) was subcloned to pET15b expression vector providing an N-terminal his$_6$-tag for affinity purification. The LSD1 expression construct lacks the first 165 amino acids but it contains the SWIRM and aminoxidase domains. This construct has previously been shown to be active toward peptide substrate *in vitro* (Forneris *et al.,* 2005). The N-terminal his$_6$-tagged LSD1 ΔN (166-852) protein was expressed in *E. coli* BL21 (DE3) star by adding 0.75 mM IPTG. The lysate was applied to Ni^{2+}affinity column and the his$_6$-tagged LSD1 was eluted with the buffer (100 mM Tris HCl pH 8.0, 300 mM imidazole). The protein was concentrated to 4 ml and then purified by size exclusion chromatography using a Superdex 200 (16/60) column. The fractions containing

recombinant LSD1 were passed through a HighTrapQ ion exchange column equilibrated with the buffer (100 mM TrisHCl pH 8.0), which resulted in the final LSD1 sample with purity higher than 95% estimated by SDS-PAGE (Figure 5.1). The purified LSD1 was stored in the buffer (20 mM Tris HCl pH 8.0, 100 mM NaCl, 5% glycerol, 2 mM DTT).

5.2.2. Establishment of LSD1-HRP coupled assay for high-throughput screening

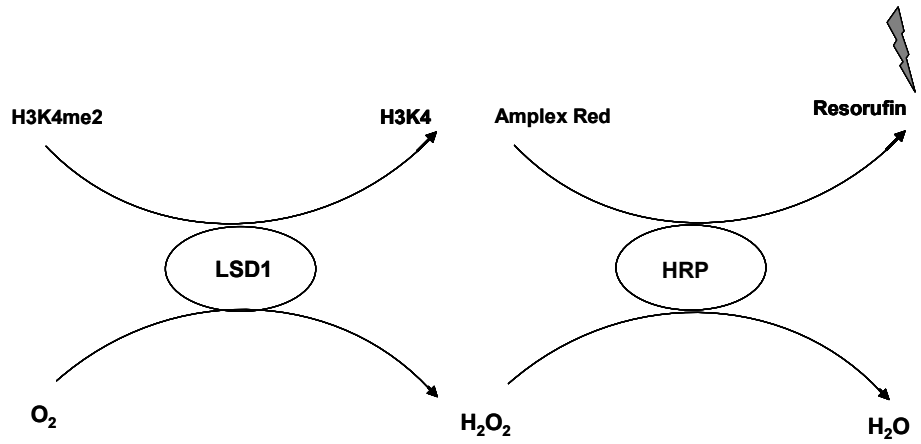

Figure 5.2. LSD1-HRP coupled assay. Recombinant his_6-tagged LSD1 (166-852aa; 0.25 μM) catalyzes the demethylation reaction of dimethylated histone H3 peptide comprising N-terminal 24 amino acids (H3K4me2; 35 μM) to H3K4 producing H_2O_2 as a byproduct. Then, horseradish peroxidase (HRP; 0.4 μM) uses Amplex Red (100 μM) as an electron donor during the reduction of hydrogen peroxide to water. The resultant product, resorufin, is a highly fluorescent compound (excitation 544, emission 590 nm). The reaction was performed in buffer (50 mM HEPES pH 7.5, 0.1% Triton-X100) at 37 °C. Concentrations represent the end-concentration of the reagents.

Recombinant LSD1 (0.25 μM) was incubated with a peptide substrate (10–100 μM) representing the N-terminal tail of histone H3 dimethylated at Lys4 (ART[dimethylK]QTARKSTGGKAPRKQLAGGK-biotin [from N- to C- terminal]). Subsequent hydrogen peroxide formation was detected using horseradish peroxidase (HRP; 0.4 μM) coupled to fluorogenic electron donor dye Amplex Red (100 μM). The resultant product resorufin is a highly fluorescent compound (excitation 544 nm, emission 590 nm) (Figure 5.2).

To analyze the sensitivity and the linear range of the assay, a standard curve using a series dilution of hydrogen peroxide was measured (Figure 5.3). In the absence of

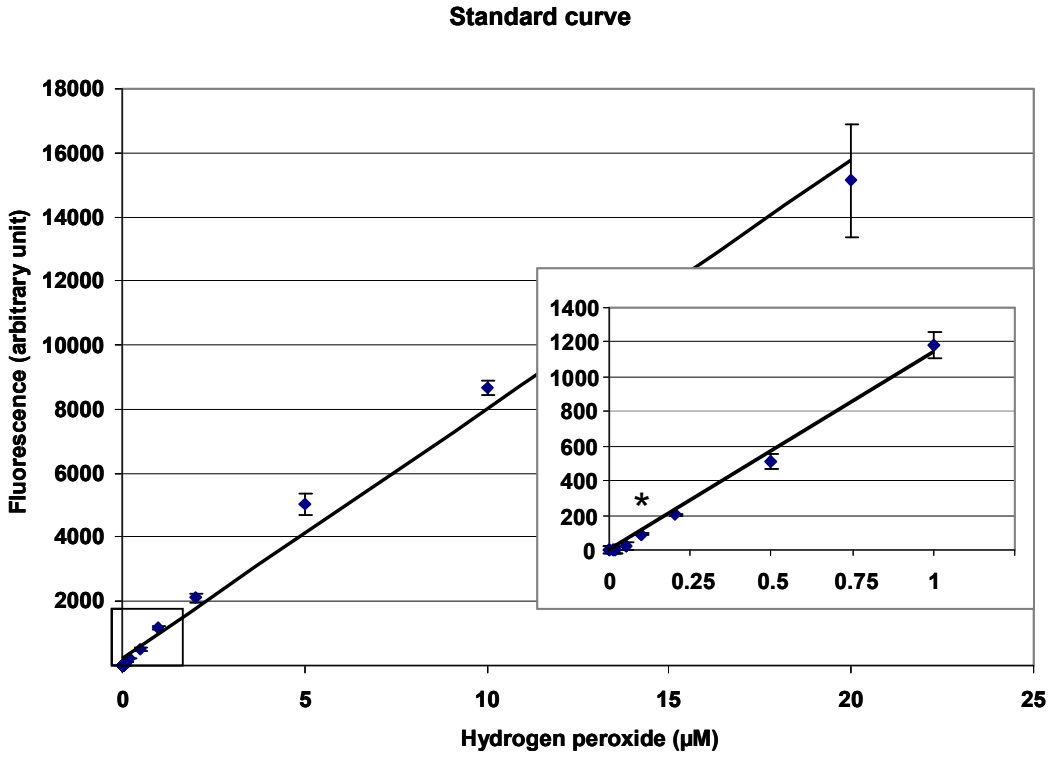

Figure 5.3. The standard curve using a serial dilution of hydrogen peroxide. Horseradish peroxidase (HRP) reduces hydrogen peroxide to water using Amplex red as an electron donor. The amount of the resulting product, resorufin (excitation 544 nm, emission 590 nm) is proportional to the hydrogen peroxide concentration. A serial dilution of hydrogen peroxide ranging from 0.01 to 20 µM was incubated with HRP (0.4 µM) and Amplex Red (100 µM) in 50 mM HEPES buffer, pH 7.5. The Linear range was 0.05 – 20 µM and the linear correlation coefficient (R^2) was 0.99. The detection limit was estimated as the minimum hydrogen peroxide concentration evoking a response significantly different from that of the zero hydrogen peroxide. The detection limit was 0.05 µM ($P < 0.01$, n=3). Fluorescence value was calculated by subtracting the background fluorescence from each value.

recombinant LSD1 and a peptide substrate, HRP reduces exogenous hydrogen peroxide to water using Amplex Red as an electron donor. The amount of the resulting product resorufin is proportional to the hydrogen peroxide concentration. A serial dilution of hydrogen peroxide ranging from 0.01 to 20 µM was incubated with HRP (0.4 µM) and Amplex Red (100 µM) in 50 mM HEPES buffer, pH 7.5. The linear range lies between 0.05–20 µM and the linear correlation coefficient (R^2) was 0.99. The detection limit was estimated as the minimum hydrogen peroxide concentration evoking a response significantly different from that of the zero hydrogen peroxide. The detection limit was 0.05 µM ($P < 0.01$, $n = 3$).

The approximate concentration of hydrogen peroxide produced by the LSD1 enzyme reaction was measured for ~ 1 h and supposed to be less than 5 μM compared the standard curve. LSD1-mediated peptide demethylation was very slow, while the HRP-mediated enzyme reaction occurred very fast, suggesting that the fluorescence development only depends on the LSD1-mediated hydrogen peroxide production.

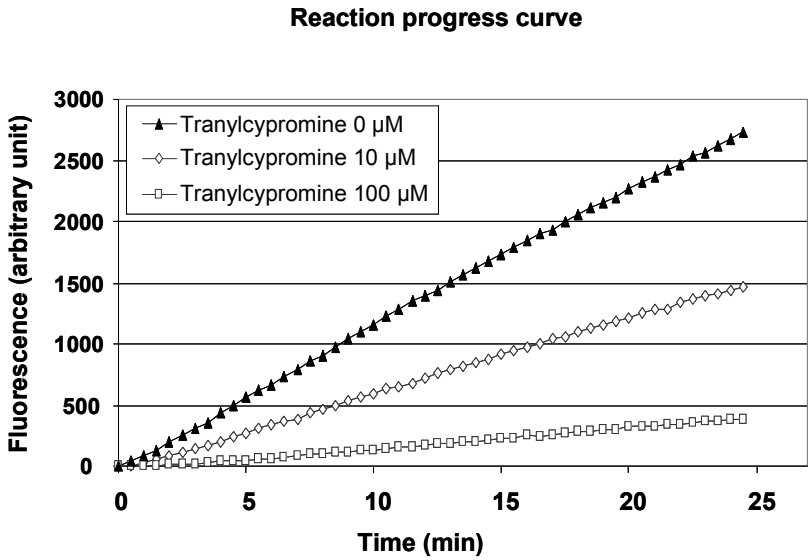

Figure 5.4. Time- and concentration-dependent inactiviation of LSD1 by tranylcypromine. A reaction progress curve was obtained by measuring resorufin over 25 min upon mixing 50 μM H3K4me2, 250 nM LSD1, 100 μM Amplex red and 0.4 μM HRP in the peroxide coupled assay system. The inactivation of LSD1 by 10 and 100 μM tranylcypromine was concluded from a decreased initial velocity (V_0) represented by decreased slope. Fluorescence value was calculated by subtracting the background fluorescence from each value.

To adapt the assay to higher throughput, 96 well microplates were used. An overall assay volume was adjusted to 40 μL which reduced the amount of reagents. In this 96 well plate format, a reaction progress curve was obtained to measure initial velocity (V_0). The inactivation of LSD1 by the addition of 10 or 100 μM tranylcypromine was observed with decreased V_0 (Figure 5.4).

Using the Michaelis-Menten plot, the Km value for the his_6-tagged LSD1 ΔN was determined as 35 ± 9 μM (Figure 5.5). Fornes et al. reported a Km of 9–50 μM for the same substrate (Fornes *et al.,* 2005; Schmidt *et al.,* 2007). Substrate concentration equal to this Km was used in further screening assays.

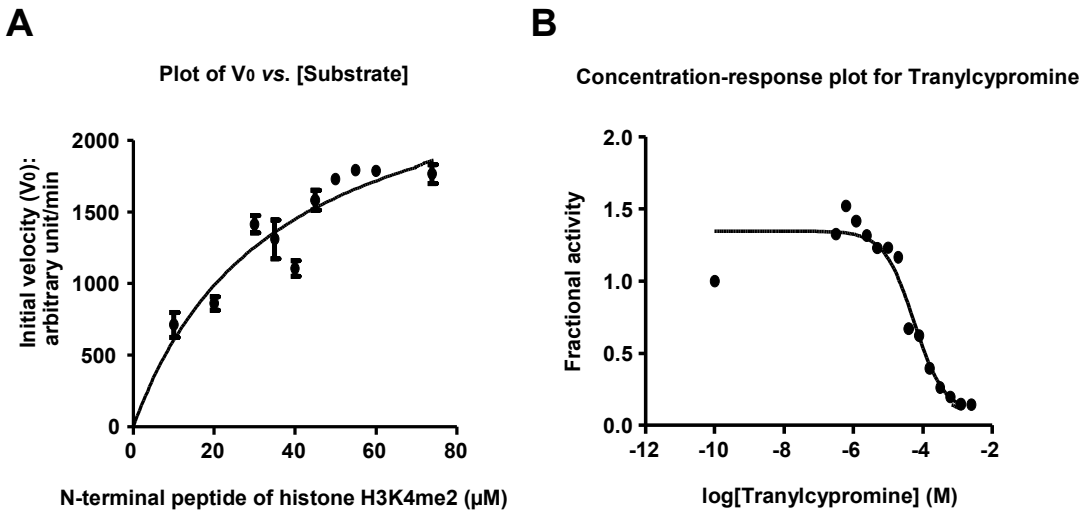

Figure 5.5. (A) Determination of Km value for recombinant LSD1. Km value for his_6-tagged recombinant LSD1 ΔN was measured as 35 ± 9 μM (95% confidence intervals (CI): 16.80 ~ 53.63 μM). (n = 3) **(B) Determination of IC50 for tranylcypromine** Tranylcypromine, a known LSD1 inhibitor was used as a reference compound in further screening assays. Inhibitory concentration yielding 50 % inhibition (IC50) for tranylcypromine was 57 μM (95% CI: 26–117 μM) Fractional activity (Y axis; V_0 [tranylcypromine X μM]/ V_0 [tranylcypromine 0 μM] is plotted as a function of inhibitor concentration (X axis).

The known LSD1 inhibitor tranylcypromine served as a reference compound in further experiments. In order to determine appropriate ranges of inhibitor concentrations to be used in screening assays, a dose-response experiment was performed with tranylcypromine (Figure 5.5). LSD1 had been preincubated with tranylcypromine for 5 min at RT and then the assay was initiated by the addition of peptide substrate. The inhibitory concentration yielding 50% decrease in initial velocity (IC_{50}) for tranylcypromine was 57 μM (95% confidence intervals: 26–117 μM). This value was higher than the IC_{50} value of 20 μM which had been reported (Schmidt *et al.,* 2007). Since tranylcypromine is an irreversible inhibitor of LSD1, rendering IC_{50} determinations is highly dependent on assay conditions and useful only as a reference point for further experiments (Schmidt *et al.,* 2007).

5.2.3. Chemical screening for LSD1 inhibitors

In cooperation with Prof. Dr. H. Waldmann of the Max-Planck-Institute (Dortmund), a compound collection comprising 768 substances was subjected to the LSD1-HRP coupled assay. This compound library was designed and prepared primarily for the screening of new MAO inhibitors using a cheminformatics approach. Given that the LSD1 catalytic domain has sequence homology with MAO enzymes, we anticipated that some compounds would inhibit LSD1 but have little potency on MAOs.

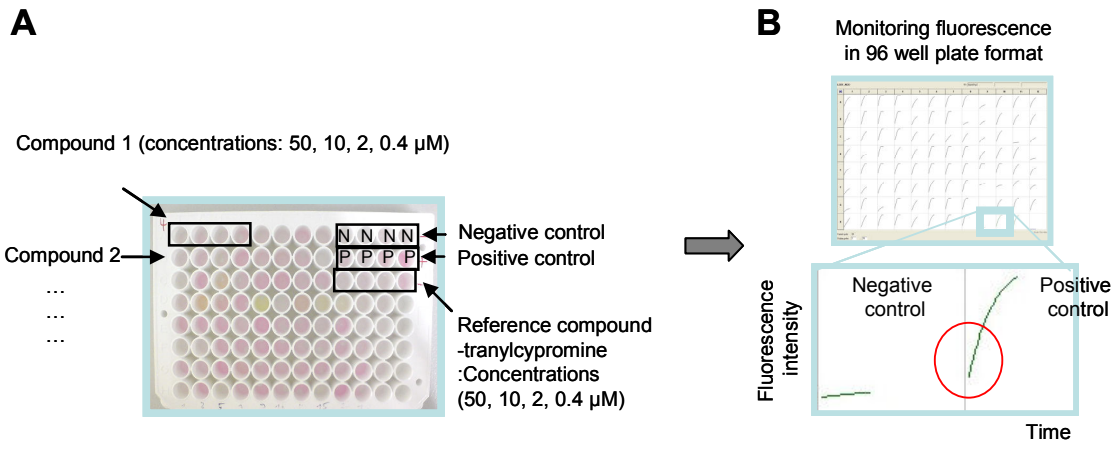

Figure 5.6. Establishment of the high-throughput screening assay. (A) The pipetting plan in the 2nd screening was illustrated. LSD1 was screened against a compound collection. Each compound was diluted in 4 different concentrations (0.4, 2, 10, 50 μM). The positive control contained LSD1, peptide substrate, Amplex red and HRP, except for the inhibitor. The negative control contained neither substrate nor inhibitor. Tranylcypromine was used as a reference compound. (B) The readout of each well in the 96 microplate is done by detection of fluorescence intensity in a time-dependent manner.

Since all compounds were solubilized in DMSO, final 2.5 % of DMSO which did not affect the *in vitro* assay was incubated in every screening plate. The positive control, negative control and reference control were also included in every screening plate. The positive control contained recombinant LSD1, peptide substrate, Amplex Red and HRP, whereas peptide substrate was excluded in the negative control. The reference control included tranylcypromine and all other reagents (Figure 5.6).

Whole screenings were accomplished in 3 steps (Figure 5.7). In a primary screening, compounds were tested at a concentration of 50 μM to cover weakly active molecules as well. 80 compounds were found as positive hits. In a secondary screening, the following 80 compounds were tested at 4 different concentrations (0.4, 2, 10 and 50 μM) to validate their inhibitory effects. During screening, some benzopyrone derivative compounds were found to be capable of reacting directly with hydrogen peroxide produced in the LSD1-mediated enzyme reaction, interfering with the HRP-coupled Amplex red oxidation. These redox-sensitive compounds appeared to scavenge hydrogen peroxide resulting in decreased conversion of Amplex red to fluorogenic resorufin. To eliminate these false positives, the additional experiment was designed in which reactivity of the compounds with 5 μM hydrogen peroxide was tested (detailed data is shown in Appendix A). Some benzopyrone derivatives having catechol moiety turned out to be highly reactive with hydrogen peroxide.

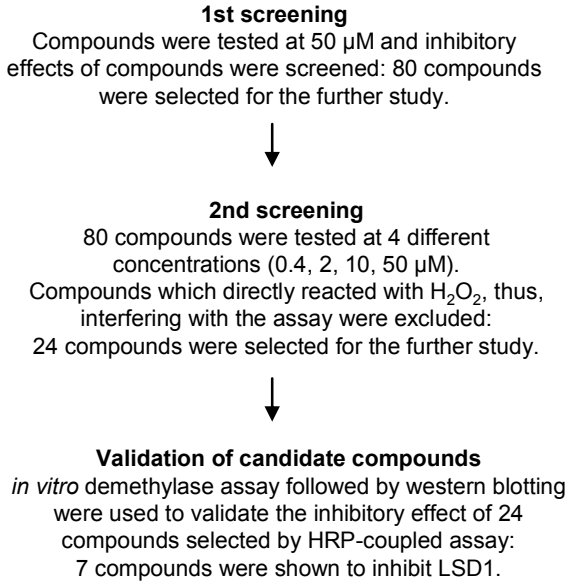

Figure 5.7. Workflow of screening the large compound library. A 768 compound collection was tested in 3 steps.

After excluding false positives, 24 compounds were selected for the third step. To validate the inhibitory activity of identified hits, the follow up screens included western blot detection followed by the *in vitro* demethylase assay. Ten µg of bulk histones were

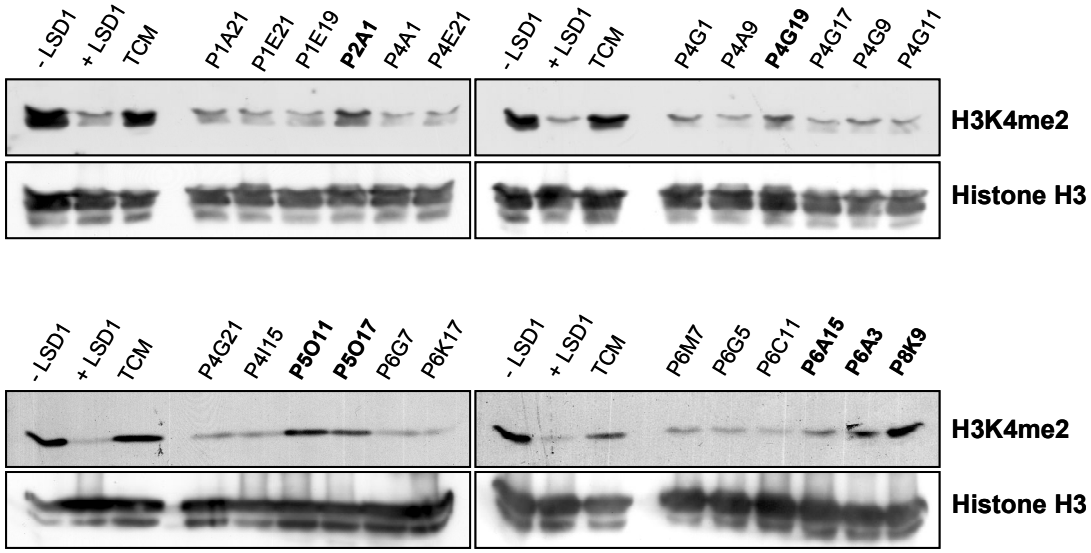

Figure 5.8. *in vitro* demethylase assay. Seven compounds (P2A1, P4G19, P5O11, P5O17, P6A15, P6A3, P8K9) were found to have inhibitory effect against LSD1 at a concentration of 50 µM. (– LSD1) and (+ LSD1) serve as controls; (+ LSD1) contains either 1 µg LSD1 enzyme or 10 µg bulk histone as the substrate, while (– LSD1) contains only 10 µg bulk histone in 50 mM hepes buffer. In the presence of LSD1 (+ LSD1), methylated H3K4 in bulk histone was demethylated by LSD1. Tranylcypromine (TCM) serves as a reference compound. Histone H3 was used as the loading control.

used as substrate for 1 µg recombinant LSD1 in the *in vitro* demethylase assay. The demethylation of H3K4 in bulk histone was detected by Western blotting using the α-H3K4me2 antibody (Figure 5.8). Seven compounds were confirmed to inhibit LSD1 enzyme activity either in LSD1-HRP coupled assay or in the *in vitro* demethylase assay /Western blot (table 5.1). Among the 24 compounds, the remaining 17 compounds showed no or very weak inhibitory effect in the *in vitro* demethylase assay/Western blot analysis. While the LSD1-HRP coupled assay used the oligo-peptide corresponding to the N-terminal 24 amino acids of histone H3 as a substrate, the *in vitro* demethylase assay used the intact bulk histones which contain whole histone H3. It seems that certain compounds could not strongly inhibit the LSD1 enzyme activity on intact bulk histones. Alternatively, immunodetection of di-methylated substrate seems to be more reliable than HRP-coupled fluorescence-based assay excluding false positives.

compounds (No.)	Inhibitory effects in LSD1-HRP assay (Relative decrease in initial velocity)				*in vitro* assay	
					followed by WB	followed by MS§
	0.4 µM	2 µM	10 µM	50 µM	50 µM*	50 µM
P2A1	0.60	0.67	0.50	0.26	++	LSD1 inhibitor
P4G19	0.47	0.49	0.39	0.24	+	-
P5O11	0.45	0.36	0.15	0.05	++	-
P5O17	0.80	0.47	0.44	0.11	+	-
P6A15	0.50	0.51	0.48	0.36	+	-
P6A3	0.78	0.63	0.62	0.49	++	-
P8K9	0.53	0.53	0.58	n.d.	+++	-
Tranylcypromine	0.34	0.53	0.52	0.35	+++	-

Table 5.1. List of final 7 compounds. The 7 compounds were found to have inhibitory effects in LSD1-HRP coupled enzyme assay and in the *in vitro* demethylase assay/western blot (WB). Mass spectromery (MS) showed, however, only P2A1 as a putative LSD1 inhibitor. Relative decrease in initial velocity was calculated at 4 different concentrations of compounds. *The inhibitory effect shown by the *in vitro* demethylase assay was arbitrarily described as +. §Mass spectrometry was done in cooperation with Prof. Dr. R. Schüle in Freiburg (data not shown).

As shown in Table 5.1, most compounds showed concentration-dependent inhibitory effects except tranylcypromine and P8K9. It may reflect the low accuracy of a microplate system. Alternately, the inhibitory effect by compounds may be caused by other factors independent on the enzyme inhibition.

In cooperation with Prof. Dr. R. Schüle from Freiburg Medical School (Freiburg), the inhibitory capability of the final 7 compounds was further investigated using mass-spectrometry which can analyze the change in methylation status of the peptide substrate after the *in vitro* enzyme reaction. Ultimately, only the compound P2A1 was confirmed as a putative LSD1 inhibitor among the 7 compounds. It remains to be elucidated why the other 6 compounds were proven to be negative in mass spectrometry. Further studies are needed to validate the assay results and inhibitory capability of compounds not only in the *in vitro* system but also in cell based experiments.

6. Discussion

6.1. LSD1 in neuroblastoma

6.1.1. LSD1 expression correlates with cell differentiation and growth in neuroblastoma

Our data clearly indicate that LSD1 expression inversely correlates with differentiation of primary neuroblastic tumors and is related to poor clinical outcome. Similar results were recently reported by Kahl *et al*. for prostate cancer (Kahl *et al*., 2006). Moreover, Wang *et al.* (Wang *et al., 2007*) reported that under physiological conditions high LSD1 expression is characteristic of undifferentiated progenitor cells. Consistently, *in vitro* differentiation of neuroblastoma cells resulted in down-regulation of LSD1. In addition, inhibition or knock-down of LSD1 led to cell differentiation by induction of differentiation associated genes *TNS1, TPM1, DNM2* and *DNAL4* and reduced cell proliferation. Although the molecular mechanism regarding the role of LSD1 in cell differentiation is not well understood, these data suggest that aggressive, undifferentiated cancer cells retain a high level of LSD1 expression, which is a characteristic of undifferentiated progenitor cells.

6.1.2. Specificity and regulatory mechanism of LSD1 are cellular complex dependent

LSD1 modulates demethylation of mono- and di-methyl-lysines at residues 4 or 9 in histone H3 (Stavropoulos *et al*., 2007). Specificity of demethylation is governed by the interaction partners of LSD1. LSD1 was previously found to be part of the chromatin modifying Co-Rest complex. The REST/Co-Rest complex, which includes LSD1 and HDAC1/2, is recruited to the promoters of neuronal-specific genes, and specifically represses the genes by epigenetic silencing (Lakowski *et al*., 2006; Lee *et al*., 2005). Recently, REST also called neuron restrictive silencer factor, was demonstrated to be down-regulated upon neuroblastoma cell differentiation (Di Toro *et al*., 2005). Therefore, highly active LSD1 in the REST/Co-Rest complex might repress a neuronal

differentiation program in neuroblastoma, and the differentiation program would be in part re-activated upon decrease of LSD1 level and REST/Co-Rest activity. Depending on cellular context, LSD1 also directly interacts with transcription factors and demethylates lysine residues in the promoter regions of specific genes. This has been shown for the interaction of LSD1 with the androgen receptor (Wissmann *et al.,* 2007). Thus, LSD1 dependent suppression of the neuronal differentiation program in undifferentiated neuroblastoma cells might be mediated by the recruitment of LSD1 protein by both transcription factors and co-repressors.

6.1.3. Epigenetic therapy may serve as an alternative to targeting transcription factors

In neuroblastomas, MYCN is known to be a central oncogene that regulates expression of cell cycle related genes. However, pharmacological intervention to modulate transcription factors like MYCN has not yet been achieved. As discussed above, LSD1 is involved in the regulation of broad gene expression programs that maintain the aggressive, undifferentiated phenotype in neuroblastoma. While this functionality is shared by LSD1 and its cooperating transcription factors, LSD1 and other histone-modifying enzymes additionally have intrinsic enzymatic activities. Thus, they can be considered as good pharmacological targets for small molecule inhibitors. LSD1 has recently been identified as a target for MAO inhibitors, including tranylcypromine, which are already in clinical use to treat depression (Huang *et al.,* 2007; Yang *et al.,* 2007; Lee *et al.,* 2006; Stavropoulos *et al.,* 2007).

6.1.4. Do MAO inhibitors qualify as LSD1 inhibitors in a clinical setting?

As MAOI are the first available small molecular inhibitors of LSD1 (Culhane *et al.,* 2007; Yang *et al.,* 2007), we analyzed their effectiveness against neuroblastoma cells. While they appeared to be very effective *in vitro*, relatively high doses were required to reduce the growth of xenograft tumor in animal models. The doses required to suppress tumor cells were higher than those effectively inhibiting neurotransmitter deamination, resulting in significant side effects such as seizures in the treated mice. For this reason, we do not

expect the currently available MAO inhibitors to be clinically applicable as LSD1 inhibitors. Instead, specific LSD1 inhibitors need to be developed, which do not inhibit the type A and B monoaminoxidases (see below). The development of small molecules modulating substrate specificity appears plausible when the surprising capability of LSD1 to change substrate specificity between H3K4 and H3K9 is taken into consideration, which might well be the effect of allosteric conformational switches (Stavropoulos *et al.,* 2007).

6.1.5. Multimodal epigenetic therapy might be applicable as targeted therapy

At present, rational tumor therapy aims to target the hallmarks of cancer cells by inhibiting angiogenesis, blocking anti-apoptotic proteins and inhibiting tumor-associated receptor tyrosine kinases that generate survival signals. Most often, tumor cells circumvent such therapeutic interventions either by mutation of the target structures or by activation of alternative pathways. We have observed such secondary mutations in response to imatinib therapy of gastrointestinal tumors (Wardelmann *et al.,* 2005). The problem of resistance to targeted therapies certainly needs to be addressed in multimodal strategies. Therefore, it is of great importance that reprogramming of tumor cells appears possible via interference with enzymes manipulating epigenetic patterns. A combination of histone demethylases and HDAC inhibitors might prove useful to prevent the development of resistance to treatment and achieve a maximal effect Indeed, inhibition of LSD1 and HDAC turned out to be synergistic for epigenetic regulation (Lee *et al.,* 2006). Furthermore, LSD1 and the jumonji domain family of proteins such as JMJD2C were reported to cooperate to stimulate the expression of androgen receptor-dependent genes (Wissmann *et al.,* 2007). Taken together, this suggests that the combination of inhibitors of different histone demethylases might act synergistically to reprogram gene expression signatures underlying the malignant phenotype of tumor cells.

In summary, we provide the first evidence that LSD1 may serve as a drug target in neuroblastoma, and that LSD1 inhibitors alone or in combination with other chromatin-modifying agents may provide potential therapeutic options to reprogram the malignant phenotype of neuroblastoma and possibly other aggressive cancers with features of undifferentiated progenitor cells.

6.2. LSD1 in breast cancer

6.2.1. Establishment of an ELISA for screening LSD1 levels in tumor tissues

In our previous works on prostate cancer and neuroblastoma, aberrantly high LSD1 expression in tumor revealed to provide a powerful marker for aggressive cancers with poor prognosis. Reliable and efficient detection of this marker would be of importance for its application in tumor diagnosis, and above all, for large screening of human tissue samples. Immunohistochemistry is the standard method to analyze the specific protein level of tissue samples but it is only a semi-quantitative method which requires independent examinations by two pathologists. Here, I established a novel direct ELISA to quantify the LSD1 protein level in patient tumor tissues. In this direct ELSIA, tissue extracts were directly coated on the 96 well microplate and incubated with a monoclonal antibody which detects the protruding tower domain of LSD1 protein. Using this LSD1 ELISA, I could detect that the LSD1 protein level in tumor region of ER-negative breast cancer is highly upregulated compared to that in matched normal tissues. The following immunohistochemistry and Western blot analysis validated the ELISA results. This new established ELISA is also useful to detect LSD1 protein amount in other tumor entities; for example, a limited number of neuroblastoma specimens was subjected to the ELISA to determine the LSD1 protein level.

6.2.2. LSD1 is highly expressed in hormone receptor-negative breast cancers

Several prognostic and predictive biomarkers are currently used to stratify patients with breast cancers for appropriate chemotherapies. Established biomarkers such as ER and PR already play a significant role in the selection of patients for endocrine therapy. In this study, we demonstrate that high expression levels of LSD1 may serve as a novel, molecular marker for malignant breast tumor. By different methods, I could show that LSD1 is significantly stronger expressed in ER-negative breast cancers which are well known to carry a poorer prognosis than ER-positive tumors (Cui *et al.*, 2005). Alteration in LSD1 expression appears not to be linked specifically to breast cancer. Importantly, aggressive, undifferentiated cancer cells appear to retain a high level of LSD1 expression. Recently, our group found that LSD1 expression is up-regulated in high-risk

prostate cancers with aggressive biology *(*Kahl *et al.,* 2006). In neuroblastomas, LSD1 expression was strongly associated with adverse outcome and inversely correlated with differentiation (Schulte *et al.,* 2009). Taken together, this study provides additional evidence that LSD1 can serve as a promising molecular marker for aggressive tumor biology.

6.2.3. LSD1 contributes to cell proliferation through regulation of CCNA2 and ERBB2

ER-negative tumors are characterized by their rapid growth, loss of differentiation and acquisition of invasive and metastastic capability. The detailed mechanism by which LSD1 overexpression contributes to neoplastic conversion of tumor cells remains to be elucidated. A recent study indicated that LSD1 might promote G2-M phase transition and cell proliferation, which is one way in which its overexpression might promote tumorigenesis (Scoumanne *et al.*, 2007). Here, *in vitro* silencing of LSD1 has shown to inhibit tumor cell-growth by down-regulating genes involved in proliferation. ChIP revealed that LSD1 was recruited to the *CCNA2* and *ERBB2* promoter, accompanied by a significant and highly reproducible increase in histone H3K9me2 upon knock-down of LSD1. Therefore, *CCNA2* and *ERBB2* seem to be direct, positively regulated targets of LSD1 in breast cancer cells. *CCNA2* encodes Cyclin A2 which functions as an activator of CDK2 kinase, and thus promotes both G1/S and G2/M cell cycle transitions. Hence, CCNA2 up-regulation by LSD1 may be one important mechanism by which LSD1 drives tumorigenesis and aggressive biology of breast cancers. Indeed, abnormal overexpression of cyclin A2 corresponds to an increase in the proliferative status of tumor cells and may play an important role in tumor development and progression (Fraczek *et al.*, 2008; Patel *et al.,* 2007). However, we did not find a significant correlation of LSD1 with HER2 overexpression in breast tumor specimens *in vivo*, although *in vitro* study showed that LSD1 positively regulates ERBB2. It appears that additional mechanisms, such as gene amplification are dominant events in HER2-positive tumors (Sunami *et al.,* 2008).

6.2.4. LSD1 functions in association with other transcriptional cofactors/epigenetic enzymes

LSD1 known as a histone H3K4 and H3K9 di- and mono-demethylase acts as a functional component of either co-activator or co-repressor complexes and regulates activation and repression programs. Transcriptional regulation by LSD1 is known to be cell type specific and the substrate specificity of LSD1 can be modulated by its associated partners such as hormone receptors (AR or ER) (Wissmann *et al.,* 2007; Shi *et al.*, 2005). LSD1 appears to regulate transcription of ERBB2 and CCNA2 possibly in concert with other genetic/epigenetic factors. As shown by qRT-PCR analysis, silencing of LSD1 caused a partial repression of gene transcription and induced the enrichment of H3K9 methylation in the promoter regions. In case of *CCNA2* or *ERBB2*, E2F and AP2 transcription factors are known to be positive regulators of gene transcription, respectively (Chen *et al.,* 2004; Pellikainen *et al.,* 2007). It is therefore possible that, in the presence of corresponding stimuli and/or in combination with knock-down of other epigenetic enzymes, silencing of LSD1 would induce even stronger down-regulation of its target genes. Therefore, the mechanism of LSD1 activity on H3K9 in partnership with other transcriptional co-factors needs to be addressed in the further study.

6.2.5. Targeting LSD1 in breast cancer provides a novel therapeutic option

Aberrant expression of LSD1 in ER-negative breast tumor and its function in driving *CCNA2* overexpression suggest that LSD1 may not only serve as a biomarker for malignant breast tumors, but also as a therapeutic target in cancer treatment. While ER-positive breast tumors respond well to anti-hormonal therapy, the treatment of ER-negative breast tumors usually includes chemotherapy by non-selective cytotoxic drugs. Targeting LSD1 in ER-negative breast cancer might provide an alternative, more specific treatment.

Both MAOI and polyamine analogues have been shown to inhibit LSD1 enzymatic activity (Metzger *et al.,* 2005; Lee *et al.,* 2006; Huang *et al.,* 2007). Polyamine analogues cause re-expression of aberrantly silenced genes that are important in the development of colon cancer (Huang *et al.,* 2007). The level of re-expression of these otherwise silenced genes was almost 30% of that observed after treatment with DNA-

methyltransferase inhibitors which are of great therapeutic interest but have many side effects. If LSD1 inhibition leads to significant de-repression of some of the same genes that are reactivated by DNA-methyltransferase inhibitors, LSD1 might be an important alternative target for therapy. Consistenly, we recently provide direct evidence that LSD1 is a target in cancer therapy. In a xenograft mouse model, MAOIs significantly decreased neuroblastoma tumor growth (Schulte *et al.,* 2009). In combination with the novel data of this study we hypothesise that LSD1 inhibitors alone or in combination with DNA demethylating drugs or/and chromatin-modifying agents might prove effective for treatment of hormone receptor-negative aggressive breast cancer.

6.3. LSD1 enzyme assay for high-throughput

6.3.1. The LSD1-HRP coupled assay can be applied for high-throughput kinetic study

To identify selective LSD1 inhibitors from a compound library comprising 768 natural compounds, we have developed a fluorescence-based *in vitro* LSD1 enzyme assay. The fluorescence-based LSD1-HRP coupled assay turned out to be much more sensitive than the standard colorimetric LSD1-HRP coupled assay (Yang *et al.,* 2007; Szewczuk *et al.,* 2007; Schmidt *et al.,* 2007). In the fluorescence-based system, the reaction volume could be minimized to 40 µl requiring only small amounts of peptide substrate and recombinant LSD1 protein. Moreover, using 96 well microplates, kinetic studies of each well could be done at the same time. Despite the lower accuracy of a microplate system, the assay system was shown to be efficient for primary screening of large compound libraries.

However, the concern must be addressed to some benzopyrone derivatives which might interfere with the HRP-coupled assay which detects hydrogen peroxide or have auto-fluorescence themselves. In combination with alternative assays such as demethylation detection using immunoblotting or biochemical test on the reactivity of compounds with hydrogen peroxide, false positive hits were excluded and the specificity of the hits could be validated (Appendix A). However, for the screening of large-scale compounds, this could be a limiting factor for high-throughput screening. The design of new assays that do not use hydrogen peroxide would be desirable especially for the screening of redox-sensitive compounds. For example, PRMT1 inhibitor screening was done using the ELISA-based screening in which methylated arginine-substrate was detected using specific primary antibody and HRP-labeled secondary antibody. This assay has the disadvantage that kinetic measurements are not possible, but it would be useful for the primary high-throughput screening (Chen *et al*., 2004).

6.3.2. The LSD1-HRP coupled assay identified a putative LSD1 inhibitor

In this study, at least 1 putative LSD1 inhibitors was identified. In collaboration with Prof. R. Schüle (Freiburg) and Prof. H. Waldmann (Dortmund), P2A1 was identified as a possible lead compound for the following reasons: 1) it inhibits LSD1 but not MAO; 2) it is cell-permeable; 3) it has a good solubility. The further studies are planned to test whether it can inhibit endogenous LSD1 activity. In this cell-based experiment, for example, accumulation of H3K4 dimethylation, reactivation of aberrantly repressed tumor suppressor genes and anti-proliferative effect by the compound will be analyzed. Ultimately, xenograft mouse models would be useful to evaluate anti-tumor effect of the inhibitor *in vivo*. The identification of a putative LSD1 inhibitor may serve as a starting point toward the development of a new class of a LSD1 selective inhibitor.

6.3.3. Is LSD1 a promising drug target for cancer therapy?

Epigenetic drugs, whether demethylating agent or HDAC inhibitor, target aberrantly heterochromatic regions leading to reactivation of tumor suppressor genes and/or other genes that are crucial for the normal functioning of cells. Some concerns were given regarding the modulation of histone methylation. The methyl marks exist as both active and inactive markers, and it might therefore be difficult to determine whether inhibiting a histone demethylase such as LSD1 would be beneficial for patients because the enzyme has opposing effects on gene regulation.

However, our experiment using a xenograft mouse model revealed for the first time that targeting LSD1 could inhibit xenograft tumor growth *in vivo*. Moreover, there are some considerations that LSD1 could be an attractive target in tumor therapy: (i) LSD1 expression is linked to tumors with aggressive biology, while some other epigenetic enzymes such as G9a have not been directly involved in tumorigenesis. Our data and other reports have shown that aberrant expression of LSD1 increases considerably when tumors enter advanced stages (Schulte *et al.,* 2009; Kahl *et al.,* 2006). Disequilibrium caused by epigenetic disregulations in tumor cells seems to promote tumorigenesis. Thus, LSD1 inhibition may selectively delay the growth of tumor cells overexpressing LSD1; (ii) LSD1 inhibitors can be useful for the treatment of hormone-

dependent cancers. For example, LSD1 assembles into the AR complex and regulates AR target gene transcription. LSD1 inhibition was shown to be capable of antagonizing AR action preventing hormone-induced tumor growth (Metzger *et al.,* 2005). Thus, targeting LSD1 can be an alternative strategy for the treatment of cancers that are hormone-dependent or resistant to hormone-therapy; (iii) in light of the fact that HDAC1/2 and LSD1 activities are synergistic with regards to transcriptional inhibition, inhibition of LSD1 will likely result in a profound effect on transcription like the inhibition of HDACs. Indeed, LSD1 inhibitors were shown to be capable of reactivating the pathologically silenced tumor suppressor genes in colon cancer cells (Huang *et al.,* 2007). Combination of LSD1 inhibitors with HDAC inhibitors might be advantageous to achieve synergistic tumor-cell growth inhibition and gene reexpression.

6.3.4. Epigenetic therapy can be used in combination with other therapeutic modalities.

Epigenetic drugs can be therapeutically used alone or as part of a combination with other therapeutic modalities, such as chemotherapy, immunotherapy or radiotherapy. So far, a number of preclinical studies have demonstrated that either DNA methylation or histone deacetylase inhibitors reverse drug resistance or increase the cytotoxicity of anticancer drugs and radiation (Mai *et al.,* 2009). In this regard, a number of clinical trials are currently testing epigenetic drugs either alone or in combination with conventional cytotoxic and radiation therapy.

Therefore, the development of LSD1 selective inhibitors would help to evaluate the therapeutic potential of targeting LSD1 as well as their use in combination with other therapeutic modalities for tumor therapy.

7. Materials and methods

7.1. Material

7.1.1. Chemicals

Acrylamide (Rotiphorese Gel 30)	Carl Roth GmbH, Karlsruhe
Agar	Merck, Darmstadt
Agarose	Sigma Aldrich, St. Louis, USA
3-amino-9-ethyl-carbazolke	Dako, Glostrup, Dänemark
Ammonium peroxisulfate (APS)	Carl Roth GmbH, Karlsruhe
Ampicillin	Carl Roth GmbH, Karlsruhe
Amplex Red	Invitrogen, Karlsruhe
Aquatex	Merck, Darmstadt
Blocking reagent (for ELISA)	Roche Diagnostics, Mannheim
Blocking reagent (for IHC)	DAKO, Glostrup, Dänemark
Bovine serum albumin (BSA)	Sigma Aldrich, St. Louis, USA
Bulk histone	Sigma Aldrich, St. Louis, USA
Clorgyline	Sigma Aldrich, St. Louis, USA
Complete Mini	Roche Diagnostics, Mannheim
Dimethyl sulfoxide (DMSO)	Sigma Aldrich, St. Louis, USA
dNTPs	Invitrogen, Karlsruhe
Dulbecco´s MEM	Invitrogen, Karlsruhe
Dynabead	Invitrogen, Karlsruhe
ECL reagent	Perbio, Bonn
Ethanol	Merck, Darmstadt
Ethidium bromide	Sigma Aldrich, St. Louis, USA
Fetal calf serum	Invitrogen, Karlsruhe
Glycerol	Sigma Aldrich, St. Louis, USA
Glycine	Sigma Aldrich, St. Louis, USA
H_2O_2	Sigma Aldrich, St. Louis, USA
HEPES	Sigma Aldrich, St. Louis, USA
HiPerFect	Qiagen, Hilden
Horse radish peroxidase (HRP)	Sigma Aldrich, St. Louis, USA
Imidazole	Sigma Aldrich, St. Louis, USA
Isopropanol	Sigma Aldrich, St. Louis, USA
IPTG	Merck, Darmstadt
Kanamycin	Carl Roth, Karlsruhe
Mayer´s hematoxylin	Sigma Aldrich, St. Louis, USA
Methanol	Merck, Darmstadt
MTT	Sigma Aldrich, St. Louis, USA
NP-40	Calbiochem, Darmstadt

Pargyline	Sigma Aldrich, St. Louis, USA
Penicillin/Streptomycin	Invitrogen, Karlsruhe
RNase-Off	Invitrogen, Karlsruhe
Roti-load 4x concentrate	Carl Roth, Karlsruhe
RPMI 1640	Invitrogen, Karlsruhe
Salmon sperm DNA	Invitrogen, Karlsruhe
siRNA	Ambion, Austin, USA; Qiagen, Hilden
Sodium bicarbonate/carbonate	Sigma Aldrich, St. Louis, USA
Sodium chloride	Merck, Darmstadt
Sodium dodecyl sulfate (SDS)	Merck, Darmstadt
Skim milk powder	Sigma Aldrich, St. Louis, USA
Sulphuric acid (2N)	Sigma Aldrich, St. Louis, USA
Synthetic peptide	CASLO, Lyngby, Denmark
TEMED	Bio- Rad, Hercules, USA
TMB substrate for ELISA	Pierce, Rockford, USA
Tranylcypromine	Biomol, Hamburg
Trishydroxymethylaminomethane (Tris)	Merck, Darmstadt
Triton-X100	Sigma Aldrich, St. Louis, USA
Trypsin EDTA (0.25% / 0.02%)	Invitrogen, Karlsruhe
Tween-20	Sigma Aldrich, St. Louis, USA
X-Gal	Invitrogen, Karlsruhe

All chemicals listed here are the molecular biology grade.

7.1.2. Apparatus

Abiprism 7900HT	Applied Biosystems, Foster City, USA
AxioCam digital camera	Zeiss, Oberkochen
Bacteria shaker Innova 4000	New Brunswick Scientific, Nürtingen
Centrifuges 5415D	Eppendorf, Hamburg
Centrifuges 5417R	Eppendorf, Hamburg
Cryostat (CM 3050 S)	Leica, Wetzlar
Digital camera KY-F70B	JVC, London, UK
ELISA Reader ELx800	BioTek Instruments, Winooski, USA
Enzyme kinetic plate reader	BMG LABTECH´s FLUOstar OPTIMA, Offenburg
FastPrep FP120 instrument	MP Biomedicals, Irvine, USA
Hoefer Dual Gel Caster	Amersham Bioscience, Freiburg
Kodak X- omat 1000 Processor	Kodak, Rochester, USA
Magnetic stirrer	Ika-Combimag RCT, IKA-Werke GmbH, Staufen
Membrane pump	M72C, Vacubrand GmbH & Co, Wertheim
Microscope Axioscop50	Zeiss, Oberkochen; Leica, Wetzlar
Mighty Small II for 8x7cm Gels	Amersham Bioscience, Freiburg

Nano Drop	Peqlab Biotechnologie, Erlangen
Peltier Thermocycler- 200 (PCR Cycler)	MJ Research, Waltham, USA
pH-meter	MP 220, Mettler Toledo, Greifensee, Switzerland
Pipettes	Gilson Pipetman, Langenfeld Eppendorf, Hamburg
Power supplies E143	Consort, Turnhout, Belgien
Shakers	Series 25 New Brunswick Scientific CO., Inc. , Edison, USA Multitron, Infors AG, Bottmingen, Switzerland
Sterilbench	Biohazard, Gelaire, Mailand, Italy Heraeus-Christ, Hanau
Thermomixer compact	Eppendorf, Hamburg
TransBlot Semi-Dry Transfer	Bio- Rad, Hercules, USA
UV-imaging system	Intas UV system, Göttingen
UV-transilluminator	Biometra, Göttingen
Water purification	Millipore-Pelicon Filtration device with polysulfone filter cassette PTGC, 10000 MW, Millipore, Molsheim, France

7.1.3. Consumables

12, 24, 48 and 96 well cell plates	Costar, Lowell, USA
75T cell culture plate	Costar, Lowell, USA
96 well MaxiSorb plate	Nunc, Wiesbaden
Autoradiography film	Kodak, New Haven, USA
Bacterial culture tubes	Costar, Lowell, USA
Cell culture plates	Costar, Lowell, USA
Cryo Tube™	Nunc, Wiesbaden
Eppendorf reaction tubes	Eppendorf, Hamburg
Falcon 2052	Costar, Lowell, USA
PCR tubes	Eppendorf, Hamburg
Petri dish (bacterial)	Costar, Lowell, USA
Transfer membrane	Millipore, Billerika, USA
Whatman paper	Schleicher & Schuell GmbH, Dassel

7.1.4. Antibodies

Mouse-monoclonal antibody ß-Actin (AC15)	Sigma Aldrich, St. Louis, USA
Rabbit-monoclonal antibody H3K4me2 (Y47)	Abcam, Cambridge, UK
Rabbit-monoclonal antibody H3K9me2 (mAbcam1220)	Abcam, Cambridge, UK
Mouse-polyclonal antibody Her2	Dako, Glostrup, Dänemark
Rabbit-polyclonal antibody Histone H3	Abcam, Cambridge, UK
Mouse-monoclonal antibody LSD1 (1B2E5)	Novus Biological, Littleton, USA
Goat polyclonal antibody anti-rabbit HRP conjugate	Dako, Glostrup, Dänemark
Goat polyclonal antibody anti-mouse HRP conjugate	Dako, Glostrup, Dänemark

7.1.5. Kits

Dako EnVision AEC kit	Dako, Glostrup, Dänemark
Plasmid isolation	Qiagen, Hilden
RNeasyMini kit,	Qiagen, Hilden
QIAquick Gel extraction kit	Qiagen, Hilden
QIAquick PCR purification kit	Qiagen, Hilden
SYBR® Green *Taq* PCR Mix™	Invitrogen, Karlsruhe
TOPO TA cloning®	Invitrogen, Karlsruhe

7.1.6. Enzymes and markers

Alkaline phosphatase	New England BioLabs, Frankfurt
DNA 100bp ladder	Invitrogen, Karlsruhe
DNA 1kb ladder	Invitrogen, Karlsruhe
***DNase* I**	Applera GmbH,Darmstadt
EcoRI	New England BioLabs, Frankfurt
Prestained SDS- PAGE standards	Invitrogen, Karlsruhe
Proteinase K	Invitrogen, Karlsruhe
Superscript II RT (200 U)	Invitrogen, Karlsruhe
T4 DNA Ligase	Invitrogen, Karlsruhe
***Taq* DNA polymerase**	Invitrogen, Karlsruhe
XhoI	New England BioLabs, Frankfurt

7.1.7. Vectors

Table 7.1. Vectors used for the cloning of recombinant LSD1 expression vector

Vector	Description	Source
pET15b	N-terminal his_6-tag expression vector	Institute of Pathology
pCMX-Flag-LSD1	Plasmid containing LSD1 gene	gift from Prof. R. Schüle
pCR®II-TOPO®	LacZa, Sp6/T7 promoter, MCS, AmpR, KanR	Invitrogen, Karlsruhe

7.1.8. Primer sequences

All oligonucleotide primers were synthesized by Invitrogen (Karlsruhe).

Table 7.2. Primers used for the cloning, qRT-PCR and ChIP assay

Name	Forward (for) Reverse (rev)	Primer sequence 5' - 3'
18s rRNA (qRT-PCR)	for	cgattggatggtttagtgagg
18s rRNA (qRT-PCR)	rev	agttcgaccgtcttctcagc
CCNA2 (qRT-PCR)	for	ggtactgaagtccgggaacc
CCNA2 (qRT-PCR)	rev	gtgacatgctcatcatttacagg
CCNA2 -70 proximal promoter (ChIP)	for	cctgctcagtttccttggt
CCNA2 -70 proximal promoter (ChIP)	rev	atcccgcgactattgaaatg
DNAL4 (qRT-PCR)	for	gaccttccctctggtcagg
DNAL4 (qRT-PCR)	rev	ggctgtgacacatagctcca
DNM2 (qRT-PCR)	for	gactgccgagtcactgtcct
DNM2 (qRT-PCR)	rev	ttgtccagaggcagcatgta
ERBB2 (qRT-PCR)	for	gggaaacctggaactcacct
ERBB2 (qRT-PCR)	rev	ccctgcacctcctggata
ERBB2 -250 proximal promoter (ChIP)	for	ggcttgggatggagtaggat
ERBB2 -250 proximal promoter (ChIP)	rev	tccctaggctgccactctta
HPRT1 (qRT-PCR)	for	tgaccttgatttattttgcatacc
HPRT1 (qRT-PCR)	rev	cgagcaagacgttcagtcct

LSD1 (for cDNA synthesis)	for	atcctcgagagtgagcctgaagaacca
LSD1 (for cDNA synthesis)	rev	aatctcgagtcacatgcttggggactg
LSD1 (cloning of expression vector)	for	gccgaattcagtgagcctgaagaacca
LSD1 (cloning of expression vector)	rev	aatctcgagtcacatgcttggggactg
LSD1 (qRT-PCR)	for	gccatggtggtaacaggtct
LSD1 (qRT-PCR)	rev	tggccagttccatatttacttg
TFPI2 (qRT-PCR)	for	cgccaacaatttctacacctg
TFPI2 (qRT-PCR)	rev	ggcaaactttgggaacttttt
TFPI2 proximal promoter (ChIP)	for	gcaggtcatttccgtctagc
TFPI2 proximal promoter (ChIP)	rev	acctgcctcccaaactttct
TPM1 (qRT-PCR)	for	ccacgctctcaacgatatga
TPM1 (qRT-PCR)	rev	cagagaggtgggacatccag
TNS1 (qRT-PCR)	for	ccccaatgagccaaacttc
TNS1 (qRT-PCR)	rev	gggatgatggagtgctggta
XRCC5 (qRT-PCR)	for	cccaaatcctcgatttcaga
XRCC5 (qRT-PCR)	rev	cccggggatgtaaagctc
XRCC5 -300 proximal promoter (ChIP)	for	caatgagagaaaagggacgtg
XRCC5 -300 proximal promoter (ChIP)	rev	ctctccattccgccgtagt

7.1.9. Bacterial strains

These bacteria were used for the transformation of recombinant plasmids.

DH5α (Invitrogen, Karlsruhe) F-, φ80*lac*ZΔM15, Δ(*lac*ZYA-*arg*F)U169, *rec*A1, *end*A1, *hsd*R17(rk-, mk+), *pho*A, *sup*E44, *thi*-1, *gyr*A96, *rel*A1 and *ton*A

TOP10 (Invitrogen, Karlsruhe) F-, *mcr*A, Δ(*mrr-hsd*RMS-*mcr*BC), Φ80*lac*ZΔM15, Δ*lac*X74, *rec*A1, *ara*D139, Δ(*araleu*)7697, *gal*U, *gal*K, *rps*L, (StrR),*end*A1 and *nup*G.

7.1.10. Cell lines

Table 7.3. Description and origin of cell lines used in this work

	Description	Source
BE2C	Human neuroblastoma cells	Institute of Pathology
IMR	Human neuroblastoma cells	Institute of Pathology
Kelly	Human neuroblastoma cells	Institute of Pathology
LAN1	Human neuroblastoma cells	Institute of Pathology
MDA-MB 231	Human breast cancer cells	Institute of Pathology
MDA- MB 453	Human breast cancer cells	Institute of Pathology
MCF7	Human breast cancer cells	Institute of Pathology
NB69	Human neuroblastoma cells	Institute of Pathology
SHEP	Human neuroblastoma cells	Institute of Pathology
SH-SY5Y	Human neuroblastoma cells	Institute of Pathology
SKNAS	Human neuroblastoma cells	Institute of Pathology
T47D	Human breast cancer cells	Institute of Pathology

7.1.11. Human breast specimens

Human breast cancer speicimens of different stages were collected for my study. 38 human breast cancers, matched pairs of normal and malignant tissue, were stored at -80 in our tumor bank (Institute of Pathology, Bonn). All tumor samples were evaluated by a panel of experienced pathologists for histopathological staging according to UICC TNM system (TNM stand for Tumor, Nodes and Metastases). The diagnosis was confirmed histologically in all cases, based mainly on examination of sections stained with Haematosilin and Eosine (HE).

7.2. Buffers and solutions

7.2.1. Bacterial culture

Luria Bertani (LB) medium

Bactotryptone 1% (w/v)
Yeast extract 0.5% (w/v)
NaCl 0.5% (w/v)

pH was adjusted to 7.5 with NaOH and then solution was autoclaved.

Luria Bertani (LB) 1.5% agar

Bactotryptone 1% (w/v)
Yeast extract 0.5% (w/v)
NaCl 0.5% (w/v)
Agar 1.5% (w/v)

The pH was adjusted to 7.5 with NaOH. The solution was autoclaved, cooled to 50°C and the corresponding antibiotics (30 µg/ml Ampicillin) were added. Approximately 25 ml medium were poured per petridish and allowed to solidify. Plates were then packed under sterile conditions and stored at 4 °C until use.

7.2.2. Cell culture

DMEM Medium	Invitrogen, Karlsruhe
DPBS	Invitrogen, Karlsruhe
FCS	Invitrogen, Karlsruhe
RPMI 1640 Medium	Invitrogen, Karlsruhe
Trypsin/EDTA (0.05% / 0.01%)	Invitrogen, Karlsruhe
10 % DMEM/RPMI	10 % (v/v) FCS, 1 % (v/v) Penicillin/streptomycin in DMEM
0.5 % DMEM/RPMI	0.5 % (v/v) FCS, 1 % (v/v) Penicillin/streptomycin in DMEM

7.2.3. Protein expression & purification

Elution buffer	300 mM Imidazole, 10 mM Tris pH 8.0
HiTrap Ion exchange column buffer	50 mM Tris pH 8.0
IPTG	100 mM in water
Lysis & Washing buffer	20 mM Imidazole in 2x PBS
Size exclusion chromatography buffer	100 mM NaCl, 10 mM Tris pH 8.0
Storage buffer	100 mM NaCl, 5 % Glycerol, 20 mM Tris pH 8.0

7.2.4. Western blotting

10% APS (w/v)	1g Ammonium peroxysulfate in 10ml water
Acrylamide solution	38 % acryamide, 2 % bisacrylamide
Coomassie staining	0.1 % Coomassie Brilliant Blue R250 25 % methanol, 10 % acetic acid
5x Electrophoresis buffer	0.125M Tris, 0.96 M Glycine, 0.5% SDS in DDW
Lysis buffer for protein preparation (RIPA)	150 mM NaCl, 0.5 % Na-Deoxycholate, 1 % NP-40, 0.1 % SDS, 50 mM Tris pH 7.5, 1x complete mini
4x Protein loading buffer	200 mM Tris HCl, pH 6.8, SDS 8% (w/v), Glycerol 40% (v/v), Bromophenol blue 0.01% (w/v), 1 M DTT 40% (v/v)
SemiDry Transfer buffer	48 mM Tris, 39 mM Glycine, 1.3 mM SDS, Methanol 5 % (v/v)
12% Separating gel buffer	Tris HCl, pH 8.8 375 mM, SDS 0.1% (w/v), Acrylamide 12% (w/v), Bisacrylamide 0.24% (w/v), Ammonium persulphate 0.1% (w/v), TEMED 0.1% (v/v)
5% Skim milk in PBST	5 % skim milk, 0.05 % Tween 20, in PBS
5% Stacking gel buffer	Tris HCl, pH 6.8 187.5 mM, SDS 0.1% (w/v), Acrylamide 5% (w/v), Bisacrylamide 0.1% (w/v), Ammonium persulphate 0.1%

	(w/v), TEMED 0.1% (v/v)
Wash buffer	1x PBST

7.2.5. DNA/RNA techniques

6x Sample buffer	Glycerol 50% (v/v), EDTA 0.002 mM, Bromo phenol blue 0.0025% (w/v), Xylene cyanol 0.0025% (w/v)
6x Sample buffer	Glycerol 50% (v/v), EDTA 0.002 mM, Orange G 0.0025% (w/v)
Solution I	50 mM Tris-HCl, pH 8.0, 10 mM EDTA
Solution II	0.2 N NaOH, 1.0% SDS
Solution III	3 M KOAc, pH 4.8
	[60 ml 5 M KOAc, 11.5 ml HOAc, 28.5 ml H_2O]
TAE (50x)	2 M Tris acetate, 50 mM EDTA (pH 8.0)
TBE (10x)	108 g Tris, 55 g boronic acid in 40 ml EDTA
TE buffer	10 mM Tris-Cl, 1 mM EDTA (pH 7.5.)

7.3. Cell culture techniques for mammalian cells

7.3.1. Mammalian cell culture method

All cell lines were cultivated at 37°C in an incubator with 5% CO_2 and humid atmosphere. Adherent growing cells were grown in tissue culture dishes on 6, 10 or 15 cm diameter dishes. The growth medium was renewed as required. Antibiotic mixtures of penicillin and streptomycin (Pen/Strep) were used to minimize bacterial contamination.

Almost confluent (80-90%) grown cells were passaged into a new culture dish. First the medium was removed and cells were washed with 10 ml PBS. Approximately 1 ml of a trypsin/EDTA solution (Invitrogen) was added and the plate was incubated at 37°C for 3-5 min to dislodge the cells. Trypsinization was inhibited by addition of 10 ml growth medium. Cells were mixed well by pipetting up and down with a 10 ml glass pipette and resuspended in growth medium and seeded at suitable density.

7.3.2. Freezing and thawing of mammalian cells

A 15 cm confluent culture dish was passaged as above. Cells were resuspended in 5 ml freezing medium with 10% DMSO and transferred with a sterile 1 ml pipette in cryotubes. The cells were stored overnight at –20°C prior to -170°C long term storage.

Cells were thawed in a 37°C waterbath as quickly as possible. In order to minimize the toxic effect of the DMSO, 5 ml fresh growth medium were added and cells were pelleted by centrifugation at 1,200 rpm for 2 min. The cell pellet was resuspended in the appropriate cell culture medium and seeded depending upon desired cell density in tissue culture dishes and cultivated under standard conditions.

7.3.3. Treatment of adherent cells with siRNAs

Cells were seeded with $1x10^5$ cells in 24 well plates, then incubated for 3 - 12 days in standard medium in the presence of 10- 20 nM siRNA directed against LSD1 (targeted on exon 8; Ambion, Austin, USA) or control siRNA (scrambled) complexed with HiPerFect Transfection Reagent (Qiagen) according to the manufacturer´s instructions.

7.3.4. Treatment of adherent cell with MAOIs

Cells were seeded at a density of $2x10^4$ cells in 96 well plate, and cultured in standard medium. Treatment with clorgyline (Sigma-Aldrich, Hamburg, Germany), pargyline (Fluka, Hamburg, Germany) or tranylcypromine (Biomol, Hamburg, Germany) was accomplished in 0.5 % DMEM or RPMI as indicated.

7.3.5. MTT cell proliferation assay

MTT (0.12 mg/ml) was added in an amount equal to 10 % of the culture medium volume and cells were incubated for 2-4 hours. After the incubation, culture mediums were removed and 100 µl DMSO were added and absorbance was measured at a wavelength of 570 nm.

7.4. DNA techniques

7.4.1. Photometric measurement of nucleic acid concentration

To determine the concentration of DNA or RNA in a solution the optical density (OD) was measured. Nucleic acids have an absorption maximum at 260 nm and proteins absorb UV light maximally at a wavelength of 280 nm. Pure DNA exhibits an OD 260/OD 280 ratio of up to 2. This ratio is inversely proportional to the amount of proteins present in the solution.
For pure nucleic acids: 1 OD 260 corresponds to a concentration:
dsDNA: 50 µg/ml
Oligonucleotide: 20 - 30 µg/ml
ssDNA: 33 µg/ml
RNA: 40 µg/ml

A nanodrop spectrophotometer was used for quantification of DNA and RNA.

7.4.2. Plasmid DNA isolation (mini/maxi preparation)

For mini preparation, 2 ml of overnight culture was centrifuged at 13,000 rpm for 1 minute. Supernatant was aspirated and cell pellet was resuspended in 300 µl Solution I (50 mM Tris-HCl, pH 8.0, 10 mM EDTA). Solution II 300 µl (0.2 N NaOH, 1.0% SDS) was added and mixed gently by inversion. Solution III 300 µl (3 M KOAc, pH 4.8 [60 ml 5 M KOAc, 11.5 ml HOAc, 28.5 ml H_2O]) was added and vortexed briefly to mix, and centrifuged for 5 minutes on high. Supernatant was transferred to fresh tube containing 0.7 volumes isopropanol and vortexed and spun for 5 minutes on high. Pellet was washed with 500 µl 75% ethanol, spin for 1 minute. Ethanol was removed as much as possible and DNA pellet was dried by leaving tubes on bench with lids open for ~5 minutes. DNA was resuspend in 40 µl of 20 µg/ml RNase A H_2O.

For maxi preparation, 100 ml - 500 ml of overnight bacterial culture was used. The plasmids were isolated with silica columns according to manufacturer's instructions (Midi/Maxi kit, Qiagen).

7.4.3. Separation of DNA by agarose gel electrophoresis

Agarose gel electrophoresis was used to resolve DNA constructs. Agarose gels (1 %) were casted in TAE Buffer. Ethidium bromide was added to the gel (final concentration 0.5 µg/ml). DNA samples were diluted in 5x loading dye before loading on agarose gels. One kb and 100 bp molecular weight ladders (Invitrogen) were used to analyze the molecular size of the DNA. Gels were run at 80 V in TAE buffer for about 1 hour. DNA on gels was viewed under UV illumination using a digital imaging system (Intas UV system).

7.4.4. Extraction of DNA from agarose gels

Under UV-light desired bands were removed from the gel using a sterile scalpel. DNA was extracted from the agarose using the QIAquick gel extraction kit (Qiagen).

7.4.5. DNA precipitation in ethanol/isopropanol

Ethanol and isopropanol precipitation was used for the purification of DNA and RNA. Ionic concentration of the aqueous DNA and/or RNA solution was increased by addition of 1/10 volume 3 M sodium acetate solution (pH 5.2). About 2.5 times volumes of ethanol/isopropanol were added. The DNA and/or RNA was incubated at -20°C for 30-60 min. Afterwards the sample was centrifuged at 13,000 rpm, the pellet was washed with 70% ethanol and dried for 10 min at 60°C. Then the DNA and/or RNA pellet was dissolved in the desired quantity of milli Q water or TE buffer (10 mM Tris-Cl, 1 mM EDTA, pH 7.5.).

7.4.6. Enzymatic restriction of plasmids

Digestions of DNA with restriction endonucleases were performed according to the instructions given by the manufacturer (New England BioLabs).

7.4.7. Dephosphorylation of DNA fragments

Vectors that were digested with restriction endonucleases have two compatible ends that can self ligate. In order to minimize such ligations and to increase the cloning efficiency, the 5'-phosphate group of the linearized vectors was removed by an alkaline phosphatase from the *shrimp* (New England BioLabs). Linearized vectors (1 µg) were treated with 1 U of *shrimp alkaline phosphatase* SAP for 30 min at 37°C. Prior to addition of insert DNA for ligation, dephosphorylation reactions were terminated by heat inactivation at 65°C for 15 min.

7.4.8. Ligation of DNA fragments

Purified linearized vector (0.01 – 0.2 µg) and PCR product were used in a molar ratio of 1:2 or 1:3 respectively. Using T4 ligase (5 U/µl, Invitrogen), the ligation reaction was carried out according to the instructions supplied by the manufacturer. The ligation reaction volume (5-10 µl) was used for transformation of competent *E. coli*.

7.4.9. Ligation of PCR products/TOPO cloning

PCR products were ligated with the TOPO® TA cloning kit (Invitrogen). To avoid auto degradation of adenosine overhangs upon longer storage intervals, freshly prepared PCR products were used. The ligation was done according to the manufacturer's directions.

7.4.10. Transformation and selection

The ligation product (1- 10 µl) was mixed with 100 µl of competent *E. coli* (*DH5* α or *Top 10*) and incubated on ice for 30 min. Next the cells were heat shocked at 42°C for 40s and were quickly placed on ice for 2 min. 1 ml LB or SOC medium was added and cells were incubated in a bacterial shaker at 37°C with for 1 h. Tubes were then centrifuged for 1 min at 12,000 rpm. The pellet was resuspended in 50- 200 µl of respective medium and cells were streaked on LB-plates with respective antibiotic. After 14-20 h of incubation at 37°C, colonies were chosen and kept for overnight cultures in 5 ml LB-growth medium with the respective antibiotic.

7.4.11. Cloning of LSD1 expression construct

cDNA comprising the coding sequence of the human LSD1 (166–852aa) were made from pCMX-flag LSD1 vector (gift from Prof. R. Schüle) by PCR using primers (forward primer: 5'-gccgaattcagtgagcctgaagaacca-3', reverse primer: 5'- aatctcgagtcacatgcttggggactg-3'). Restriction sites for XhoI was incorporated in the sense and antisense primers, in order to facilitate subsequent cloning. The PCR amplicon was subcloned into the cloning vector pCR2®II-TOPO and then the cDNA was subcloned into XhoI sites of pET-15b expression vector.

7.4.12. Sequencing of DNA

The DNA sequence of plasmids was performed by Entelechon (Regensburg).

7.4.13. Sequence analysis

The DNA sequence for the LSD1 gene (166 -852 aa) was analyzed using the sequence alignment tool in NCBI homepage.

7.4.14. PCR: *in vitro* amplification of DNA

DNA sequence for the respective gene was obtained from the NCBI web site.

Primers for PCR were designed based on the following general considerations: the length of the primer should be around 19 bp, the melting temperature (Tm) of the primer should be close to 60°C, and the nucleotide at the 3' end should be either G or C. Primers used in the same PCR reaction were checked carefully to avoid formation of primer-primer dimers.

The melting temperature of the primer was calculated according to the following formula:
Tm = 4 (G+C) + 2 (A+T)

PCR reactions were performed in a total volume of 50 µl.

Detail	**End concentration**
DNA template (cDNA, plasmid DNA)	2 ng/µl
Primer sense	0.3 µM
Primer antisense	0.3 µM
Taq DNA polymerase 10x buffer	1x
$MgCl_2$	2 mM
dNTPs	25 nM
Taq DNA polymerase	1 U
Made upto 50 µl with milli Q water	

The reaction parameters (temperature, cycle) were adapted to the respective PCR setup.

The standard PCR program consists of the following steps:

1) Initial denaturation	94°C	5 min
2) Denaturation	94°C	45 sec
3) Annealing	50–60°C	45 sec
4) DNA synthesis (extension)	72°C	2 min
5) 20-35 Cycles of 2-4)		
6) Terminal DNA-Synthesis	72°C	10 min
7) Cooled at 4°C.		

7.4.15. Purification of PCR-Products

PCR products were cleaned up over spin columns in accordance to the manufacturer´s datasheet (Qiagen).

7.4.16. Real-time RT-PCR

Total RNA was isolated from cells using the RNeasyMini kit (Qiagen), and cDNA synthesis was performed using the SuperScript Reverse Transcription Kit (Invitrogen). Gene expression was monitored by quantitative real-time PCR (Applied Biosystems). SYBR GreenER qPCR SuperMix for ABI PRISM (invitrogen) was used with ABI real-time instrument (ABI7900HT). Expression values were normalized to the mean of 18s rRNA.

PCR reactions were performed in a total volume of 20 µl.

Detail	**End concentration**
DNA template (cDNA)	0.5 – 4 µl (cDNA generated from up to 1 µg of RNA
Primer sense	200 nM
Primer antisense	200 nM
SYBR GreenER qPCR SuperMix	1x
DEPC-treated water	to 20 µl

The standard real-time RT-PCR program consists of the following steps:

50°C for 2 minutes hold
95°C for 10 minutes hold
40 cycles of:
  95°C, 15 seconds
  60°C, 60 seconds
Followed by melting curve analysis

7.4.17. Chromatin Immunoprecipitaiton

Cells were transfected 3-6 days before harvesting for Chromatin immunoprecipiation (ChIP) with or without LSD1 siRNA (Ambion) following the manufacturer's instructions. Immunoprecipitation was performed with specific antibodies to H3K4me2 (Abcam), H3K9me2 (Abcam) and LSD1 (Novus Biologicals) on protein A coupled Dynabeads (Invitrogen). Purified DNA were subjected to real-time PCR using a SYBR green probe (Invitrogen) in an ABI Prism 7900 (Applied Biosystems), according to the manufacturer's specified parameters. Amplicons were normalized to the 1/100 diluted input DNA or to the DNA immunoprecipitated with antibody to histone H3 (Abcam). The following TaqMan real-time PCR primers were used for the proximal promoter region of *TFPI2, XRCC5*, *CCNA2* and *ERBB2* are listed in table 7.2.

7.5. RNA techniques

7.5.1. Isolation of RNA

Total RNA from adherent cells was isolated from cell using RNeasyMini kit according to manufacturer's instructions (Qiagen). The RNA concentration was estimated using the Nanodrop.

7.5.2. Reverse transcription/cDNA synthesis

About 1-5 µg of RNA were used for cDNA synthesis and volume was adjusted to 10 µl with DEPC water. One µl of oligo (dT) primer was added to RNA and mixture was incubated at 60°C for 5 min. In the meantime, master mix was prepared as follows: 1 µl DEPC water, 1 µl 10 mM dNTPs, 4 µl 5x first strand buffer, 2 µl 0.1 M DTT and 1 µl reverse transcriptase. Nine µl of master mix was added to each tube and tubes were incubated at 42°C for 1 h followed by 15 min incubation at 70°C for cDNA synthesis.

7.6. Protein techniques

7.6.1. Preparation of protein samples from adherent cells

Cells were washed and scrapped off in ice cold PBS. Cells were pelleted by centrifugation at 1,000 rpm/ 5 min/ 4°C and lysed with RIPA buffer (200 µl for 6 cm dish and 400 µl for 10 cm dish) on ice for 30 min in the presence of protease inhibitor mix. The lysates were cleared by centrifugation at 12,000 rpm.

7.6.2. Preparation of protein samples from tissues

20-50 mg tumor tissues from patients were homogenized using FastPrep kit (MP biomedicals) by homogenating 3 x 5 min in FastPrep FP120 instrument (MP Biomedicals). Following centrifuge, the supernatant in 200 – 500 µl of RIPA lysis buffer in the presence of the complete mini protease inhibitor cocktails (Roche) was transferred to a new tube and one aliquot was used for protein measurement.

7.6.3. Tissue preparation – Cryosectioning

The prepared tumor tissues were sectioned in the cryostat (CM 3050 S, Leica) at a temperature of -18 to -24°C to a thickness of 12-20 µm. After cutting, the sections were dried for 10-15 min at room temperature and prepared for the HE staining.

7.6.4. Hematoxylin and Eosin (HE) staining

Cryosections of tumor tissues were incubated in 1% Hematoxylin solution for 3 min. Slides were then washed 10 min with milli Q water, followed by eosin staining in 0.1% Eosin solution for 1 min. Slides were then wahed with increasing gradient of ethanol (80%-100%) prior to incubating 2X5 min with Xylol solution. Excessive xylol was removed with clean tissue paper and slides were covered with Roti Histo-Kit II (Roth) mounting medium and dried. Microscopic visualization of slides was done using digital-camera KY-F70B (JVC, London) connected to microscope Axioskop 50 (Zeiss).

7.6.5. Immunohistochemistry

Tissue slides were cut 4 µm thick from formalin-fixed and paraffin embedded human colon cancer or breast cancer specimens and used for staining with haematoxilin and eosine (HE) or by immunohistochemistry. Indirect immunohistochemistry was done by the avidin-biotin-method. Tissue sections were incubated overnight at 60°C, deparaffinized for 10 min in xylene, then washed for 5 min with 100 %, 96 %, 70 %, 50 % ethanol and finally washed in PBS. For better antigen retrieval, samples were boiled in a microwave oven in citrate buffer pH 6.0 (Merck) for 15 min. Then samples were washed in PBS.

The samples were incubated for 1 h at RT with the primary antibodies diluted in blocking buffer (DAKO) by using the TechMate 500 semiautomatic machine (DAKO). Slides were incubated overnight with LSD1 primary antibody diluted 1:250. After slides were washed twice for 5 min in PBS, a horseradish peroxidase /HRP)-labelled polymer conjugated with a secondary antibody was applied (Dako EnVision AEC kit). After 2x washing with PBS, slides were treated with endogenous peroxidase for 5 min in (0.03 % H_2O_2). The staining was visualized with 3-amino-9-ethyl-carbazolke (DAKO) and after a final washing step. Slides were counterstained with Mayer´s hematoxylin (Fluka), dehydrated and mounted by using Aguatex (Merck). Negative controls were performed using blocking solution alone instead of the primary antibody diluted in blocking solutions and resulted in complete absence of signal.

Nuclear immunostaining results for LSD1 were evaluated using a semi-quantitative scoring system. Briefly, the number and intensity of positive cells were counted and scored between 0 and 3 (0 = no positive nuclei, 1 = < 20% nuclei display intense staining or more nuclei display weak staining, 2 = 20-80% intense staining, or more nuclei display moderate staining, 3 = 80-100% nuclei display intensive staining).

Tissue images were taken by using a microscope (Leica) and by using the analysis system software Diskus (Hilgers).

7.6.6. Protein quantification

The method developed by Bradford was employed using coomassie blue dye (Bio-Rad protein assay) and BSA, bovine serum albumin as standard. In the range between 1.2 and 10 µg/ml, the protein concentration can be determined photometrically according to the Lambert-Beer law. Ten µl of standards or 1 µl protein sample are added to 200µl of Bradford reagent diluted 1:4 in PBS. Absorption measurements and calculation of sample concentrations are carried out photometrically on an ELISA reader (Biotek instrument).

7.6.7. Protein staining with Coomassie Brilliant Blue R250

Gel was washed thoroughly with H2O and stained with Coomasie Blue for at least 30 minutes to 1 hr. Gel was incubated with the Destain solution, until the background is gone and blue bands are clearly visible.

7.6.8. SDS-PAGE/Western blot

About 10 – 50 µg of protein samples were loaded in polyacrylamide gel and gel was run (25 mA per gel) in 1x SDS running buffer. After electrophoresis, proteins from a polyacrylamide gel were transferred to a PVMF membrane using blotting chamber (BioRad). Membrane was blocked with 5% skim milk in PBST for 1 h or overnight at 4°C. The blot was then incubated with appropriately diluted primary antibody solution for 1 h at room temperature. The following antibodies and dilutions were used: α-LSD1 (Novus Biologicals) 1:1000; α-H3K4me2 (Abcam) 1:1000; β-actin (Sigma-Aldrich) 1:5000; Her2/erbB2 (DAKO), 1:1000. The blots were washed 3 times each for 5 min with PBS-T and later incubated with appropriate secondary antibody conjugated to HRP (Horseradish peroxidase) for 1 h at RT. The blots were again washed with PBST and chemiluminescent peroxidase substrate was used to visualize protein bands.In the dark, X-ray film was exposed to the membrane and developed using Kodak X-omat 1000 Processor (Kodak). Coomassie staining was used as a loading control in some experiment, since the frequently used reference protein ß-actin was clearly up-regulated in the cancer specimen.

7.6.9. ELISA

For ELISA analysis, 20 normal breast tissues, 26 ER-positive and 37 ER-negative breast tumor tissues were used. Hematoxylin-eosin-stained sections were prepared for assessment of the percentage of tumor cells; only samples with >70% tumor cells were selected.

96-well Maxisorb microplates (Nunc, Wiesbaden, Germany) were incubated with tissue protein lysates (40 µg) in coating buffer (50 mM sodium carbonate buffer, pH 9.2) overnight at 4 °C. After removal of the coating solution by inverting the plate, the wells were blocked with 200 µl blocking buffer (Roche, Mannheim, Germany) for 1 h at room temperature. After rinsing with washing buffer (0.05 % Tween in PBS, PBS-T), the wells were incubated with α-LSD1 solution (1: 400, Novus Biologicals, Cat. No NB 100-1762) in 100 µl blocking buffer for 1 h at 25 °C followed by three washing steps with 200 µl PBS-T. After addition of 100 µl HRP-labelled α-mouse (1:1000, DAKO, Glostrup, Denmark, Cat. No. P-0448), the wells were incubated for 0.5 h and washed three times. Finally, 100 µl of the TMB substrate solution (1 Step Ultra TMB, Thermo Scientific, Rockford, USA) were added to each well. The conversion of substrate was stopped by addition of 100 µl of 2 N sulphuric acid solution. The optical density was determined in an ELISA reader (ELX 800 Universal, Biotek Instruments, Winooski, USA) at 450 nm.

For standard curve, microplates were incubated with a series of dilution of recombinant 6x his-tagged LSD1 protein (1.0, 3.1, 9.3, 27.8, 83.3 and 250.0 µg/L) and breast tumor tissue protein lysate (3, 10, 30 and 60 µg/well) in coating buffer (50 mM sodium carbonate buffer, pH 9.2) overnight at 4 °C. Antibody dilution ratio was modified for the recombinant LSD1. (α-LSD1, 1:4000; HRP-labelled α–mouse, 1:1000). Otherwise, all steps were performed as described above.

7.6.10. Expression and purification of recombinant human LSD1

Genes encoding LSD construct (166 – 852 amino acids) was inserted into the vector pET15b (Novagen). The final construct is missing the first 165 amino acid but N-terminal his_6-tagged LSD1 ΔN (166-852) still contains the SWIRM and amino oxidase domains, which has previously been shown to have a enzyme activity toward peptide substrate *in vitro* (FEBS lett. 579,2203, 2005).

E. coli BL21 (DE3) Star was transformed with LSD1 expression vector and colonies were inoculated directly to 3L Terrific Broth, grew at 37C until saturation. The expression vector contains the promoter of the lac-operon, so that the expression of the recombinant gene can be induced by the synthetic lactose analogon IPTG (isopropylthio- galactopyranoside). Protein expression is induced by addition of 100 mM IPTG solution (final concentration 0.75 – 1 mM IPTG) and incubated overnight at 20 °C. Samples are taken prior to and after induction and analyzed by SDS-PAGE.

Cells were harvested and lysed with 2X PBS buffer containing 20 mM Imidazole. The lysate was applied to Ni^{2+} affinity column (Gravity column) and washed with lysis buffer. His-tagged LSD1

protein was eluted with elution buffer (100 mM Tris-HCl pH 8.0, 300 mM Imidazole). The protein was concentrated to 4 ml and then purified on a Superdex 200 (16/60) size exclusion chromatography (GE Healthcare, Piscataway, U.S.A.) in 20 mM Tris-HCl pH 8.0, 100 mM NaCl. Three fractions were passed through HitrapQ ion exchange column (50 mM Tris pH 8.0). Finally, purified N-terminal his_6-tagged LSD1 ΔN (166-852) was stored in 20 mM Tris-HCl pH 8.0, 100 mM NaCl, 5 % Glycerol. The protein yield was estimated ~ 1mg/L.

7.6.11. LSD1 enzyme assay for high-throughput screening

Peroxide production by LSD1 was monitored using a HRP coupled assay (Forneris, 2005, JBC; Forneris, 2005, FEBS Lett) with exception that Amplex red (100 µM) was used as the fluorogenic electron donor in fluorescene-based assays.

The demethylase activity of N-terminal his_6-tagged LSD1 ΔN (166-852) was assayed with synthetic peptide corresponding to the first 24 amino acids of N-terminal tail of histone H3, incorporating dimethylated Lys at residue 4 (H3K4me2; CASLO, Lyngby, Denmark). The total LSD1 assay volume was 40 µl and all the assay components were diluted in HEPES buffer (50 mM HEPES/NaOH pH 7.4, 0.1% Triton X100). The reaction was carried out in white 96-well plates (Costar 3693). In brief, reaction was started by adding peptide substrate (50 µMl) to the LSD1 assay mixture contained LSD1 (0.25 µM), inhibitor (0.4, 2, 10, 50 µM), Amplex red (100 µM) and HRP (0.4 µM). Concentrations represent the end-concentration of the reagents. Positive controls contained all the above components except the inhibitor. The negative controls contained neither substrate nor inhibitor. In each case, these were replaced with an equivalent volume of buffer. The assay components were incubated at 37 °C for 30 min to obtain progress curves. The fluorescence generated was monitored at wavelengths 560 nm (excitation) and 590 nm (emission) in the plate reader (BMG LABTECH´s FLUOstar OPTIMA, Offenburg). The linear range for LSD1 was determined (0.05 - 1 µM), resulting in the use of final concentration of 0.25 µM LSD1.

For assessment of inhibition of LSD1, the Km for the dimethylated peptide substrate (H3K4me2) was assayed and found to be 35 µM. The use of Km reflects the conversion of dimethylated substrate to unmethylated product via two demethylation events. This substrate concentration was then used in all subsequent inhibition assays.

Inhibitos were prepared as 10 mM stocks in diemethyl sulfoxide (DMSO) and stored at -20 °C. IC50 value was determined by preincubating LSD1 with varying concentrations of inhibitor for 5 min at room temperature prior to initiation of the reaction via the addition of substrate. In control experiments, DMSO was found to have no effect on enzyme activity at concentrations used (2.5 %) (Data not shown).

7.6.12. *in vitro* demethylase assay

1 µg of N-terminal his_6-tagged LSD1 ΔN (166-852) was incubated with 10 µg bulk histone in 50 mM Hepes buffer pH 7.5 at for 3 hours 37 °C. The methlyation status of lys4 at histone H3 in bulk histone was analyzed using western blotting. 7 compounds were tested for their LSD1 inhibitory effect, while tranylcypromine served as a reference compound. Histone H3 was used as the loading control. α-H3K4me2 antibody was diluted 1:1000, while α-Histone H2 antibody was diluted in 1:10,000.

7.7. Growth of xenograft tumors in nude mice

SH-SY5Y neuroblastoma cells were cultured to 80 % confluency, harvested, and suspended in Matrigel (BD Bioscience, Heidelberg, Germany). Four week-old female athymic NCR (*nu/nu*) mice were inoculated s.c. in the flank with 2 x 10^7 cells/ in 200µl Matrigel. Mice were injected with 2mg tranylcypromine (in 100µl NaCl) or NaCl alone i.p. once per day. Mice were sacrificed at day 21, and tumors were weighed, formalin fixed and analyzed.

7.8. Statistical methods

Statistical significance of the ELISA results was tested by two-sided, non-parametrical Mann-Whitney U-test to analyze differences in protein levels among distinct groups using SPSS 17.0 program (SPSS, Inc., Zürich, Switzerland). Association between categorical variables was assessed by two-sided Fisher´s exact test using GraphPad Prism 5 (La Jolla, USA).

8. Reference

1. Allis, D. *et al.* (2007) Epigenetics. CSHL Press.
2. Anand, R. *et al.* (2007) Structure and mechanism of lysine-specific demethylase enzymes. *J Biol Chem*, **282**, 35425-35429.
3. Attiyeh, E.F. *et al.* (2005) Chromosome 1p and 11q deletions and outcome in neuroblastoma. *N Engl J Med*, **353**, 2243-2253.
4. Bernstein, B.E. *et al.* (2007) The mammalian epigenome. *Cell*, **128**, 669-681.
5. Bestor, T.H. (2000) The DNA methyltransferases of mammals. *Hum Mol Genet*, **9**, 2395-2402.
6. Bird, A. (2007) Perceptions of epigenetics. *Nature*, **447**, 396-398.
7. Brodeur, G.M. (2003) Neuroblastoma: biological insights into a clinical enigma. *Nat Rev Cancer*, **3**, 203-216.
8. Chen, Q. *et al.* (2004) Distinct capacities of individual E2Fs to induce cell cycle re-entry in postmitotic lens fiber cells of transgenic mice. *Dev Neurosci*, **26**, 435-445.
9. Chen, Q.R. *et al.* (2006) Increased WSB1 copy number correlates with its over-expression which associates with increased survival in neuroblastoma. *Genes Chromosomes Cancer*, **45**, 856-862.
10. Chen, T. *et al.* (2004) Structure and function of eukaryotic DNA methyltransferases. *Curr Top Dev Biol*, **60**, 55-89.
11. Cheng, D. *et al.* (2004) Small molecule regulators of protein arginine methyltransferases. *J Biol Chem*, **279**, 23892-23899.
12. Cuende, J. *et al.* (2008) Retinoic acid downregulates Rae1 leading to APC(Cdh1) activation and neuroblastoma SH-SY5Y differentiation. *Oncogene*, **27**, 3339-3344.
13. Cui, X. *et al.* (2005) Biology of progesterone receptor loss in breast cancer and its implications for endocrine therapy. *J Clin Oncol*, **23**, 7721-7735.
14. Culhane, J.C. *et al.* (2006) A mechanism-based inactivator for histone demethylase LSD1. *J Am Chem Soc*, **128**, 4536-4537.
15. Dallman, J.E. *et al.* (2004) A conserved role but different partners for the transcriptional corepressor CoREST in fly and mammalian nervous system formation. *J Neurosci*, **24**, 7186-7193.
16. de Ruijter, A.J. *et al.* (2004) The novel histone deacetylase inhibitor BL1521 inhibits proliferation and induces apoptosis in neuroblastoma cells. *Biochem Pharmacol*, **68**, 1279-1288.
17. Dehmelt, L. *et al.* (2006) A microtubule-based, dynein-dependent force induces local cell protrusions: Implications for neurite initiation. *Brain Cell Biol*, **35**, 39-56.

18. Di Stefano, L. *et al.* (2007) Mutation of Drosophila Lsd1 disrupts H3-K4 methylation, resulting in tissue-specific defects during development. *Curr Biol*, **17**, 808-812.
19. Di Toro, R. *et al.* (2005) Expression of the repressor element-1 silencing transcription factor (REST) is influenced by insulin-like growth factor-I in differentiating human neuroblastoma cells. *Eur J Neurosci*, **21**, 46-58.
20. Edmunds, J.W. *et al.* (2008) Dynamic histone H3 methylation during gene induction: HYPB/Setd2 mediates all H3K36 trimethylation. *Embo J*, **27**, 406-420.
21. Esteller, M. (2008) Epigenetics in cancer. *N Engl J Med*, **358**, 1148-1159.
22. Feinberg, A.P. *et al.* (2006) The epigenetic progenitor origin of human cancer. *Nat Rev Genet*, **7**, 21-33.
23. Feinberg, A.P. *et al.* (2004) The history of cancer epigenetics. *Nat Rev Cancer*, **4**, 143-153.
24. Forneris, F. *et al.* (2007) Structural basis of LSD1-CoREST selectivity in histone H3 recognition. *J Biol Chem*, **282**, 20070-20074.
25. Forneris, F. *et al.* (2008) LSD1: oxidative chemistry for multifaceted functions in chromatin regulation. *Trends Biochem Sci*, **33**, 181-189.
26. Forneris, F. *et al.* (2005) Human histone demethylase LSD1 reads the histone code. *J Biol Chem*, **280**, 41360-41365.
27. Forneris, F. *et al.* (2005) Histone demethylation catalysed by LSD1 is a flavin-dependent oxidative process. *FEBS Lett*, **579**, 2203-2207.
28. Fraczek, M. *et al.* (2008) Clinicopathologic significance and prognostic role of cyclin E and cyclin A expression in laryngeal epithelial lesions. *Acta Otolaryngol*, **128**, 329-334.
29. Garcia-Bassets, I. *et al.* (2007) Histone methylation-dependent mechanisms impose ligand dependency for gene activation by nuclear receptors. *Cell*, **128**, 505-518.
30. Godmann, M. *et al.* (2007) Dynamic regulation of histone H3 methylation at lysine 4 in mammalian spermatogenesis. *Biol Reprod*, **77**, 754-764.
31. Goldberg, A.D. *et al.* (2007) Epigenetics: a landscape takes shape. *Cell*, **128**, 635-638.
32. Groth, A. *et al.* (2007) Chromatin challenges during DNA replication and repair. *Cell*, **128**, 721-733.
33. Hanahan, D. *et al.* (2000) The hallmarks of cancer. *Cell*, **100**, 57-70.
34. Heintzman, N.D. *et al.* (2007) Distinct and predictive chromatin signatures of transcriptional promoters and enhancers in the human genome. *Nat Genet*, **39**, 311-318.
35. Hu, Q. *et al.* (2008) Enhancing nuclear receptor-induced transcription requires nuclear motor and LSD1-dependent gene networking in interchromatin granules. *Proc Natl Acad Sci U S A*, **105**, 19199-19204.
36. Huang, J. *et al.* (2004) Lsh, an epigenetic guardian of repetitive elements. *Nucleic Acids Res*, **32**, 5019-5028.

37. Huang, J. *et al.* (2007) p53 is regulated by the lysine demethylase LSD1. *Nature*, **449**, 105-108.
38. Huang, Y. *et al.* (2007) Inhibition of lysine-specific demethylase 1 by polyamine analogues results in reexpression of aberrantly silenced genes. *Proc Natl Acad Sci U S A*, **104**, 8023-8028.
39. Jaenisch, R. *et al.* (2003) Epigenetic regulation of gene expression: how the genome integrates intrinsic and environmental signals. *Nat Genet*, **33 Suppl**, 245-254.
40. Jaenisch, R. *et al.* (2008) Stem cells, the molecular circuitry of pluripotency and nuclear reprogramming. *Cell*, **132**, 567-582.
41. Jenuwein, T. *et al.* (2001) Translating the histone code. *Science*, **293**, 1074-1080.
42. Jones, P.A. *et al.* (2007) The epigenomics of cancer. *Cell*, **128**, 683-692.
43. Jones, P.A. *et al.* (2005) A blueprint for a Human Epigenome Project: the AACR Human Epigenome Workshop. *Cancer Res*, **65**, 11241-11246.
44. Jones, P.A. *et al.* (2001) The role of DNA methylation in mammalian epigenetics. *Science*, **293**, 1068-1070.
45. Kahl, P. *et al.* (2006) Androgen receptor coactivators lysine-specific histone demethylase 1 and four and a half LIM domain protein 2 predict risk of prostate cancer recurrence. *Cancer Res*, **66**, 11341-11347.
46. Katz, D.J. *et al.* (2009) A C. elegans LSD1 demethylase contributes to germline immortality by reprogramming epigenetic memory. *Cell*, **137**, 308-320.
47. Koch, C.M. *et al.* (2007) The landscape of histone modifications across 1% of the human genome in five human cell lines. *Genome Res*, **17**, 691-707.
48. Kouzarides, T. (2007) Chromatin modifications and their function. *Cell*, **128**, 693-705.
49. Krivtsov, A.V. *et al.* (2008) H3K79 methylation profiles define murine and human MLL-AF4 leukemias. *Cancer Cell*, **14**, 355-368.
50. Kuendgen, A. *et al.* (2008) Current status of epigenetic treatment in myelodysplastic syndromes. *Ann Hematol*, **87**, 601-611.
51. Laird, P.W. (2003) The power and the promise of DNA methylation markers. *Nat Rev Cancer*, **3**, 253-266.
52. Lakowski, B. *et al.* (2006) CoREST-like complexes regulate chromatin modification and neuronal gene expression. *J Mol Neurosci*, **29**, 227-239.
53. Lee, M.G. *et al.* (2006) Histone H3 lysine 4 demethylation is a target of nonselective antidepressive medications. *Chem Biol*, **13**, 563-567.
54. Lee, M.N. *et al.* (2007) Epigenetic inactivation of the chromosomal stability control genes BRCA1, BRCA2, and XRCC5 in non-small cell lung cancer. *Clin Cancer Res*, **13**, 832-838.
55. Lengauer, C. *et al.* (1998) Genetic instabilities in human cancers. *Nature*, **396**, 643-649.

56. Li, B. *et al.* (2007) The role of chromatin during transcription. *Cell*, **128**, 707-719.
57. Li, E. *et al.* (1992) Targeted mutation of the DNA methyltransferase gene results in embryonic lethality. *Cell*, **69**, 915-926.
58. Luger, K. *et al.* (1997) Characterization of nucleosome core particles containing histone proteins made in bacteria. *J Mol Biol*, **272**, 301-311.
59. Lund, A.H. *et al.* (2004) Epigenetics and cancer. *Genes Dev*, **18**, 2315-2335.
60. Mai, A. *et al.* (2009) Epi-drugs to fight cancer: from chemistry to cancer treatment, the road ahead. *Int J Biochem Cell Biol*, **41**, 199-213.
61. Margueron, R. *et al.* (2005) The key to development: interpreting the histone code? *Curr Opin Genet Dev*, **15**, 163-176.
62. Maris, J.M. *et al.* (2007) Neuroblastoma. *Lancet*, **369**, 2106-2120.
63. Metzger, E. *et al.* (2005) LSD1 demethylates repressive histone marks to promote androgen-receptor-dependent transcription. *Nature*, **437**, 436-439.
64. Muegge, K. (2005) Lsh, a guardian of heterochromatin at repeat elements. *Biochem Cell Biol*, **83**, 548-554.
65. Nobeyama, Y. *et al.* (2007) Silencing of tissue factor pathway inhibitor-2 gene in malignant melanomas. *Int J Cancer*, **121**, 301-307.
66. Okamoto, P.M. *et al.* (2001) Dynamin isoform-specific interaction with the shank/ProSAP scaffolding proteins of the postsynaptic density and actin cytoskeleton. *J Biol Chem*, **276**, 48458-48465.
67. Okano, M. *et al.* (1999) DNA methyltransferases Dnmt3a and Dnmt3b are essential for de novo methylation and mammalian development. *Cell*, **99**, 247-257.
68. Ooi, S.K. *et al.* (2007) DNMT3L connects unmethylated lysine 4 of histone H3 to de novo methylation of DNA. *Nature*, **448**, 714-717.
69. Osborne, C. *et al.* (2004) Oncogenes and tumor suppressor genes in breast cancer: potential diagnostic and therapeutic applications. *Oncologist*, **9**, 361-377.
70. Ozanne, S.E. *et al.* (2007) Mechanisms of disease: the developmental origins of disease and the role of the epigenotype. *Nat Clin Pract Endocrinol Metab*, **3**, 539-546.
71. Patel, R.S. *et al.* (2007) Cyclin A expression and its diagnostic value in pleomorphic adenoma and carcinoma expleomorphic adenoma of the parotid gland. *Histopathology*, **51**, 21-25.
72. Pellikainen, J.M. *et al.* (2007) Activator protein-2 in carcinogenesis with a special reference to breast cancer--a mini review. *Int J Cancer*, **120**, 2061-2067.
73. Peterson, C.L. *et al.* (2004) Histones and histone modifications. *Curr Biol*, **14**, R546-551.
74. Reik, W. (2007) Stability and flexibility of epigenetic gene regulation in mammalian development. *Nature*, **447**, 425-432.

75. Roh, T.Y. *et al.* (2005) Active chromatin domains are defined by acetylation islands revealed by genome-wide mapping. *Genes Dev*, **19**, 542-552.
76. Ruthenburg, A.J. *et al.* (2007) Methylation of lysine 4 on histone H3: intricacy of writing and reading a single epigenetic mark. *Mol Cell*, **25**, 15-30.
77. Ruthenburg, A.J. *et al.* (2007) Multivalent engagement of chromatin modifications by linked binding modules. *Nat Rev Mol Cell Biol*, **8**, 983-994.
78. Saleque, S. *et al.* (2007) Epigenetic regulation of hematopoietic differentiation by Gfi-1 and Gfi-1b is mediated by the cofactors CoREST and LSD1. *Mol Cell*, **27**, 562-572.
79. Schevzov, G. *et al.* (2005) Specific features of neuronal size and shape are regulated by tropomyosin isoforms. *Mol Biol Cell*, **16**, 3425-3437.
80. Schleiermacher, G. *et al.* (2007) Chromosomal CGH identifies patients with a higher risk of relapse in neuroblastoma without MYCN amplification. *Br J Cancer*, **97**, 238-246.
81. Schmidt, D.M. *et al.* (2007) trans-2-Phenylcyclopropylamine is a mechanism-based inactivator of the histone demethylase LSD1. *Biochemistry*, **46**, 4408-4416.
82. Schneider, R. *et al.* (2002) Unsafe SETs: histone lysine methyltransferases and cancer. *Trends Biochem Sci*, **27**, 396-402.
83. Schramm, A. *et al.* (2007) Translating expression profiling into a clinically feasible test to predict neuroblastoma outcome. *Clin Cancer Res*, **13**, 1459-1465.
84. Schulte, J.H. *et al.* (2008) MYCN regulates oncogenic MicroRNAs in neuroblastoma. *Int J Cancer*, **122**, 699-704.
85. Schulte, J.H. *et al.* (2009) Lysine-specific demethylase 1 is strongly expressed in poorly differentiated neuroblastoma: implications for therapy. *Cancer Res*, **69**, 2065-2071.
86. Scoumanne, A. *et al.* (2007) The lysine-specific demethylase 1 is required for cell proliferation in both p53-dependent and -independent manners. *J Biol Chem*, **282**, 15471-15475.
87. Seligson, D.B. *et al.* (2005) Global histone modification patterns predict risk of prostate cancer recurrence. *Nature*, **435**, 1262-1266.
88. Shi, Y. *et al.* (2004) Histone demethylation mediated by the nuclear amine oxidase homolog LSD1. *Cell*, **119**, 941-953.
89. Sidell, N. *et al.* (1983) Effects of retinoic acid (RA) on the growth and phenotypic expression of several human neuroblastoma cell lines. *Exp Cell Res*, **148**, 21-30.
90. Silva, C.M. *et al.* (2007) Integration of steroid and growth factor pathways in breast cancer: focus on signal transducers and activators of transcription and their potential role in resistance. *Mol Endocrinol*, **21**, 1499-1512.
91. Spannhoff, A. *et al.* (2009) Cancer treatment of the future: inhibitors of histone methyltransferases. *Int J Biochem Cell Biol*, **41**, 4-11.

92. Stavropoulos, P. *et al.* (2006) Crystal structure and mechanism of human lysine-specific demethylase-1. *Nat Struct Mol Biol*, **13**, 626-632.
93. Steger, D.J. *et al.* (2008) DOT1L/KMT4 recruitment and H3K79 methylation are ubiquitously coupled with gene transcription in mammalian cells. *Mol Cell Biol*, **28**, 2825-2839.
94. Stupack, D.G. *et al.* (2006) Potentiation of neuroblastoma metastasis by loss of caspase-8. *Nature*, **439**, 95-99.
95. Su, S.T. *et al.* (2009) Involvement of histone demethylase LSD1 in Blimp-1-mediated gene repression during plasma cell differentiation. *Mol Cell Biol*, **29**, 1421-1431.
96. Sunami, E. *et al.* (2008) Estrogen receptor and HER2/neu status affect epigenetic differences of tumor-related genes in primary breast tumors. *Breast Cancer Res*, **10**, R46.
97. Szewczuk, L.M. *et al.* (2007) Mechanistic analysis of a suicide inactivator of histone demethylase LSD1. *Biochemistry*, **46**, 6892-6902.
98. Talbert, P.B. *et al.* (2006) Spreading of silent chromatin: inaction at a distance. *Nat Rev Genet*, **7**, 793-803.
99. Tsai, W.W. *et al.* (2008) p53-targeted LSD1 functions in repression of chromatin structure and transcription in vivo. *Mol Cell Biol*, **28**, 5139-5146.
100. Valk-Lingbeek, M.E. *et al.* (2004) Stem cells and cancer; the polycomb connection. *Cell*, **118**, 409-418.
101. Vandesompele, J. *et al.* (2005) Unequivocal delineation of clinicogenetic subgroups and development of a new model for improved outcome prediction in neuroblastoma. *J Clin Oncol*, **23**, 2280-2299.
102. Vargo-Gogola, T. *et al.* (2007) Modelling breast cancer: one size does not fit all. *Nat Rev Cancer*, **7**, 659-672.
103. Wang, J. *et al.* (2009) The lysine demethylase LSD1 (KDM1) is required for maintenance of global DNA methylation. *Nat Genet*, **41**, 125-129.
104. Wang, J. *et al.* (2007) Opposing LSD1 complexes function in developmental gene activation and repression programmes. *Nature*, **446**, 882-887.
105. Wardelmann, E. *et al.* (2005) Acquired resistance to imatinib in gastrointestinal stromal tumours caused by multiple KIT mutations. *Lancet Oncol*, **6**, 249-251.
106. Wei, L. *et al.* (2008) Rapid recruitment of BRCA1 to DNA double-strand breaks is dependent on its association with Ku80. *Mol Cell Biol*, **28**, 7380-7393.
107. Widschwendter, M. *et al.* (2007) Epigenetic stem cell signature in cancer. *Nat Genet*, **39**, 157-158.
108. Wijermans, P.W. *et al.* (2008) Efficacy of decitabine in the treatment of patients with chronic myelomonocytic leukemia (CMML). *Leuk Res*, **32**, 587-591.

109. Wissmann, M. *et al.* (2007) Cooperative demethylation by JMJD2C and LSD1 promotes androgen receptor-dependent gene expression. *Nat Cell Biol*, **9**, 347-353.

110. Witt, O. *et al.* (2009) Targeting histone deacetylases in neuroblastoma. *Curr Pharm Des*, **15**, 436-447.

111. Wojtukiewicz, M.Z. *et al.* (2003) Immunohistochemical localization of tissue factor pathway inhibitor-2 in human tumor tissue. *Thromb Haemost*, **90**, 140-146.

112. Wong, C.M. *et al.* (2007) Tissue factor pathway inhibitor-2 as a frequently silenced tumor suppressor gene in hepatocellular carcinoma. *Hepatology*, **45**, 1129-1138.

113. Yang, M. *et al.* (2007) Structural basis for the inhibition of the LSD1 histone demethylase by the antidepressant trans-2-phenylcyclopropylamine. *Biochemistry*, **46**, 8058-8065.

114. Yokoyama, A. *et al.* (2008) Transrepressive function of TLX requires the histone demethylase LSD1. *Mol Cell Biol*, **28**, 3995-4003.

9. Acknowledgements

First and foremost I want to thank my supervisor Prof. Dr. Reinhard Büttner who gave me the possibility to carry out a very exciting Ph.D here in Germany. I appreciate all his guidance and support throughout my Ph.D work and for this I will be forever indebted to him. I would also like to express my sincere thanks to Dr. Jutta Kirfel for all her contributions of time, her guidance and excellent support in the Ph.D. pursuit. I am also gratefull to Prof. Michael Gütschow for his interest and many helpful comments. Without his support, it would have been impossible to perform the enzyme assay. I wish to express my gratitude to Prof. Dr. Christa Müller for her interest in me, to be my second supervisor. I would like to thank Prof. Dr. Hubert Schorle and Prof. Dr. Evi Kostenis for being reviewers for my Ph.D. thesis.

I would like to acknowledge the financial support by GRK 804 program organized by Prof. Famulok and Dr. Sven Jan Freundenthal. I am also very thankful for the people that collaborated with me during my Ph.D: Johannes Schulte (Essen), Prof. Dr. Roland Schüle of Freiburg Medical School, Dr. Dominica Willmann, Prof. Dr. H. Waldmann of the Max-Plank-Institute (Dortmund). I would like to give special thanks to Hans-Georg Häcker (Institute of Pharmaceutical Chemistry) for his very constructive discussion and cordial support and to Doris Schmidt (Institute of Urology) for her technical help.

My time during my Ph.D was made enjoyable in large part due to all my colleagues in the lab. I want to give many thanks from my heart to Katrin, Andreas, Claudine, Paloma, Carmen, Annemarie, Anke and all the other colleagues from the neighbour-laboratoris: Dr. Richard Jäger, Daniel, Dawid, Peter, Sabine, Tatjana, Jasmin and Swapna. Sincere thanks are given to my colleagues from GRK 804 for nice and constructive time together.

Finally, I am forever indebted to my parents and my two older brothers, Young-Kwan and Young-Jun for their endless encouragement and practical help. I am also very grateful to Martin for being a great supporter to me.

10. Curriculum Vitae

Educational background

12/2005 – present	Ph.D study, Institute of Pathology Bonn medical school, University of Bonn, Germany Under the supervision of Prof. Dr. Reinhard Buettner
03/2001 – 02/2003	Master of Science, College of Pharmacy Seoul National University, South Korea Under the supervision of Prof. Dr. Young-Joon, Surh
03/1997 – 02/2001	Bachelor of Science, College of Pharmacy Seoul National University, South Korea

Publications

Lim, S., Janzer, A., Schüle, R., Buettner, R., and Kirfel, J. (2009) Lysine-specific demethylase 1 (LSD1) is highly expressed in ER-negative breast cancers and a biomarker predicting aggressive biology. *Carcinogenesis*, submitted.

Schulte, J.H.[*], **Lim, S**.[*], Schramm, A., Friedrichs, N., Koster, J., Versteeg, R., Ora, I., Pajtler, K., Klein-Hitpass, L., Kuhfittig-Kulle, S., Metzger, E., Schüle, R., Eggert, A., Buettner, R. and Kirfel, J. (2009) Lysine-specific demethylase 1 is strongly expressed in poorly differentiated neuroblastoma: implications for therapy. *Cancer Res.*, **69**, 2065-71.

[*]Both authors contributed equally to this work.

Schulte, J.H., Kirfel, J., **Lim**, **S**., Schramm, A., Friedrichs, N., Deubzer, H.E., Witt, O., Eggert, A. and Buettner, R. (2008) Transcription factor AP2alpha (TFAP2a) regulates differentiation and proliferation of neuroblastoma cells. *Cancer Lett*., **271**, 56-63.

Lim, S.Y., Jang, J.H., Na, H.K., Lu, S.C., Rahman, I. and Surh, Y.J. (2004) 15-Deoxy-Delta12,14-prostaglandin J(2) protects against nitrosative PC12 cell death through up-regulation of intracellular glutathione synthesis. *J. Biol. Chem.,* **279,** 46263-70.

Kim, S.H., Song, S.H., Kim S.G., Chun, K.S., **Lim, S.Y.**, Na, H.K., Kim, J.W., Surh, Y.J., Bang, Y.J. and Song, Y.S. (2004) Celecoxib induces apoptosis in cervical cancer cells independent of cyclooxygenase using NF-kappaB as a possible target. *J. Cancer Res. Clin. Oncol.,* **130**, 551-60.

Lim, S.Y., Jang, J.H. and Surh, Y.J. (2003) Induction of cyclooxygenase-2 and peroxisome proliferator-activated receptor-gamma during nitric oxide-induced apoptotic PC12 cell death. *Ann. N. Y. Acad. Sci.*, **1010**, 648-58.

Meetings and Courses

Bonner Forum Biomedizin Meeting, February 2009, Bad Breisig, Germany
Poster Presentation

Cold Spring Harbor Course, "The Genome Access Course", November 2008, Cold Spring Harbor, USA

59 Mosbacher Kolloquium, "Epigenetics – Molecular Principles and Mechanisms", March 2008, Mosbach, Germany
Poster Presentation

Bonner Forum Biomedizin Meeting, February 2008, Bad Breisig, Germany
Poster Presentation

Cold Spring Harbor Meeting, "Mechanisms of Eukaryotic Transcription", June 2007, Cold Spring Habor, USA
Poster presentation

Bonner Forum Biomedizin Meeting, February 2007, Bad Breisig, Germany
Poster Presentation

11. Appendix

Table. LSD1-HRP coupled assay, H_2O_2 interference test and *in vitro* demethylase assay

LSD1-HRP coupled assay was performed using 4 different concentrations of 80 compounds. Some compounds were found to react directly with hydrogen peroxide, thus interfering with the LSD1-HRP coupled assay. To screen out the compounds reacting with hydrogen peroxide, exogenous hydrogen peroxide (5 μM) was incubated with 50 μM compounds, 0.4 μM HRP and 100 μM Amplex red. The consumed hydrogen peroxide in the presence of the compounds was calculated.

		LSD1-HRP coupled assay				Reactivity of compounds to H_2O_2	*in vitro* demethylase assay	
No.	Compounds No.	Relative decrease of initial velocity				Conc. of H_2O_2 reacting to 50 μM compound (μM)	√[§]	Inhibition at 50 μM compound conc.
		50μM	10 μM	2 μM	0.4 μM			
	Tranylcypromine	**0.34**	**0.53**	**0.52**	**0.35**	**0.00**		**LSD1 inhibitor**
1	P1 A11	0.60	0.72	0.19	1.12	0.06		
2	P1 A15	0.21	0.37	0.69	0.81	0.72		
3	P1 A21	n.d.	0.35	0.50	0.66	0.00	√	
4	P1 E11	0.30	0.39	0.45	0.48	1.87		
5	P1 E19	0.61	0.48	0.99	0.55	0.08	√	
6	P1 E21	n.d.	0.51	0.49	0.31	0.01	√	
7	P1 M19	n.d.	0.48	0.60	0.59	2.07		
8	P2 A1	0.26	0.50	0.67	0.60	0.00	√	LSD1 inhibitor
9	P3 E15	0.26	0.19	0.40	0.36	2.29		
10	P3 G7	0.36	0.40	0.43	0.47	2.20		
11	P3 K21	n.d.	0.28	0.65	0.56	1.21		
12	P3 O1	0.42	0.39	0.39	0.33	2.37		
13	P4 A1	n.d.	0.48	0.48	0.68	0.17	√	
14	P4 A5	n.d.	0.62	0.72	0.62	0.40		
15	P4 A9	n.d.	0.25	0.64	0.60	0.03	√	
16	P4 A11	0.67	0.24	0.82	0.84	0.00		
17	P4 A15	0.29	0.43	0.69	0.77	0.55		
18	P4 A17	0.33	0.76	0.81	0.88	0.00		
19	P4 A19	0.74	0.77	0.82	1.01	0.00		
20	P4 A21	0.77	0.71	0.61	0.73	0.00		

		LSD1-HRP coupled assay				Reactivity of compounds to H_2O_2	*in vitro* demethylase assay	
No.	Compounds No.	Relative decrease of initial velocity				Conc. of H_2O_2 reacting to 50 μM compound (μM)	√[§]	Inhibition at 50 μM compound conc.
		50μM	10 μM	2 μM	0.4 μM			
21	P4 C1	0.30	0.85	0.94	0.83	0.00		
22	P4 C5	0.57	0.10	0.86	0.80	0.17		
23	P4 C9	0.50	0.77	0.74	0.58	0.70		
24	P4 C15	0.65	0.73	1.03	0.75	0.02		
25	P4 C17	0.67	0.83	1.07	1.03	0.00		
26	P4 C19	0.70	0.99	0.88	0.83	0.00		
27	P4 E1	0.73	0.79	0.98	0.78	0.00		
28	P4 E17	0.56	0.74	0.76	0.47	0.00		
29	P4 E19	0.68	0.94	0.86	0.20	0.00		
30	P4 E21	0.35	0.36	0.47	0.61	0.00	√	
31	P4 G1	0.40	0.38	0.40	0.51	0.17	√	
32	P4 G9	0.17	0.48	0.45	0.56	0.08	√	
33	P4 G11	0.37	0.61	0.76	0.55	0.03	√	
34	P4 G13	0.41	0.43	0.60	0.55	2.07		
35	P4 G15	0.53	0.61	0.61	0.65	1.04		
36	P4 G17	0.28	0.29	0.45	0.55	0.00	√	
37	P4 G19	0.24	0.39	0.49	0.47	0.00	√	inhibition
38	P4 G21	0.19	0.17	0.15	0.16	0.13	√	
39	P4 I15	0.16	0.33	0.29	0.73	0.00	√	
40	P4 I19	0.60	0.90	0.87	0.97	0.00		
41	P4 I21	0.68	0.69	0.71	0.83	0.00		
42	P4 K1	0.66	0.77	0.99	1.02	0.00		
43	P4 K3	0.63	0.96	0.70	0.56	0.00		
44	P4 K19	0.39	0.54	0.74	0.82	0.05		
45	P4 K21	0.58	0.87	0.91	0.77	0.00		
46	P4 M21	0.76	0.27	0.83	0.72	0.00		
47	P4 O1	0.47	0.89	0.97	0.73	0.00		
48	P4 O5	0.61	0.89	0.95	0.87	0.00		
49	P4 O15	0.75	0.87	0.36	0.80	0.00		
50	P4 O21	0.53	0.79	0.85	0.18	0.00		
51	P5 E13	0.56	0.60	0.62	0.59	0.42		
52	P5 G9	0.43	0.85	1.04	0.82	0.03		

		LSD1-HRP coupled assay				Reactivity of compounds to H_2O_2	*in vitro* demethylase assay	
No.	Compounds No.	Relative decrease of initial velocity				Conc. of H_2O_2 reacting	√§	Inhibition at 50 μM
		50μM	10 μM	2 μM	0.4 μM	to 50 μM compound (μM)		compound conc.
53	P5 M21	0.37	0.68	0.82	0.75	0.00		
54	P5 O11	0.06	0.25	0.49	0.47	0.00	√	inhibition
55	P5 O17	0.11	0.44	0.47	0.80	0.13	√	inhibition
56	P5 O21	0.22	0.33	0.18	0.35	0.27		
57	P6 A1	0.67	0.28	0.77	0.93	0.02		
58	P6A3	0.49	0.62	0.63	0.78	0.00	√	inhibition
59	P6 A7	0.19	0.38	0.59	0.63	0.76		
60	P6 A11	0.10	0.47	0.62	0.29	1.24		
61	P6 A13	0.14	0.21	0.29	0.46	0.73		
62	P6 A15	0.36	0.48	0.51	0.50	0.00	√	inhibition
63	P6 A17	0.31	0.68	0.96	1.05	0.16		
64	P6 A21	0.34	0.55	0.67	0.77	1.52		
65	P6 C7	n.d	0.45	0.58	0.56	0.15		
66	P6 C11	0.45	0.52	0.49	0.37	0.05	√	
67	P6 C17	0.33	0.34	0.41	0.32	1.58		
68	P6 E3	n.d	0.31	0.36	0.85	0.83		
69	P6 G5	0.58	0.67	0.69	0.67	0.00	√	
70	P6 G7	0.60	0.19	0.67	0.66	0.00	√	
71	P6 G19	0.17	0.35	0.53	0.60	1.20		
72	P6 I15	n.d	0.78	0.84	0.60	0.00		
73	P6 I19	0.81	0.72	0.86	0.74	0.00		
74	P6 K17	n.d	0.57	0.67	0.84	0.00	√	
75	P6 K19	n.d	0.15	0.71	0.91	0.00		
76	P6 M7	0.52	0.58	0.60	0.54	0.00	√	
77	P6 M13	0.40	0.32	0.40	0.32	1.40		
78	P7 A9	0.69	0.82	0.65	0.77	0.00		
79	P7 I19	0.47	0.71	0.85	0.75	0.00		
80	P8 K9	n.d	0.58	0.53	0.53	0.00	√	inhibition

§ 24 compounds (√) which showed LSD1 inhibitory effect and didn't react with H_2O_2 were selected for the further in vitro demethylase assay.

n.d., not determind